LEUKOTRIENE B_4 LEVELS DETERMINE *STAPHYLOCOCCUS AUREUS* SKIN INFECTION OUTCOME

Stephanie Lillian Brandt

Submitted to the faculty of the University Graduate School
in partial fulfillment of the requirements
for the degree
Doctor of Philosophy
In the Department of Microbiology and Immunology,
Indiana University

October 2017

Accepted by the Graduate Faculty, Indiana University, in partial fulfillment of the requirements for the degree of Doctor of Philosophy.

_____
C. Henrique Serezani, Ph.D., - Co-Chair

Doctoral Committee

_____
Janice S. Blum, Ph.D. - Co-Chair

August 18, 2017

_____
Mark H. Kaplan, Ph.D.

_____
Carmella Evans-Molina, M.D., Ph.D.

ACKNOWLEDGEMENTS

There are many great people I need to acknowledge for helping me along my journey through graduate school. I first want to thank my mentor and co-chair, Dr. Henrique Serezani, for his guidance, encouragement, and support. Next I want to thank my committee, co-chair Dr. Janice Blum, Dr. Mark Kaplan, and Dr. Carmella Evans-Molina for their constructive advice and support.

A special thanks to all of the Serezani lab members, past and present, who helped create a collaborative lab environment. I'd like to give a very special thanks to Soujuan Wang for being a wonderful person to work with. I want to thank Luciano Filgueiras for helping me when I first joined the lab. I would also like to thank Naiara Dejani for being a great coworker and friend. I also thank all of the rotation students and summer students I had the opportunity to work with, which helped me become a better teacher.

I would also like to thank the Indiana University department of Microbiology & Immunology faculty, staff, and all the collaborators throughout the years. Thanks to Seth Winfree with the Indiana Center for Biological Microscopy for helping with intravital microscopy imaging and analysis. Thanks to Brian McCarthy with the Indiana Institute for Biological Imaging Sciences for helping with the in vivo imaging and analysis. Thanks to Dr. David Morris, Dr. Jeff Travers, and Dr. Lloyd Miller for collaborating and providing helpful advice in our discussions. Thanks to the Indiana University Research in Pediatric & Developmental Pharmacology for U54 funding to collaborate on a pilot project. This project gave me the opportunity to travel to Dr. Victor Nizet's lab at

University of California San Diego to learn new lab techniques from Ross Corriden, Simon Doehrmann, and other lab members. I would also thank the Indiana University Immunology and Infectious Diseases T32 training grant, which provided funding for three years.

In August 2016, Dr. Serezani moved his laboratory to Vanderbilt University School of Medicine. I am grateful I had the opportunity to relocate with the lab. I would like to thank Dr. Janice Blum again, who became a co-chair on my committee, which facilitated the move to Vanderbilt. I would also like to thank the Division of Infectious Diseases and the department of Pathology, Microbiology, and Immunology for welcoming me to their groups. Thanks to Dr. David Aronoff, the director of the Division of Infectious Diseases at VUMC, for providing helpful discussions. Thanks to the new members in the Serezani lab, Sarah Sturgeon, Nathan Klopfenstein, and Allison Judge, for being great friends and colleagues.

Importantly, I would like to thank my family and friends, old and new, for their continuous support.

Lastly, I would like to give a special thanks to Cayman Chemical Company for providing me a thesis-printing award.

Stephanie Lillian Brandt

LEUKOTRIENE B_4 LEVELS DETERMINE *STAPHYLOCOCCUS AUREUS* SKIN INFECTION OUTCOME

Methicillin-resistant *Staphylococcus aureus* (MRSA) is a major cause of severe skin infections and due to antibiotic resistance there is an intrinsic need to develop new immunotherapeutic strategies. Skin immune responses to infections require the cross-talk between phagocytes and structural cells that involves the secretion of cytokines, chemokines, and lipids. Leukotriene B_4 (LTB_4) is a pleiotropic lipid mediator known as a chemoattractant, but is also necessary to promote antimicrobial activity through B leukotriene receptor 1 (BLT1) signaling. However, chronic LTB_4 production is associated with inflammatory diseases, including diabetes. People with diabetes are more susceptible to infections. The determinants by which LTB_4/BLT1 promotes protective or detrimental immune responses in homeostasis and diabetes are unknown. We hypothesize that LTB_4 levels determine infection outcome; while LTB_4 is necessary for infection control, excessive LTB_4 levels promote overwhelming inflammation that impairs host defense. Our data show that skin macrophages were necessary for LTB_4 production and that LTB_4 was vital for neutrophil direction, abscess formation, IL-1β production, and MRSA clearance through reactive oxygen species production. Importantly, topical LTB_4 ointment treatment enhances neutrophil direction, abscess formation, and bacterial clearance. Conversely, in the setting of

diabetes, skin macrophages drove excessive LTB_4 production that promoted overwhelming inflammation, uncontrolled neutrophil recruitment, poor abscess formation, and lack of bacterial control. Diabetic mice treated with a topical ointment to inhibit BLT1 dampened inflammation and restored host defense by improving abscess formation, bacterial clearance, and overall inflammatory responses in the skin. These data demonstrate the balance of LTB_4-induced inflammation is critical for regulating optimal immune responses during infections. This work highlights the importance of investigating the role of inflammatory mediators in the settings of health and disease. Targeting LTB_4/BLT1 has therapeutic potential to regulate inflammation during MRSA skin infection by enhancing immune responses in settings of vulnerability or decrease inflammation in diabetes.

C. Henrique Serezani, Ph.D., Co-Chair

Janice S. Blum, Ph.D., Co-Chair

TABLE OF CONTENTS

LIST OF TABLES

LIST OF FIGURES

LIST OF ABBREVIATIONS

12-HHT	12-Hydroxyheptadecatrenoic acid
AA	Arachidonic acid
Alox-5 (5-LO)	5-lipoxygenase
ASC	Apoptosis-associated speck-like protein containing a carboxy-terminal CARD
BLI	Bioluminescence imaging
BSA	Bovine serum albumin
cAMP	cyclic AMP
cDNA	Complementary DNA
CFSE	Carboxyfluorescein succinimidyl ester
CFU	Colony forming unit
CRAMP	Cathelicidin-related antimicrobial peptide
CT	Control/nondiabetic
ctNOD	Nondiabetic NOD control
cysLT	cysteinyl leukotriene
DAB	3,3’-diaminobenzidine
DAMP	Danger associated molecular pattern
DAPI	4’,6-diamidino-2-phenylindole
DB	Diabetic
dbNOD	Diabetic NOD
DMEM	Dulbecco’s modified Eagle medium
DT	Diphtheria toxin

DTR	Diphtheria toxin receptor
ECM	Extracellular matrix
EDTA	Ethylenediaminetetraacetic acid
EGFP	Enhanced green fluorescent protein
EIA	Enzyme immunoassay
FACS	Fluorescence-activated cell sorting
FBS	Fetal bovine serum
FITC	Fluorescein isothiocyanate
FLAP	5-lipoxygenase-activating protein
fMLP	*N*-formylmethionine-leucyl-phenylalanine
GFP	Green fluorescent protein
H&E	Hematoxylin and eosin
HETE	Hydroxyeicosatetraenoic acid
HK-MRSA	Heat-killed methicillin-resistant *Staphylococcus aureus*
IAC	Infected apoptotic cell
ICAM-1	Intercellular adhesion molecule 1
IF	Immunofluorescence
IHC	Immunohistochemistry
IL	Interleukin
IL1B (IL-1β)	Interleukin-1 beta
LT	Leukotriene
LTA4H	Leukotriene A4 hydrolase
LTB_4	Leukotriene B4

LTB4DH/PTGR1	LTB_4, leukotriene B_4 dehydrogenase/prostaglandin reductase 1
Ltb4r1 (BLT1)	B leukotriene receptor 1
Ltb4r2 (BLT2)	B leukotriene receptor 2
MALDI	Matrix-assisted laser desorption/ionization
MFI	Mean fluorescence intensity
MMDTR	Monocyte/macrophage diphtheria toxin receptor
MMP	Matrix metalloproteinase
MOI	Multiplicity of infection
MRSA	Methicillin-resistant *Staphylococcus aureus*
MyD88	Myeloid differentiation primary response gene 88
NADPH	Nicotinamide adenine dinucleotide phosphate
NFκB	Nuclear factor kappa B
NLRP3/NALP3	NACHT, LRR and PYD domains-containing protein 3
NO	Nitric oxide
NOD	Non-obese diabetic
PAMP	Pathogen associated molecular pattern
PBS	Phosphate buffered saline
PG	Prostaglandin
PLA	Proximity ligation assay
PLA2	phospholipase A2
PPR	Pattern recognition receptor
PS	phosphatidylserine serine

PTAH	Phosphotungstic acid-hematoxylin
qRT-PCR	Quantitative real-time polymerase chain reaction
RNA	Ribonucleic acid
RNS	Reactive nitrogen species
ROS	Reactive oxygen species
Sirpa (SIRPα)	Signal-regulatory protein alpha
SOCS1	Suppressor of cytokine signaling 1
STAT1	Signal transducer and activator of transcription 1
STZ	Streptozotocin
T1D	Type 1 diabetes
T2D	Type 2 diabetes
TLR	Toll-like receptor
TRIF	TIR-domain-containing adapter-inducing interferon-β
TSA	Tryptic soy agar
TSB	Tryptic soy broth
TUNEL	Terminal deoxynucleotidyl transferase dUTP nick end labeling
WT	wild type

INTRODUCTION

Immune system

The immune system encompasses numerous cell types with specialized functions that work together to recognize and respond to microorganisms, self-antigens, and environmental stimuli. These cell types are broadly categorized into the innate or adaptive immune system.

The innate immune system functions as a first line of defense and the cells are the first responders to infection or injury [1]. Skin and mucous membranes serve as mechanical barriers and also produce antimicrobial molecules that prevent harmful microorganisms from colonizing these tissues. During injury or infection, the cells in the tissues (such as keratinocytes, fibroblasts, endothelial cells, and epithelial cells) produce inflammatory mediators. Additionally, hematopoietic innate immune cells (such as monocytes, macrophages, neutrophils, dendritic cells, and NK cells) also produce inflammatory mediators that contribute to inflammation. These cell types function together to quickly eliminate invading pathogens or damaged cells. The various inflammatory mediators and effector functions of innate immune cells are discussed in more detail in the following sections.

It was traditionally considered that innate immune responses were generic to the class of pathogen and do not develop immunological memory. However, more recently, the concept of innate cell memory, also referred as trained immunity, is becoming more appreciated [2]. Innate immune cells, such as macrophages can be primed with a pathogen to induce metabolic reprogramming

or epigenetic changes that can alter their activation to a subsequent infection [3, 4]. Macrophages and dendritic cells are professional antigen presenting cells meaning they process and present antigens on major histocompatibility complexes (MHC) to T cells, which can activate the cells.

The adaptive immune system provides protective immunity. Cells of the adaptive immune system include B cells and T cells. Initial adaptive responses take longer to be activated compared to innate immune responses due to the activation, proliferation, and affinity maturation steps [5]. B cells are professional antigen presenting cells and produce antibodies. Antibodies can neutralize antigens and also enhance phagocytosis of pathogens by macrophages through opsonization. There are two major types of T cells, CD8 cytotoxic T cells and CD4 helper T cells. Cytotoxic T cells are able to directly kill cells, which is important for eliminating infected cells and tumor cells. There are multiple classes of helper T cells, which produce various cytokines that modulate immune responses, such as T regulatory cells that suppress activation and Th1 cells that aid in activating macrophages [6, 7].

There is great importance for the immune system to recognize self from non-self. Recognition of self-antigens contributes to autoimmune diseases, such as type 1 diabetes. Additionally, the activation of these cells and the balance of inflammatory mediators are important for promoting beneficial immune responses. Impaired activation contributes to unregulated inflammation and poor host defense to infections [8-10].

Inflammation

Inflammation is a complex process involving immune cell activation in response to injury or infection **(Figure 1).** This process involves a wide variety of mediators: lipids, chemokines, cytokines, complement factors, and clotting factors.

There are five cardinal signs of acute inflammation: pain, heat or fever, redness, swelling, and loss of function. Injury or infection induces tissue-resident immune cells and endothelial cells to produce inflammatory mediators such as chemokines and cytokines. Cytokines (TNF-α, IL-6 and IL-1α) as well as other mediators (prostaglandins, leukotrienes, and platelet-activating factor) induce vasodilation and stimulate the permeability of blood vessels that cause pain,

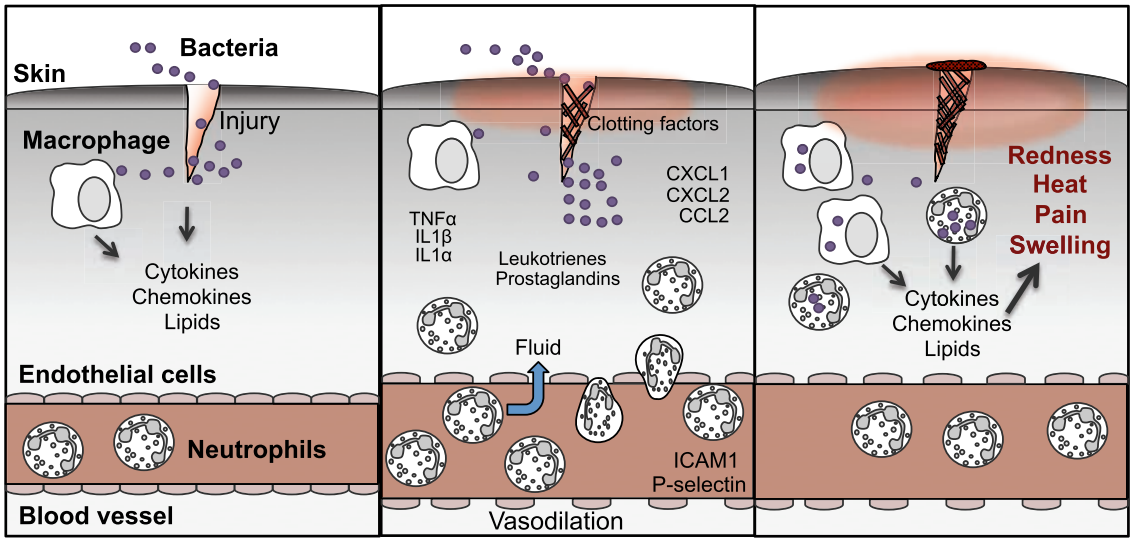

Figure 1. Inflammatory response to bacteria in the skin. Left panel: Macrophages and other cells in skin respond to injury and pathogens by producing inflammatory mediators. Middle panel: Vasodilation promotes fluid accumulation and cell recruitment to the site of infection and injury. Right panel: Innate immune cells destroy invading pathogens and produce more inflammatory mediators, which are responsible for the symptoms of inflammation: Redness, heat, pain, and swelling.

heat, and redness [11, 12]. These responses result in increased blood flow and fluid accumulation, causing swelling. Chemokines (such as CXCL1, CXCL2, and CCL2) recruit neutrophils, monocytes, and other cells to the site of injection/injury [13]. The severity and location of inflammation could result in loss of function such as in instances of extreme swelling or pain. Inflammation is resolved when infection and debris are removed, swelling and redness are eliminated, and tissue remodeling occurs [14].

Inflammation is necessary for regulating physiological homeostasis and promoting immune responses to eliminate invading pathogens and removing damaged cells [15]. Once infection or injury is eliminated, homeostasis is returned. However, certain circumstances alter or delay the onset of inflammation or resolution. These circumstances can result in immunosuppression or chronic inflammation. Infections that fail to be cleared can lead to poor wound healing, autoimmune diseases, and hypersensitivity which are all associated with poorly controlled inflammation [16]. Unbalanced or unregulated inflammation impairs host activation, which can increase susceptibility to infections such as with malnutrition-induced immunosuppression [17] or obesity-induced chronic inflammation [10]. The balance of inflammatory mediators is critical for maintaining homeostasis and for responding to infections.

Innate immunity and phagocytes

Some innate immune system cells are phagocytes: monocytes, macrophages, neutrophils, and dendritic cells. Although many other cells also

participate in innate immune responses, the research goals for this work focus on the roles of macrophages and neutrophils.

Monocytes are immune cells that arise from common-myeloid progenitors from the bone marrow. Monocytes migrate to tissues and differentiate into the tissue-resident macrophages [18]. Macrophages can also arise from the yolk sac or fetal liver and many tissue-specific macrophages proliferate locally to replenish populations in situ [19]. Macrophages reside within tissues and develop specialized functions depending on the tissue-environment. Macrophages exhibit plasticity, meaning that their functions can change depending on microenvironment and activation [20]. It was thought that macrophages are either classically-activated (M1) or alternatively-activated (M2), which promote pro-inflammatory or anti-inflammatory processes, respectively [21]. However, it is more recently appreciated that macrophages have many more functions, which is better represented as a spectrum of macrophage activation and function [22]. At the site of injury or infection, tissue-resident macrophages produce signals, such as chemokines and lipid mediators, to induce the recruitment and activation of other cell types that participate in the inflammatory process. Macrophages are phagocytic cells, meaning that they “eat” or engulf pathogens. Along with pathogens, macrophages are also able to engulf apoptotic cells, a process known as efferocytosis. Macrophages also have anti-inflammatory or resolution functions, which serve to dampen pro-inflammatory signaling and to promote wound healing and tissue repair.

Neutrophils, like monocytes/macrophages, also arise from common myeloid progenitor cells. Neutrophils are the most abundant type of white blood cell in circulation in human blood, comprising 40-60% of leukocytes [23]. In mice, neutrophils make up 10-25% of leukocytes in the blood [24]. In response to infection or injury, neutrophils are typically the first cells to be recruited to the area where they can exert their effector functions. Similar to macrophages, neutrophils are phagocytic cells that can engulf pathogens. Unlike macrophages, neutrophils are granulocytes and contain various types of granules [25]. These granules contain antimicrobial molecules and enzymes and that function to destroy pathogens and degrade extracellular matrix (ECM) molecules [26]. Inside neutrophils, granules fuse with the phagosome to aid in intracellular pathogen killing. Also, granule contents can be released from the cell in a process known as neutrophil degranulation. Neutrophils also produce neutrophil-extracellular traps (NETs), which are DNA and proteases released from the cells that aid in trapping pathogens [27]. Macrophages are also capable of producing extracellular traps, termed METs [28], however these are less characterized than NETs.

Leukotriene synthesis

Leukotrienes (LTs) are part of the large family of lipids termed eicosanoids, which also include prostaglandins and hydroxyeicosatetraenoic acids (HETEs). Eicosanoids are polyunsaturated fatty acids composed of twenty carbons, aptly named from the Greek word “eicosa” meaning twenty. These lipids

are important mediators in amplifying or dampening inflammation and promoting tissue remodeling and wound healing. Eicosanoids are not typically stored within cells, but are produced rapidly after activation.

The synthesis of LTs involves several rate-limiting steps that include activation of phospholipase A_2 (PLA_2) and arachidonic acid (AA) release from phospholipids in cellular membranes **(Figure 2)**. Activation of 5-LO and 5-LO activation protein (FLAP) together metabolize AA to LTA_4, which is converted to LTB_4 by LTA_4 hydrolase (LTA_4H). LTA_4 could alternatively be modified with glutathione by LTC_4 synthase to form LTC_4. Further modifications of LTC_4 give rise to LTD_4 and LTE_4. Since LTC_4, D_4, and E_4 contain cysteine, they are known as the cysteinyl leukotrienes (CysLTs), which are involved in allergy and asthma [29]. The main cellular sources of LTB_4 in both murine and humans are granulocytes, monocytes, and macrophages **(Table 1)** [30]. However, murine (RAW264.7 and J774) and human (THP1 and U937) macrophage cell lines express low levels of 5-LO and produce barely detectable levels of LTB_4, which

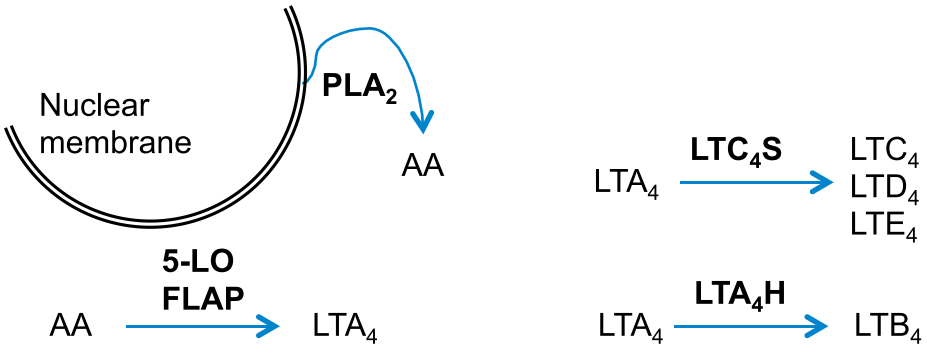

Figure 2. Leukotriene synthesis. PLA_2 releases AA from cellular membranes. AA is metabolized by 5-LO and FLAP to produce LTA_4. LTA_4 is hydrolyzed by LTA_4H to produce LTB_4. LTA_4 is also metabolized by LTC_4S to produce the cysteinyl LTs (LTC_4, LTD_4, and LTE_4).

make these cell lines unsuitable models for LT research [31]. Some cell types, even non-immune cells, have been reported to express some but not all of the LT-synthesis enzymes, which render these cells incapable of synthesizing leukotrienes independently. However, these cells may contribute to the synthesis of LTs in a process known as transcellular biosynthesis [32]. Examples of transcellular biosynthesis of LTB_4 are with neutrophils/erythrocytes and keratinocytes/endothelial cells [33-37]. The capabilities of individual cells types to produce various types of LTs depend on the expression of LT synthesis enzymes **(Table 1).**

5-LO activity relies on various signals including calcium release and phosphorylation, which control the catalytic site and translocation of 5-LO within the cell. In a resting cell, 5-LO location varies depending on the cell type [38]. In

Cell type	5-LO	FLAP	LTA_4 hydrolase	LTC_4 synthase
Neutrophil	+++	+	+++	±
Monocyte/ macrophage	++	+	+++	+
Dendritic cell	+	+	++	+
Mast cell	+	+	+	++
Eosinophil	+	+	+	++
Endothelial cell	-	-	+	+
Red blood cell	-	-	+	-
Keratinocyte	±	-	+	+

Table 1. Expression of LT synthesis enzymes. + indicates relative amounts of enzymes or receptors produced by various cell type. - indicates a lack of expression. ± indicates minimal to no expression.

neutrophils and peritoneal macrophages, 5-LO is located in the cytosol whereas in alveolar macrophages and Langerhans cells, 5-LO is located within the nucleus [39-41]. Upon cell activation, increased intracellular calcium levels induce 5-LO translocation to the perinuclear or cytoplasmic membrane where it can metabolize AA into LTA_4 [42]. 5-LO activity is triggered by various stimuli such as pathogens, cytokines, and immune complexes **(Table 2)** [43]. However, some pathogens are less effective at increasing phagocyte intracellular calcium levels suggesting that these are not effective 5-LO activators alone. Treating infected cells with a calcium ionophore or opsonized particles is able to greatly enhance LT synthesis [44, 45]. The molecular mechanisms that regulate 5-LO activation are reviewed here [46, 47]. While 5-LO metabolites include other lipids such as HETEs and cysteinyl leukotrienes, the research goals presented here focus on the actions of LTB_4.

Cell type	Cytokines/ Growth factors	Bacteria	Opsonized pathogen	Fungi	Viral
Neutrophil	++	++	+++	++	++
Monocyte/ macrophage	++	++	+++	++	++
Dendritic cell	+	++	ND	+	+
Mast cell	+	+	ND	+	+
Endothelial cell	±	±	±	±	±

Table 2. Relative induction of LTB_4 produced in response to various stimuli. + indicates relative amounts of LTB_4 produced in response to various stimuli or receptors produced by various cell type. ± indicates minimal to no production of LTB_4. ND not determined.

Leukotriene B_4 receptors

There are two G protein-coupled receptors for LTB_4, BLT1 and BLT2. BLT1 is the high-affinity receptor and BLT2 is the low-affinity receptor. The distribution of BLT1 and BLT2 on cells and tissues vary between mouse and human [48]. On human cells, BLT1 expression is limited to leukocytes and BLT2 is ubiquitously found on many cell types **(Table 3)**. On mouse cells, BLT1 expression is detected on leukocytes and BLT2 is reported to be limited to intestinal epithelium and keratinocytes [48, 49]. BLT1 can be coupled to Gαi or Gαq that decreases cyclic AMP (cAMP) levels or increases intracellular calcium levels, respectively [50]. LTB_4 activation of BLT1 enhances antimicrobial effector function activities in macrophages and neutrophils **(Figure 3).** The mechanisms

Cell type	BLT1	BLT2
Neutrophil	+	+
Monocyte/ macrophage	+	+
Dendritic cell	+	+
Mast cell	+	+
Eosinophil	+	+
Endothelial cell	+	+
Red blood cell	-	-
Keratinocyte	+	+

Table 3. Expression LTB_4 receptors. + indicates relative amounts of enzymes or receptors produced by various cell type. - indicates no expression detected.

by which LTB_4 enhances phagocyte effector functions mediated through BLT1 signaling are discussed in more detail in the following sections.

Although there are reports that leukocytes in mice do not express BLT2, others have detected BLT2 expression in murine phagocytes [51, 52], but its role in host defense is not well understood. Blocking BLT2 does not influence phagocytosis and killing of *Streptococcus pyogenes* by alveolar macrophages [53], however blocking BLT2 in bone marrow-derived macrophages impairs phagocytosis of *Borrelia burgdorferi* [52]. Also, other lipid mediators have higher affinity than LTB_4 for BLT2. BLT2 plays a beneficial role in skin wound healing through 12-hydroxyheptadecatrenoic acid (12-HHT) actions which mediate TNF-

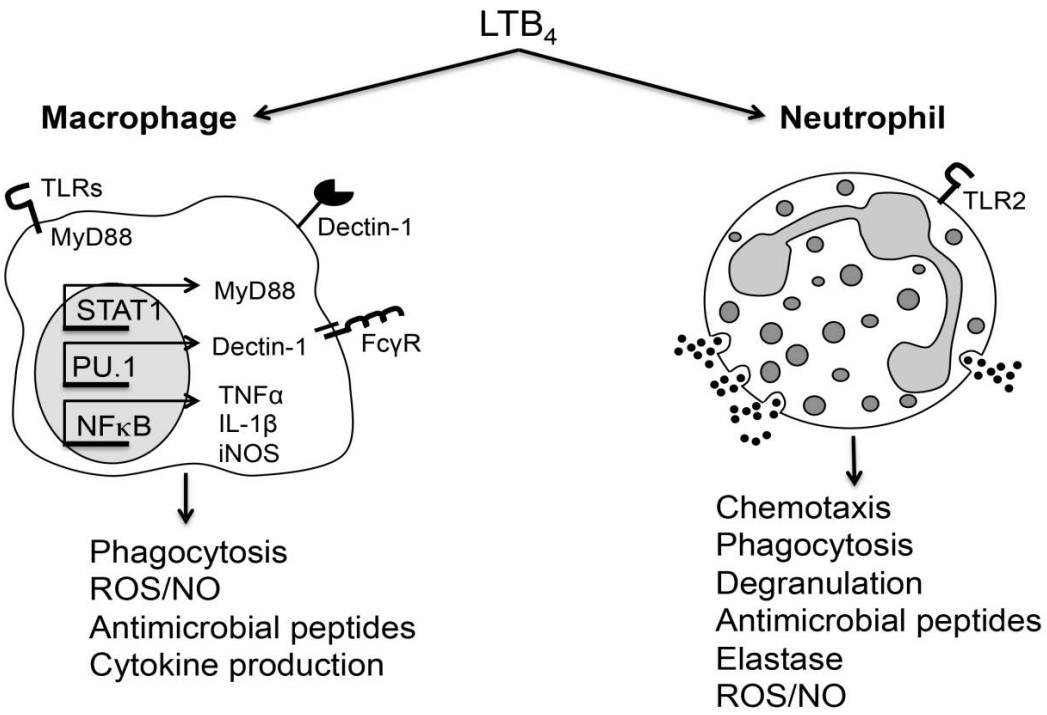

Figure 3. LTB_4 enhances antimicrobial effector functions in macrophages and neutrophils. LTB_4 activation of BLT1 induces expression of PRRs, enhances phagocytosis and killing potency, and induces production of cytokines and antimicrobial peptides.

α and MMP production [48]. 12-HHT has been shown to be important for keratinocyte wound healing in diabetic mice [54]. Additionally 12-HETE and BLT2 effects have been shown to be important for enhancing VEGF expression and promoting wound healing [55]. Although other lipid mediators promote beneficial wound healing responses through BLT2 signaling, less is known about specific LTB_4/BLT2 effects on phagocyte effector functions during infections. The research goals here focus on LTB_4/BLT1 effects.

Pattern recognition receptors and signaling

Innate immune cells use pattern recognition receptors (PRRs) to detect pathogen-associated and danger-associated molecular patterns (PAMPs and DAMPs, respectively). The functions of PRRs include stimulating phagocytosis, inducing production of cytokines and other inflammatory mediators, and facilitating chemotaxis [56].

Toll-like receptors (TLRs) are known to detect both PAMPs and DAMPs. There are 11 TLRs in human and 13 in mouse. TLRs can be found on the cell surface or located within endosomes in the cytoplasm and are activated by different agonists [57]. TLR1/2 and TLR2/6 on the cell surface recognize lipopeptides that are found on gram-positive bacteria [58]. TLR activation is dependent on different adaptors such as myeloid differentiation factor 88 (MyD88) and TIR-domain-containing adapter-inducing interferon-β (TRIF). Most TLRs, except TLR3, utilize MyD88. Only TLR3 and TLR4 utilize TRIF. MyD88 activation is followed by phosphorylation of downstream molecules such as

IRAKs and TAK-1. Signaling cascades activate transcription factors to promote gene expression. Activation of nuclear factor kappa B (NFκB) induces transcription of pro-inflammatory cytokines such as TNF-α and IL-1β [59].

LTB_4 is involved in TLR activation [60-62]. TLR signaling induces pro-inflammatory cytokine responses [57, 63]. LTB_4 stimulation upregulates the expression of TLR2 (cell surface receptor that recognizes peptidoglycan molecules) and TLR9 (endosomal receptor that recognizes DNA) in human neutrophils [64]. Enhanced expression of TLRs could allow for neutrophils to better sense various pathogens and induce a stronger signaling cascade, which allows for a more potent immune response. Furthermore, LTB_4 is also known to amplify the actions of different PRRs. LTB_4 enhances MyD88 expression and MyD88-dependent activation of NFκB, which are able to intensify the signaling potential of TLRs and other PPRs [60]. The mechanisms involved in LTB_4-enhanced MyD88 expression relies on enhancing the activation of signal transducer and activator of transcription 1 (STAT1) [65]. BLT1 activation leads to mRNA degradation of suppressor of cytokine signaling 1 (SOCS1), a major STAT1 negative regulator, which contributes to elevated MyD88 expression and subsequent enhancement of TLR-mediated macrophage activation [60]. Furthermore, it has been shown that LTB_4 amplifies the phosphorylation of IRAK and TAK-1 in human neutrophils [62]. Through TLR and PRR activation, LTB_4 amplifies the induction of cytokine production. LTB_4 is known to induce cytokines and chemokines that have roles in inflammatory responses: GM-CSF, TNF-α, IL-6, IL-1β, CXCL1, MCP-1, and CXCL2 [66, 67].

Migration and chemotaxis

The production of chemokines and lipid mediators after infection or injury induce the migration of cells to the area. Neutrophils are typically the first cells to migrate to the site, followed by monocytes. Neutrophil recruitment from the bloodstream to the site of infection or injury involves a series of events: rolling, chemokine-activation, firm adhesion, and transendothelial migration [68]. Neutrophil rolling involves weak interactions between P-selectin glycoprotein-1 (PSGL-1) and P-selectin on endothelial cells [69]. Chemokine activation induces stronger neutrophil adhesion through activating integrins including intercellular adhesion molecule 1 (ICAM-1) [70]. Neutrophil transendothelial migration occurs when the cells migrate through the tight junctions between endothelial cells and follow chemoattractant gradients.

Once cells migrated to the site of infection or injury, cells must then be directed towards a location. Chemotaxis is the migration of a cell towards a molecular signal. These signals include chemokines, lipid mediators, complement factors, and bacterial peptides. Two major classes of chemokines include the CC (e.g. CCL2 – MCP-1, CCL3- MIP-1α, and CCL5 – RANTES) and the CXC (e.g. CXCL1 – KC and CXCL2 – MIP2α) families. CC chemokines bind to CCR (e.g. CCR2 and CCR7) and CXC chemokines bind to CXCR (e.g. CXCR1 and CXCR2) receptors. Lipid mediators, including leukotriene B_4 (LTB_4) and platelet-activating factor (PAF) are chemotactic molecules for leukocytes. Complement factor C5a and bacterial products *N*-formylmethionine-leucyl-phenylalanine (fMLP) activate innate immune cells and are end-target

chemotactic molecules. Since there are many molecules that are chemotactic for cells, there is a hierarchy of signals that allow cells to prioritize end-target chemoattractants over intermediate signals, such as CXC chemokines and LTB_4 [71].

LTB_4 is well known for its role as a neutrophil chemoattractant from distant sites to the site of inflammation [72-74]. LTB_4 is also chemotactic for other cells such as cytotoxic CD8 effector T cells [75], dendritic cells [76], and monocytes [77]. Also, LTB_4 participates with chemokine gradients to further enhance neutrophil chemotaxis towards other chemoattractants such as fMLP, C5a, and heme [78-80], aiding to guide cells to end-target signals and promote neutrophil accumulation. Directed neutrophil accumulation and clustering is termed swarming. *Ltb4r1*$^{-/-}$ neutrophils have smaller neutrophil clusters than wild type (WT) neutrophils [81], demonstrating the importance of LTB_4/BLT1 signaling in neutrophil accumulation. Additionally, neutrophil recruitment is not unidirectional. Reverse transendothelial migration has been reported where neutrophils reenter the blood stream after migration to the site of infection or injury [82]. In a model of ischemia-reperfusion injury, LTB_4 and neutrophil elastase create an important axis that drives reverse transendothelial migration. Neutrophils that reenter the vasculature are able to migrate to secondary organs and have the potential to cause injury [83].

Phagocytosis

Phagocytosis is the engulfment of pathogens or other insoluble materials [84]. Phagocytosis receptors detect pathogen particles and stimulate phagocytosis. There are different receptors that recognize various particulates. C-type lectin receptor family members include dectin-1 and mannose receptor, which recognize sugar molecules that are cell wall components found in fungi, bacteria, and viruses [85]. Other phagocytic receptors include scavenger receptors, including MARCO which recognizes bacterial ligands [86], and CD36 which recognizes microbial ligands as well as lipoproteins and phosphatidylserine (PS) found on the surface of dead cells [87]. Additionally, phagocytosis can be enhanced with opsonins that coat the surface of the pathogen, such as antibodies and complement proteins. Antibodies and complement proteins are recognized by Fc receptors (FcR) and complement receptors that stimulate phagocytosis [88].

Engulfment is an actin-dependent process mediated by F-actin polymerization [89]. The cytoskeleton of the phagocyte surrounds the particulate forming a phagocytic cup. Engulfed pathogens are internalized into the phagosome. Phagosomes are fused with lysosomes, which contain digestive enzymes, and form the phagolysosome [90]. The phagolysosome acidifies, which activates enzymes that degrade pathogens and cellular debris. These digested particles can be loaded and presented on MHC proteins or released from the cell by exocytosis [91, 92].

LTB_4/BLT1 signaling amplifies the actions of different signaling components required for ingestion of particles. The first demonstration that LTB_4 enhances phagocytosis was shown by Wirth et al using a model of *Trypanosoma cruzi* infection [93]. After this, Dr. Peters-Golden's group pioneered in demonstrating the role of endogenous LTs in amplifying phagocytosis of antibody-opsonized targets [94, 95]. Both genetic and pharmacologic blockage of LTB_4/BLT1 actions greatly reduces ingestion of a myriad of pathogens, including both gram-positive bacteria (*Streptococcus pneumoniae* [53]), gram-negative bacteria (*Klebsiella pneumoniae* [96]), fungi (*Histoplasma capsulatum* [97, 98], *Candida albicans* [99], and *Paracoccidioides braziliensis* [100]), and parasites (*Leishmania braziliensis* [101], *L. amazonensis* [102], and *T. cruzi* [93, 103]).

The molecular mechanisms involved in LTB_4-mediated amplification of phagocytosis have been studied. BLT1 signaling enhances activation of Syk, a protein tyrosine kinase, important for FcγR-mediated phagocytosis [43, 50]. When macrophages are challenged with opsonized-targets, LTB_4 enhances phagocytosis of opsonized red blood cells in an FcγR1-dependent manner. This enhancement is attributed to the association of BLT1 with lipid raft formation and heightened signaling capabilities [104]. Furthermore, LTB_4 amplifies phagocytosis by increasing phosphorylation of kinases involved in the formation of a phagocytic cup, such as PKC-α, PKC-δ, PI3K, and ERK1/2 [105, 106]. However, the hierarchical role of these kinases in amplifying phagocytosis remains to be determined. It has been shown that LTB_4 enhances *C. albicans* phagocytosis via activation of Gαi-mediated PKC-δ and PI3K activation resulting

in F-actin polymerization [107]. LT enhancement of yeast phagocytosis involves the activation of PKC and PI3K, with subsequent activation of LIM kinase, decreased cofilin-1 activation, and ultimately, F-actin polymerization [107]. Furthermore, LTB_4 enhances phagocytosis of fungi by increasing the expression of dectin-1, a main phagocytic receptor detecting fungal pathogens [97]. LTB_4-mediated dectin-1 expression is dependent on GM-CSF production and activation of the transcription factor PU.1 [99].

Antimicrobial activity

Antimicrobial effector functions are necessary for destroying and killing pathogens. These functions include the production of antimicrobial peptides, reactive oxygen species (ROS), reactive nitrogen species (RNS), and antimicrobial activity facilitated by cytokines, such as inflammasome activation and IL-1β production.

Antimicrobial peptides include cathelicidins, LL37 found in human and the mouse homolog cathelicidin-related antimicrobial peptides (CRAMP), and defensins. These peptides interact and disrupt bacterial membranes. Neutrophils kill pathogens by producing toxic components within granules that are released in a process known as neutrophil degranulation [108]. When human neutrophils are infected in vitro with the parasite *L. amazonensis*, endogenous and exogenous LTB_4 promotes neutrophil degranulation [102]. Also, LTB_4 induces release of myeloperoxidase [109] and elastase in neutrophils [83, 110]. LTB_4 treatment in mice infected with influenza virus induced production of antimicrobial peptides

including β-defensins and CRAMP [111]. In human neutrophils, LTB_4 induces the production of LL37 in a dose-dependent manner [112].

ROS species include superoxide and hydrogen peroxide. The major source of ROS in phagocytes is through nicotinamide adenine dinucleotide phosphate (NADPH) oxidase activity. NADPH oxidase is composed of several subunits: $gp91^{phox}$ and $gp22^{phox}$ are membrane bound subunits and $gp47^{phox}$, $p40^{phox}$ and $p67^{phox}$ are cytosolic subunits. Once activated, the cytoplasmic subunits and Rac GTPase translocate and associate with the membrane bound subunits. NADPH activity generates superoxide (O_2^-). NADPH oxidase is an important complex and the functions are necessary for eliminating infections. Defects in these enzymes or activity greatly increase susceptibility to infections. People with the genetic disease chronic granulomatous disease (CGD) have defective NADPH oxidase functions, which prevent the ability to effectively eliminate infections. LTB_4 enhances the production of NADPH oxidase-dependent ROS generation in phagocytes [113, 114]. LTB_4 enhances NADPH oxidase activation via phosphorylation of the cytosolic subunit $p47^{phox}$ that is dependent on PKC-δ [114], ERK-1/2 and PI3K activation [115]. LTB_4 is part of a positive-feedback loop in human neutrophils infected with *L. amazonensis,* which is important to kill parasites [102]. LTB_4-mediated ROS production in macrophages is dependent on PKC-δ-mediated $p47^{phox}$ and $p40^{phox}$ phosphorylation and membrane translocation in alveolar macrophages challenged with opsonized *K. pneumonia* [106]. Furthermore, aerosolized LTB_4

increases p47^{phox} expression and membrane translocation during *Streptococcus pneumoniae* lung infection [116].

Nitric oxide (NO) is a major reactive nitrogen species (RNS) and is produced from nitric oxide synthase. NO has various functions that include antimicrobial activity and anti-tumor activity [117]. NO induces smooth muscle cells to contract, resulting in vasodilation. Additionally, NO is also involved in regulating cytokine production and immune cell activation. LTB_4-dependent RNS production is dependent on NFκB and STAT1 activation [101]. LTB_4 treatment further enhances the production of NO in murine macrophages, which improves killing of different pathogens such as *L. amazonensis* and *T. cruzi* [106, 118].

Other antimicrobial activity functions are a result of cytokine production, such as IL-1β. IL-1β is produced as an inactive pro-IL-1β, which requires maturation to be functional. The NLRP3 inflammasome is a major mechanism that processes IL-1β and facilitates antimicrobial activities and enhances immune effector functions [119]. In a model of monosodium urate (MSU)-induced gout, LTB_4 was shown to mediate inflammasome activation [120]. NLRP3 inflammasomes are multi-subunit protein complexes involving NLRP3, ASC, and caspase-1. Once assembled, caspase-1 is activated and cleaves pro-IL-1β to form mature IL-1β. Effective IL-1β processing by NLRP3 requires two signals: 1) TLR activation to induce expression of *Il1b* and 2) activation signal to induce inflammation assembly and activity. Alternatively, IL-1β can also be processed in noncanonical NLRP3 activation, mediated through caspase-11 activation. Also, IL-1β can be processed via inflammasome-independent mechanisms by serine

proteases from neutrophils and bacterial proteases [121]. The majority of IL-1β produced in the skin of *S. aureus* infected mice is processed primarily through NLRP3 inflammasome activity as opposed to non-canonical inflammasome activation or inflammasome-independent processes [122].

Methicillin-resistant *Staphylococcus aureus*

Staphylococcus aureus is a gram-positive bacterium and is commonly found as part of normal human skin microbiota in ~30-50% of the population. Often referred as an opportunistic pathogen, *S. aureus* colonization can occur asymptomatically. However, if presented an opportunity, such as through a break in the skin, inhalation, or ingestion, *S. aureus* can cause symptomatic infections.

Antibiotic resistant strains have emerged which pose a challenge to effectively treat infections caused by these pathogens. A notable example is methicillin-resistant *S. aureus* (MRSA). MRSA infections were traditionally limited to hospital settings but community-acquired MRSA (CA-MRSA) strains emerged [123]. In addition to antibiotic resistance, some CA-MRSA strains such as USA300 produce more potent virulence factors, which enable these strains to cause infections in otherwise healthy individuals [124-126]. These virulence factors can induce tissue damage, which can cause more severe infections [125]. Infections with MRSA strains, especially in immunocompromised hosts, pose a serious public health risk.

The development of other strategies to treat antibiotic-resistant infectious diseases is greatly needed. One strategy includes immunomodulatory therapies,

which enhance or suppress immune responses leading to improved host defense mechanisms [127]. The mediators involved during inflammation may provide a target for immunomodulatory therapies to promote or restrain immune activation in various settings of infectious diseases or chronic inflammatory diseases.

Skin biology and immune response to *S. aureus*

The skin is composed of the epidermis and the dermis, and serves as an immune barrier preventing pathogen entry. Keratinocytes form the outer layer of the epidermis. The inner layer of the skin, the dermis, contains extracellular matrix proteins (ECM), blood vessels, subcutaneous adipose tissue, fibroblasts, and tissue-resident immune cells including macrophages.

Keratinocytes produce antimicrobial peptides, which provide a chemical barrier to pathogens. The epidermis also serves as a mechanical barrier preventing entry of harmful pathogens. During infection, the tissue-resident cells along with keratinocytes produce cytokines, chemokines, and lipids, which aid in the recruitment of immune cells to the site of infection. Neutrophils are recruited in to the site and promote the development of an abscess. Abscesses develop in stages: cell death surrounded by live neutrophils, all encapsulated with a fibrous material [128].

Cell death is another common characteristic of *S. aureus* skin infections. MRSA produces toxins, such as panton-valentine leukocidin (PVL) that is a pore forming toxin that induces necrosis and apoptosis [124]. The dead cells and other debris require clearance by phagocytes, which is a processed called

efferocytosis. The removal of apoptotic cells by macrophages typically does not activate immune responses. However, if apoptotic cells are not cleared properly, they can become necrotic and secrete DAMPs, further stimulating inflammation. Ingestion of necrotic cells by macrophages can activate different cell functions compared to ingestion of apoptotic cells. Necrotic-neutrophil uptake by macrophages enhances MHC presentation and T cell activation, which does not occur with apoptotic-cell ingestion [129]. After infection and debris are eliminated, fibroblasts and macrophages produce molecules to aid in the ECM remodeling.

Aberrant LTB_4 and poor host defense

Chronic inflammatory morbidities are accompanied by aberrant LTB_4 production and high production of inflammatory cytokines. Diseases in which LTB_4 plays a detrimental role include type-1 and type-2 diabetes, arthritis, and atherosclerosis [130-136]. LTB_4 has beneficial roles in promoting antimicrobial effector functions in phagocytes, but the bad reputation of LTB_4 comes from its capacity to maintain inflammatory programs in monocytes and macrophages and prolonging neutrophil recruitment to the inflammatory foci. LTB_4/BLT1 blockade is expected to dampen inflammatory responses and restore tissue homeostasis during chronic inflammation.

Besides increased production of LTB_4, chronic inflammatory diseases are often associated with co-morbidities, including the major threat of increased susceptibility to infections. Although LTB_4 plays a beneficial role in promoting pathogen clearance, the counterintuitive effect of LTB_4 in chronic inflammatory

diseases could be explained by the overwhelming inflammatory response and lack of proper phagocyte response to pathogens. Abundant LTB_4 production and detrimental host defense responses have been associated in a zebrafish model of *Mycobacterium marinum* infection. The authors showed that LTA_4 hydrolase (LTA4H), the enzyme that converts LTA_4 to LTB_4, is an important susceptibility factor involved in Mycobacterium infection. Zebrafish expressing hyperactive LTA4H are hypersusceptible to *M. marinum* infection [137]. Additionally, overexpression of LTA4H produces high levels of LTB_4 that drive aberrant TNF-α production and uncontrolled mycobacterial infections [138]. Furthermore, zebrafish expressing the enzyme that inactivates LTB_4, leukotriene B_4 dehydrogenase/prostaglandin reductase 1 (LTB4DH/PTGR1), exhibit lower bacterial numbers than WT zebrafish. The susceptibility to infection of LTB4DH mutant animals can be reversed with BLT1 antagonism, further implicating LTB_4 as detrimental to host defense during Mycobacteria infection in zebrafish [139].

Exaggerated LTB_4 is also detrimental to systemic infection such as sepsis. *Alox5*$^{-/-}$ mice or pharmacological inhibition of BLT1 protect mice during cecum ligation and puncture (CLP). *Alox5*$^{-/-}$ mice and WT mice treated with a LT synthesis inhibitor, AA861, have drastically lower levels of neutrophil infiltrates and lower levels of inflammatory cytokines such as IL-1β in the peritoneal cavity [140]. During CLP-induced sepsis, treatment with the BLT1 antagonist U-75302 decreases lung injury [141] as evidenced by decreased neutrophil recruitment. Therapeutically regulating 5-LO products or blocking BLT1 during or after sepsis may help prevent organ injury.

Diabetes

Diabetes represents a family of diseases characterized by an inability to produce insulin or reduced sensitivity to insulin signaling. Insulin is a hormone produced from pancreatic β cells that aids in regulating blood glucose levels. Insulin signaling through the insulin receptor induces muscle and adipocytes to express glucose transporters on the cell surface, which in turn induces the uptake of glucose by these cells thereby reducing blood glucose levels.

There are two major types of diabetes, Type 1 (T1D) and Type 2 (T2D). T1D is an autoimmune disease in which the insulin-producing pancreatic β cells are targeted for destruction. T1D is associated with the development of autoreactive T cells and production of autoreactive antibodies. People with T1D are typically diagnosed in adolescence. The lack of insulin requires T1D patients to take recombinant insulin to help regulate blood glucose levels. The exact cause of T1D is not well understood. There is likely a genetic component but other factors such as viral infection or other environmental factors may also be involved [142]. People with T2D are typically in adulthood when diagnosed and the disorder is often associated with obesity. T2D is caused by insulin resistance, in which insulin receptor signaling is no longer effective at regulating blood glucose levels. Pancreatic β cells produce more insulin to compensate for the insulin resistant tissues. However, β cells can become fatigued and fail to produce insulin. Treatments for people with T2D include medication to improve insulin receptor sensitivity or to reduce blood glucose levels.

Diabetes and infection risk

Uncontrolled hyperglycemia is often associated with numerous co-morbidities such as neuropathy, kidney disease, eye disease, and risk for infections. People with diabetes, including both T1D and T2D, are more susceptible to developing infections that affect the lung, urinary tract infections, and skin and soft tissue infections [143, 144]. Diabetic foot ulcers that fail to heal often require amputation [145]. Infections and wounds inflicting skin and soft tissues take significantly longer to heal, and have the risk of developing polymicrobial infections. There is an additional risk of infections disseminating to other organs that can cause life-threatening infections such as sepsis, osteomyelitis, and endocarditis.

Phagocytes from people with diabetes are reported to have impaired function. Poor respiratory burst and defective phagocytosis are associated with poor bacterial clearance. Immune cells from mice and rats with diabetes are reported to have poor phagocytosis and cytokine production [146-148]. Others suggest that neutrophils in people with diabetes have poor recruitment to the site of infection or injury, contributing to the susceptibility to infections [149].

Since people with diabetes are more susceptible to infections, an initial hypothesis would be that people with diabetes produce lower levels of inflammatory mediators, which promote host defense. However, many of these mediators, such as LTB_4, promote host defense mechanisms by boosting inflammation. Since diabetes is associated with chronic low-grade inflammation, the levels of inflammatory mediators are altered even in the absence of infection.

The role of these inflammatory mediators in infections complicated with diabetes is unknown. Along with other inflammatory mediators, LTB_4 levels are higher in the serum of mice and people with diabetes [150]. A better understanding on how diabetes alters immune functions could allow for the development of new therapies to restore host defense in this vulnerable population to prevent infection risk and severity.

Research goals

The ability to regulate inflammation is critical for maintaining homeostasis and promoting effective immune responses during infection. However, chronic inflammatory diseases alter the homeostatic levels of these mediators that contribute to low-grade inflammation, including elevated LTB_4 levels. Diabetes is a chronic inflammatory disease and is a risk factor for comorbidities including enhanced susceptibility to infections. The hypothesis for this work is that the threshold of LTB_4 production determines the outcome of MRSA skin infection. This hypothesis was tested by investigating the role of LTB_4 during MRSA skin infection under both homeostasis and diabetes-like conditions.

Due to the immunostimulatory effects of LTB_4, one research goal was to evaluate its role in orchestrating the immune response to MRSA skin infection in wild type (WT) C57BL/6 mice. For this goal, the aims were to: 1) determine whether endogenously produced LTB_4 promotes host defense mechanisms, 2) determine the role of skin resident macrophages in MRSA skin infection, and 3)

evaluate the effectiveness of topical LTB_4 application as use as an immunotherapeutic strategy for treating MRSA skin infection.

The second research goal was to evaluate the role of LTB_4 in MRSA skin infections in mice with a disease model that exhibit exaggerated LTB_4 levels, such as diabetes. The aims in this goal were to: 1) determine how excessive LTB_4 levels in the skin drive overwhelming inflammation in diabetic mice, 2) determine the role of tissue macrophages on LTB_4 production during MRSA skin infection, and 3) evaluate the therapeutic potential of blocking BLT1 actions in diabetic mice during MRSA skin infection.

This work highlights the importance of studying inflammation and the mediators that regulate immune responses. Targeting LTB_4/BLT1 has therapeutic potential for enhancing or dampening inflammation as necessary. This suggests that people who are immunocompromised may benefit from exogenous LTB_4 treatment. Conversely, people with chronic inflammatory diseases may benefit from BLT1 antagonist treatment. This treatment strategy may help restore host defense mechanisms during infections.

MATERIALS AND METHODS

Mice

Mice were purchased through Jackson Mice or were donated from other investigators. *Lys*^{EGFP} mice were a gift from Dr. Nadia Carlesso (City of Hope, Duarte, CA) and pIL1DsRED mice were a gift from Dr. Akiko Takashima (University of Toledo, Toledo, OH). Colonies of mice were bred and maintained at Indiana University School of Medicine in Indianapolis, IN or Vanderbilt

Strain	Information	Reference
C57BL/6	Wild type (WT) mice	Jackson Laboratory
Ltb4r1$^{-/-}$	LTB4 Receptor 1 total knockout (C57BL/6 background)	Jackson Laboratory
Alox5$^{-/-}$	5-lipoxygenase total knockout (C57BL/6 background)	Jackson Laboratory
pIL1DsRED	Il1beta reporter mouse expressing DsRED (C57BL/6 background)	[151]
Cybb$^{-/-}$	Total knockout for gp91^{phox} (membrane bound subunit of NADPH oxidase) (C57BL/6 background)	Jackson Laboratory
MMDTR	*Csf1rL*$^{LsL\text{-}DTR\text{-}mCherry}$ crossed with *LysM*^{cre} Monocyte-macrophage DTR-mCherry (C57BL/6 background)	Parent strains available at Jackson Laboratory [152]
Lys^{EGFP}	*LysM*^{EGFP} Myeloid lineage express GFP (C57BL/6 background)	[153]
NOD	Non-obese diabetic (type 1 diabetes mouse model).	Jackson Laboratory

Table 4. List of mouse strains.

University Medical Center in Nashville, TN. All experimental procedures were approved by the Institution Animal Care and Use Committee (IACUC) at Indiana University or Vanderbilt University Medical Center. Mouse strains utilized are listed in **Table 4.**

C57BL/6 and NOD mouse colonies were maintained by breeding brother-sister mating pairs. *Ltb4r1*$^{-/-}$, *Alox5*$^{-/-}$, and *Cybb*$^{-/-}$ mouse colonies were maintained by breeding homozygous knockout brother-sister mating pairs to maintain homozygosity.

pIL1DsRED mice are *Il1b* reporter mice that have a DsRED construct under the promoter of *Il1b* [151]. C57BL/6 mice were bred with pIL1DsRED heterozygous mouse to maintain heterozygosity, which was determined by genotyping for DsRED by PCR. Littermate controls lacking DsRED were used as non-fluorescent controls.

Monocyte/macrophage diphtheria toxin receptor (MMDTR) mice are *Csfr1*$^{LsL\text{-}DTR\text{-}mCherry}$*_LysM*^{cre} [152]. *Csfr1*$^{LsL\text{-}DTR\text{-}mCherry}$ mice have a construct containing a floxed stop codon followed by diphtheria toxin receptor (DTR) and mCherry which is under the *Csfr1* gene. When bred with *LysM*^{cre} mice, cre expressed in monocytes and macrophages excise the floxed stop codon, which allows for expression of the DTR-mCherry fusion protein. MMDTR mice allow for the detection of monocytes/macrophages by mCherry fluorescence and specific cell ablation when mice are treated with diphtheria toxin (DT). Mice containing the floxed stop codon-DTR-mCherry construct but lacking cre expression were used as controls.

Lys^{EGPF} mice express enhanced green fluorescent protein (EGFP) in all myeloid cells [153]. Mouse colonies were maintained by breeding brother-sister pairs that are GFP^{+}. Mice were monitored for GFP fluorescence by collected a drop of blood from tail vein puncture and analyzing cells by flow cytometry or by genotyping for GFP by PCR.

MRSA preparation

The MRSA USA300 LAC strain was a gift from Dr. Bethany Moore (University of Michigan, Ann Arbor, MI) [154]. The bioluminescent USA300 (NRS384 lux) strain was a gift from Dr. Roger Plaut (Food and Drug Administration, Silver Spring, MD) [155]. The GFP-expressing USA300 strain was a gift from Dr. William Nauseef (University of Iowa, Iowa City, IA) [156]. MRSA stocks were stored in the -80°C freezer. Frozen MRSA aliquots were transferred to a 50mL conical tube containing 10mL tryptic soy broth (TSB) and allowed to incubate overnight shaking at 200rpm at 37°C with a loose cap to generate a saturated culture. The following day, the saturated culture was sub-cultured 1:100 (100µL of culture into 10mL new TSB in 50mL conical tube) and allowed to shake at 200rpm for 3 hours at 37°C. To determine bacterial density, the culture was diluted 1:10 in TSB and the OD_{600} was measured and compared to the growth chart that was previously generated for each MRSA strain **(Table 5)**. The growth chart was created by measuring the OD_{600} on 2-fold serial dilutions from a saturated culture of MRSA. Each sample in the 2-fold series was further diluted by 10-fold serial dilutions and spotted onto tryptic soy agar (TSA)

plates to determine the colony forming units. A chart of OD_{600} on the y-axis vs. CFU/mL on the x-axis was created and used to estimate bacterial density in future experiments.

According to the growth chart, a minimum of $1x10^9$ bacteria was centrifuged in a 1.5mL tube at 12,000g for 10 minutes at 4°C. Supernatant was carefully removed and bacteria was resuspended in 1mL PBS and centrifuged as before to wash bacteria. Bacteria were washed twice. Following final wash, bacteria were resuspended in 1mL sterile PBS for $1x10^9$ MRSA/mL. For MRSA skin infections, the washed MRSA preparation was diluted to $1x10^8$ MRSA/mL in PBS. For in vitro assays, the washed MRSA preparation was diluted to $1x10^8$

OD_{600}	CFU/mL
2.593	$3.58x10^9$
2.005	$1.94x10^9$
1.370	$8.50x10^8$
0.803	$3.71x10^8$
0.437	$2.71x10^8$
0.219	$1.60x10^8$
0.117	$8.53x10^7$
0.055	$3.52x10^7$
0.027	$2.33x10^7$
0.013	$9.22x10^6$
0.006	$3.92x10^6$
0.002	$1.96x10^6$

Table 5. MRSA growth chart. OD_{600} readings and corresponding CFU/mL used to estimate bacterial density.

MRSA/mL in PBS. Bacteria preparations used for MRSA skin infections were serially diluted and plated onto TSA plates to determine actual infection inoculum.

In order to generate heat-killed MRSA (HK-MRSA), MRSA was pelleted, washed in PBS, and resuspended in $1x10^9$ MRSA/mL. Bacteria was heat-killed by incubating tubes on a heating block at 60°C for 1 hour. In order to confirm bacterial killing, HK-MRSA was plated onto TSA plates.

MRSA skin infection model

Murine skin infection model was adapted from [157]. Male and female mice between 6-12 weeks of age were used for MRSA skin infection. Fur from the back of mice was removed with a fur trimmer, cleansed with 70% ethanol, and injected with 50µL of approximately $1x10^8$ MRSA/mL subcutaneously using a 1mL syringe and 30G1/2 needle to aim for approximately $3x10^6$ MRSA to infect. Infection areas were measured with a caliper and areas were calculated by area X width for mm^2. Biopsies and sample collection were taken at various times after infection ranging from 6 hours to 9 days post infection. To collect biopsy samples, mice were euthanized with CO_2. The exterior of the skin was cleansed with 70% ethanol, allowed to dry, and a 8mm-diameter biopsy punch was used to collect the infected area of skin (or naive skin, for uninfected controls). Biopsy punches were sectioned and processed for the following analyses: histology, RNA for qRT-PCR, cytokine for enzyme immune assay (EIA)/enzyme-linked immunosorbant assay (ELISA)/multiplex, bacterial burden colony forming units

(CFU) counts, dissociation for flow cytometry analysis, sample prep for eicosanoid core mass spectrometry analysis, or sample prep for MALDI analysis. Processing methods for these various samples are described in more detail in the following sections.

Immunohistochemistry of skin biopsy sections

Histology samples were collected by 8mm biopsy bunch. Tissue was fixed overnight in 100µL 4% paraformaldehyde and transferred to 70% ethanol for storage prior to paraffin embedding. Paraffin embedding and sectioning was performed at the histology core at Indiana University School of Medicine or at the Translation Pathology Resource Core (TPSR) at Vanderbilt University. Tissue staining for the following stains were performed at the Vanderbilt TPSR core: H&E, Masson's trichrome blue for collagen, Phosphotungstic acid-hematoxylin (PTAH) for fibrin and collagen, F4/80 IHC for macrophage, Ly6G/C IHC for neutrophil, and gram stain for bacteria. Slides were visualized and pictures acquired on Nikon Eclipse Ci and camera Nikon Ds-Qi2.

IHC for 5-LO was performed on 5µm paraffin-embedded sections by the following steps: 1) Deparaffinized tissue with sequential washes in xylene, 100% ethanol, 95% ethanol, 70% ethanol, 50% ethanol, and water. Slides were incubated for 2 minutes in each buffer. 2) Antigen exposure in Tris-EDTA buffer (10mM Tris base, 1mM EDTA, 0.05% Tween 20, pH 9.0) by submerging slides in the buffer in plastic slide holder. Slides were heated in a microwave for 20 minutes. Slides were washed in Tris buffered saline (TBS) + 0.025% Triton-X. 3)

Slides were blocked with Vectastain blocking serum (provided in VectaLabs Vectastain ABC kit) for 2 hours at room temperature. 4) Blocking solution was removed and primary antibody to 5-LO (1:100 dilution) in TBS + 1% BSA was added and incubated overnight at 4°C. 5) Washed three times in wash buffer as described in step 2. Endogenous peroxidase activity was quenched in 0.3% hydrogen peroxide for 15 minutes. Slides were washed as before. 5) Using Vectastain ABC kit, added biotinylated antibody for slides for 1 hour at room temperature. Slides were washed as before. 6) Added ABC reagent to slides (from VectaLabs Vectastain ABC kit) and incubated for 30 minutes at room temperature. Slides were washed as before. 7) Developed slides with 3,3'-diaminobenzidine (DAB) (Sigma) and reaction was stopped with water. 8) Slides were counterstained with hematoxylin (Sigma) for 1-5 minutes. Slides were rinsed in water. 9) Tissues were dehydrated in sequential washes in water, 50% ethanol, 70% ethanol, 95% ethanol, 100% ethanol, and xylene. Slides were incubated in each buffer for 2 minutes each. 10) Slides were mounted with Organo/limonene (Sigma) mounting medium and sealed with a glass coverslip and allowed to air-dry overnight.

Quantification of collagen thickness was performed in ImageJ. The scale bar was used to calibrate the measurement scale. A line was drawn over the edge of the collagen border surrounding the abscess and measurement taken. Quantification of cells in the skin were performed in ImageJ. Images were converted to 8-bit and adjusted the image threshold. Cells were quantified by analyzing particles by setting the size threshold for 10-15μm. Quantification of

fluorescence intensity was performed in ImageJ. An area was drawn around the cell and the mean area integrated intensity was measured. Background was determined by measuring the mean fluorescence intensity of a region next to the cells with no fluorescence. Background values were subtracted from the cell fluorescence values.

Immunofluorescence staining. Frozen tissue sections were blocked with 3% BSA in PBS. Sections were labeled with 1:100 dilution of Ly6G-AlexaFluor 594 (Biolegend) overnight at 4°C, washed with PBS + 0.005% Tween 20 for 5 minutes for 3 washes. Tissues were mounted with ProLong Gold Antifade Mountant with DAPI (Thermo Fisher Scientific). Apoptotic cells were labeled with fluorescein isothiocyanate (FITC) by TUNEL staining kit (Millipore) following manufacturer's instructions (Millipore). After staining, tissue sections were counterstained and mounted in ProLong Gold Antifade Mountant with DAPI (Thermo Fisher Scientific) and sealed with a coverglass. Slides were visualized and pictures acquired on Nikon Eclipse Ci with filters for DAPI, GFP, and Texas Red and camera Nikon Ds-Qi2.

RNA isolation and gene expression analysis (qRT-PCR)

Skin biopsy sections for RNA isolation were homogenized in 400μL RLT buffer (Qiagen) + β-mercaptoethanol. Tissue was homogenized with a disposable pestle (Bel-Art) compatible with 1.5mL tubes. Samples were centrifuged at 12,000g for 10 minutes at 4°C to pellet cell debris. Supernatant was transferred to a new 1.5mL tube + 400μL of isopropanol. Samples were

incubated on a rocker at room temperature for 10 minutes. Samples were spun at 12,000g for 10 minutes at 4°C to pellet RNA. Supernatant was discarded and RNA pellets were washed with 800µL of 75% ethanol. Samples spun at 12,000g for 10 minutes at 4°C to pellet RNA. Supernatants were discarded and excess ethanol was evaporated prior to resuspending RNA in 50µL of nuclease-free water.

Isolated RNA samples were used to make cDNA with BioRad iScript following kit-provided instructions. The cDNA samples were used to run qRT-PCR on the BioRad CFX-Connect system using BioRad sybr green following kit-provided instructions. List of primers (IDT) utilized are listed in **Table 6.**

Gene	Protein name	Primer name
Actb	β-actin	Mm.PT.39a.22214843
Alox5	5-LO	Mm.PT.58.30176779
Ltb4r1	BLT1	Mm.PT.58.29472157
Ltb4r2	BLT2	Mm.PT.58.42703902
Il1b	IL-1β	Mm.PT.58.41616450
Cd36	CD36	Mm.PT.58.7548967
Cd47	CD47	Mm.PT.58.5992165
Sirpa	Sirpα	Mm.PT.58.41676998

Table 6. List of primers for qRT-PCR. Primers from IDT Primetime.

Multiplex and EIA/ELISA

Skin biopsy sections were homogenized in TNE cell lysis buffer containing 1x protease inhibitor (Sigma). Samples were homogenized with a pestle and centrifuged at 12,000g for 5 minutes at 4°C to pellet insoluble debris. Supernatant was transferred to a new tube. Skin biopsy homogenates were diluted 1:2 in diluent buffer provided in the kit (R&D). A custom 19-panel

magnetic bead multiplex array was designed and purchased through R&D **(Table 7).** The kit also provided materials for standards, wash buffer, and antibody reagents. Plates were read and analyzed with BioRad Bio-Plex Magmix reader.

For detection of IL-1β ELISA (R&D), skin biopsy homogenates were diluted 1:4 or 1:10 in assay diluent following manufacturer's instructions. Skin biopsy homogenates for LTB_4 EIA (Cayman) were diluted 1:10 in assay diluent following manufacturer's instructions. Assay plates were read and analyzed on Molecular Devices Spectramax M3 and SoftMax Pro software.

Analyte	Bead region
CCL2/MCP-1/JE	BR18
CCL4/MIP-1β	BR51
CCL7/MARC	BR39
CCL8/MCP-2	BR38
CXCL1/KC	BR13
CXCL2/MIP-2	BR20
ICAM-1	BR35
IFN-γ	BR33
IL-1α	BR47
IL-1β	BR19
IL-12 p70	BR15
IL-33	BR43
MMP-12	BR73
MMP-8	BR61
MMP-9	BR62
P-Selectin	BR46
RAGE	BR78
TIM-1/KIM-1	BR72
VEGF	BR21

Table 7. R&D 19-panel magnetic bead multiplex assay. BR = bead region**.**

Bacterial burden in skin

Bacterial burdens from skin biopsies were determine by homogenizing tissue sections in a 1.5mL tube containing 200µL of TSB using a pestle. Undiluted, 1:100 and 1:10,000 dilutions of tissue samples were plated (5µL) onto TSA plates. Plates were incubated in 37°C overnight and CFUs were counted. Bacterial burdens were normalized to tissue weight and calculated by the following equation: ((CFU/mL plated)*(dilution factor))/(tissue weight in mg). Bacterial burdens in the skin are represented by CFU/mg tissue.

Dissociation of skin biopsy for flow cytometry

Skin biopsy sections were cut into small pieces with sterile scissors and incubated with 1mg/mL of Collagenase-D (Roche) for 3 hours in 37°C in 0.5-1mL DMEM cell culture media in a 24-well tissue culture plate. Reactions were

Marker detected	Antibody clone	Fluorophores	Company
Annexin V		APC	Biolegend
7AAD			eBioscience
F4/80	BM8 BM8	PE-Cy7 Alexafluor-700	Biolegend Biolegend
Ly6G	IAC IAC	PerCP/Cy5.5 Alexafluor-488	Biolegend Biolegend
BLT1	203/14F11	PE	BD
BLT2	1-55/389	Alexafluor-647	Bioss
Viability dye		Zombie UV e780	Biolegend eBioscience
SIRPα	P84	PerCP/Cy5.5	Biolegend
CD47	miap301	PECy7	Biolegend
CFSE			Sigma

Table 8. List of antibodies and fluorescent dyes used for flow cytometry. Blank cells indicate information is not applicable.

quenched with 10mM final concentration of EDTA. Tissue sections were passed through a 70µm cell strainer and washed with PBS. Single cells were stained with fluorescent antibodies or dyes for flow cytometry analysis on the BD LSR II flow cytometer. Analysis was performed using Flow Jo software. List of fluorescent antibodies or dyes utilized are in **Table 8.**

Gating strategy for dissociated skin biopsy samples are as followed: Cells were gated from FSC vs. SSC **(Figure 4A)** followed by doublet exclusion by

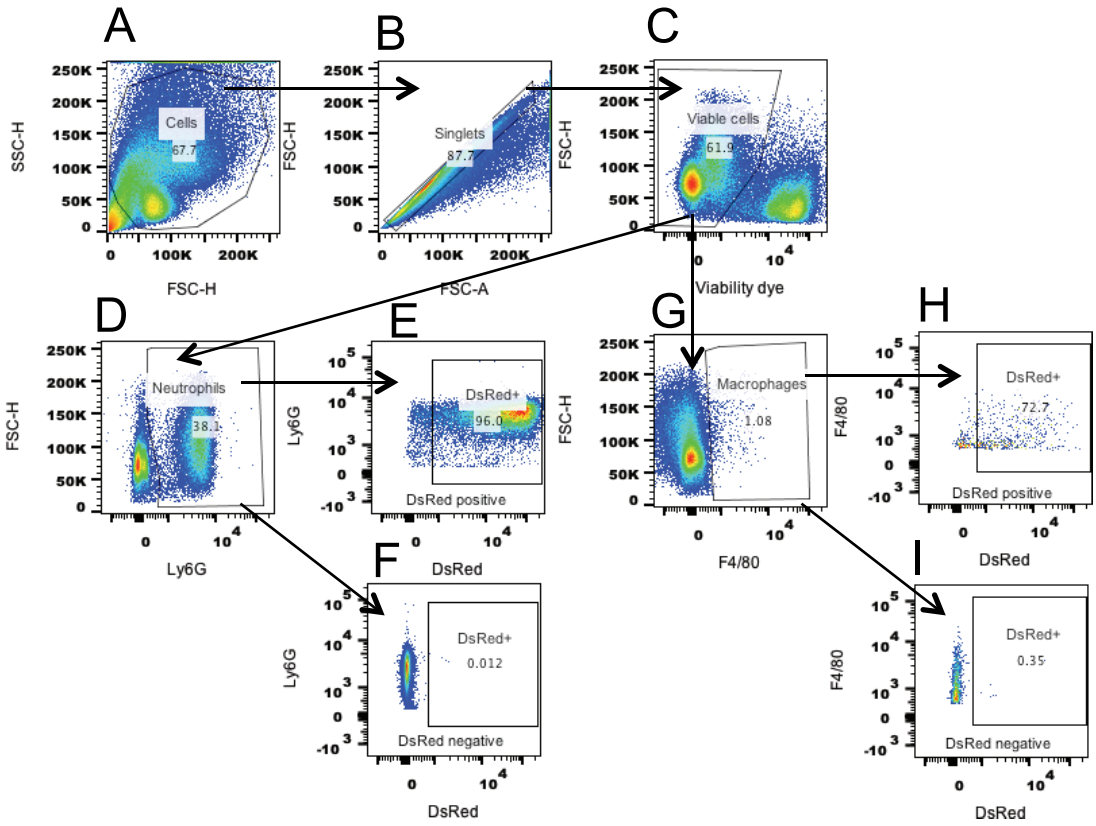

Figure 4. Gating scheme for flow cytometry. A) Gated on all cells. **B)** Gated on singlets (single cells) by plotting area vs. height. **C)** Gated on viable cells (viability dye) which are cells that did not take up the dye. **D** and **G)** Gated on neutrophils ($Ly6G^+$) or macrophages ($F4/80^+$). **E** and **H)** For pIL1DsRED mice, neutrophils and macrophages were then gated on DsRED cells. **F** and **I** show DsRed negative control.

FSC-A vs. FSC-H **(Figure 4B)**. Dead cells were excluded by viability dye **(Figure 4C)**. Viable cells were then gated on $Ly6G^+$ for neutrophils **(Figure 4D)** or $F4/80^+$ for macrophages **(Figure 4G)**. For pIL1DsRED mice, neutrophils **(Figure 4E-F)** and macrophages **(Figure 4H-I)** were then gated for DsRed expression to determine percentage of cells expressing DsRed and MFI calculated to determine expression of DsRed (a readout for *Il1b* expression).

Sample preparation for mass spectrometry

Skin biopsy sections were collected with a 8mm-diameter biopsy punch, sectioned in two equal pieces and flash frozen with dry ice. Samples were submitted and processed at the Vanderbilt University Eicosanoid Core Laboratory and processed as previously described [158]. Briefly, skin samples were homogenized and extracted in ice-cold methanol with indomethacin and butylated hydroxytoluene (BHT). Samples were injected for liquid chromatography - mass spectrometry (LC-MS). Eicosanoids were identified and quantified based on the mass and amount of known standards.

Sample preparation for MALDI

Skin biopsy sections were flash frozen with dry ice. Samples were submitted and processed at the Vanderbilt University Mass Spectrometry Research Center - Tissue Core Laboratory.

Lipid imaging: Plates designated for lipid imaging were not washed. DHA was sublimed at 110°C for approximately 6 minutes at <45 torr onto the plates

using a glass sublimation apparatus. Images were acquired with a 9.4T Fourier transform ion cyclotron resonance mass spectrometer (FT-ICR MS, Solarix, Bruker, Billerica, MA) equipped with a MALDI source (Smartbeam Nd:YAG laser, 355 nm). Serial sections were imaged in positive ion mode and negative ion mode with a pixel spacing of 75µm in both the x and y directions. Positive ion mode images were acquired from m/z 400-1600, and negative mode ion images were acquired from m/z 200-1300. Images were processed and visualized with flexImaging (Bruker).

Ointment preparations

Ointments were prepared by emulsifying the active ingredient into 100% petroleum jelly (Vaseline) and prepared daily prior to treatment application **(Table**

	Active ingredient per 1g petroleum jelly	Percent	Chemical supplier
LTB_4	33.65ng	3.37E-06%	Cayman Chemicals
U-75302	10µg	0.001%	Cayman Chemicals
Apocynin	166.17µg	16.6%	Sigma-Aldrich
Mupirocin	1mg 20mg	0.1% 2%	Applichem
LY255283	10µg	0.001%	Cayman Chemicals
Vancomycin HCL	10mg	1%	Dot scientific
MyD88 peptide	333.907µg	0.033%	Novus Biologicals

Table 9. Ointment preparations. Percentages are the amount of active ingredient per 1g of petroleum jelly.

9). Treatments were applied to cover the infected area with a clean cotton swab. Mice were treated once a day throughout the course of infection (ranging from 6 hours – 9 days).

IVIS in vivo imaging

IVIS spectrum/CT (Perkin Elmer) machine was used to image bioluminescence or fluorescence in the mice. Mice were anesthetized with isoflurane and imaged while under gas anesthesia. Mice were positioned facing the CCD camera and imaged for the appropriate bioluminescence/fluorescence.

Bioluminescence imaging (BLI) and analysis: The mice were scanned for determinant amount of time to allow for bioluminescent signal detection from each mouse (maximum acquisition time of 4 minutes). Mice were scanned longitudinal throughout the course of MRSA skin infection. A region was drawn around each infection and total flux (photons/second) was measured for each infection site. A background region was drawn to determine the background signal of each scan. To obtain background-free total flux signal the mouse infection region was subtracted from the background region. The background-free total flux was compared to a standard curve to obtain the bacteria amount in each infection. The standard curve was prepared by spotting known bacterial CFU TSA plates (for in vitro) and infected subcutaneously in mice (for in vivo) and imaged. A graph of luminescence total flux on the y-axis and CFU on the x-axis was referred to in order to quantify bacterial burden in the skin.

DsRed and mCherry scans and analysis: WT mice that were DsRed negative (or mCherry negative) served as the autofluorescence background. Mice were scanned using filter pairs for DsRed fluorescence or mCherry fluorescence. Living Image software (Perkin Elmer) was used to spectrally unmix the DsRed signal. A region was drawn around the spectrally unmixed DsRed signal (or mCherry signal) and total radiant efficiency was measured ([photons/second]/[$\mu W/cm^2$]).

Two-photon intravital microscopy

Mice were anesthetized with a solution of ketamine/xylazine. A skin flap was created surrounding the infection area, adapted from [159]. Tissues were moistened with PBS were used to maintain moisture on the mouse. The skin flap was placed in a coverslip-bottomed cell culture dish for imaging and moistened with PBS. Temperature of mice was maintained at 36°C with two ReptiTherm pads. Mice were imaged for up to 1 hour. Imaging was performed using an Olympus FV1000-MPE confocal/multiphoton microscope. This imaging technique was a terminal procedure. Immediately following imaging and while still anesthetized, mice were euthanized by cervical dislocation. Analysis was performed using FIJI (Image J) tracking software using TrackMate plugin.

Diabetes induction with streptozotocin

C57BL/6 male mice induced with 40mg/kg of streptozotocin (STZ) dissolved in 0.1M sodium citrate buffer [160]. Female mice were not used since

female mice are more resistant to developing hyperglycemia with STZ-treatment [161]. Mice aged 6-8 weeks were induced with the multiple low dose strategy (40mg/kg), one intraperitoneal injection with 0.2mL daily for 5 consecutive days. Nondiabetic control mice received citrate buffer as vehicle control. STZ induces cell death in the insulin-producing pancreatic beta cells, resulting in low insulin production and subsequent hyperglycemia [162]. Mice were considered diabetic when blood glucose levels were >250mg/dL. Mice were treated with STZ to induce diabetes 30 days prior MRSA skin infection. Mice were 10-12 weeks old at the time of MRSA skin infection.

Both *Alox5*$^{-/-}$ and *Ltb4r1*$^{-/-}$ mice were more resistant to developing hyperglycemia after STZ treatments compared to C57BL/6 WT mice. These knockout mice were treated with 3-5 more injections of 40 mg/kg of STZ. Age-matched WT and KO mice with similar blood glucose levels were used for experiments.

NOD diabetes model

Non-obese diabetic (NOD) mice are a model for T1D. These mice spontaneously develop diabetes approximately 12+ weeks of age. Female NOD mice develop diabetes at a higher frequency than male NOD mice by week 30 of age (80% of females vs. 45% males). NOD breeders were maintained at Indiana University School of Medicine. Starting at 10 weeks of age, blood glucose levels were monitored weekly in female NOD mice, using OneTouch Ultra glucose meter and strips. When blood glucose levels reached 250mg/dL, mice were

considered diabetic (dbNOD). Age-matched female NOD mice that did not become diabetic (glucose levels ~100mg/dL but <150mg/dL) were used as nondiabetic NOD controls (ctNOD). Once NOD mice became diabetic, they were used in experiments within 1-2 weeks. Body weight was monitored and mice that lost more than 20% of original body weight were excluded from experimentation. NOD mice were approximately 12-20 weeks of age at the time of MRSA skin infection.

Neutrophil depletion

Ly6G depleting antibody (clone 1A8) and IgG control (BioXcell) were prepared by diluting antibodies in BioXcell pH 7.0 dilution buffer. 200µg in 200µL of antibody was administered via intraperitoneal injection18-hours prior MRSA skin infection, adapted from [163]. Affected region areas were measured with calipers at 24 hours post infection. Skin biopsies were collected from naive animals, and at 6 hours and day 1 post MRSA infection and processed for histology as described in “Immunohistochemistry of skin biopsy sections”.

Macrophage depletion

In order to deplete macrophages, MMDTR mice were treated with 100ng DT or PBS vehicle control once a day for three consecutive days prior to MRSA skin infection **(Figure 5)**. Biopsy punches were collected at 6 hours or 1 day post MRSA skin infection. Mice used for 2 day post MRSA skin infection were treated with 100ng DT in PBS at day 1 to continual deplete monocytes/macrophages.

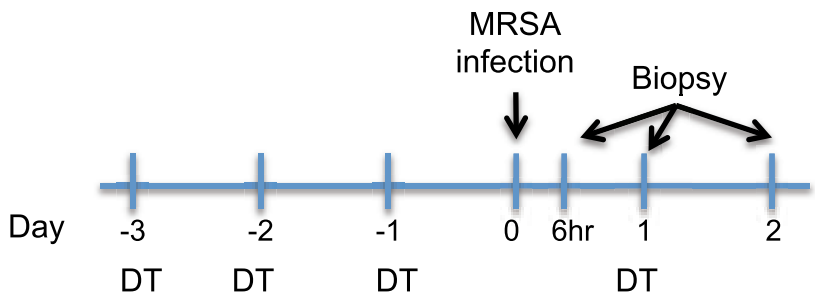

Figure 5. Macrophage depletion protocol in MMDTR mice. 100ng of diphtheria toxin (DT) 100ng in PBS administered via intraperitoneal injection once daily for three consecutive days prior to MRSA skin infection. Mice biopsied on day 2 post infection received 100ng DT on day 1 post infection.

Primary cell isolation

Resident peritoneal macrophages were isolated by PBS lavage from euthanized mice. Cells were centrifuged and red blood cell lysis was performed if necessary. The cells were counted and plated for assays. After resting, non-adherent cells were washed away with warm PBS washes. Cells were rested for at least 1 hour prior to experimentation.

To isolate bone marrow neutrophils, both tibias and femurs were isolated from euthanized mice. Bone marrow was flushed with PBS with a 26G needle and 20mL syringe. Neutrophils were negatively isolated for using neutrophil isolation kit (Macs Miltenyi).

The media used to culture primary cells was Dulbecco's Modified Eagle's Medium (DMEM) supplemented with 5% fetal bovine serum (FBS), HEPES, and 1X antibiotic/antimycotic. DMEM containing 1g/L glucose was used to culture

macrophages/neutrophils to mimic low glucose (control - nondiabetic) and 4.5g/L glucose was used to culture cells to mimic high glucose (diabetic) conditions.

Efferocytosis assay

Peritoneal macrophages were isolated as described in “Primary cell isolation” and plated in 500µL at a cell density of $1x10^6$ cells/mL in 24-well plates and rested overnight. Bone marrow neutrophils were isolated as described in "Primary cell isolation" and labeled with CFSE (Sigma). Briefly, neutrophils were labeled with 2µM CFSE in PBS in $1x10^6$ cells/mL volume for 30 minutes incubated at 37°C and washed with PBS. Labeled neutrophils were allowed to rest in DMEM for at least 30 minutes prior to experimentation. Labeled neutrophils were incubated with MRSA at MOI of 50:1 for 18 hours to generate infected apoptotic cells (IACs). IACs were confirmed apoptotic by flow cytometry analysis of 7AAD and AnnexinV staining. IACs were washed with PBS and given to macrophages at a ratio of 2 IACs per 1 macrophage. Co-cultures were incubated for 2 hours and cells were collected by placing plate on ice and scraping cells into a 5mL tube for flow cytometry activated sorting (FACS). Macrophages were labeled with fluorescent F4/80 antibody. Samples were collected on BD LSR II and analyzed using Flow Jo software. All cells were gated on and doublets were excluded to eliminate bound cells from the analysis. F4/80 positive cells were gated on and analyzed for CFSE, indicating efferocytosis. The percent of $CFSE^+$ $F4/80^+$ cells were called efferocytosis macrophages. The mean

fluorescence intensity (MFI) was determined. Efferocytosis index was calculated by multiplying the percent of efferocytosis macrophages by the MFI.

Macrophages were cultured with 30nM siRNA for SCRAMBLE negative control or *Sirpa* (Dharmacon) with 1:1000 dilution of lipofectamine 3000 transfecting agent (Thermo Fisher Scientific) for 24 hours prior to efferocytosis assay. Transfection took place in DMEM media containing no FBS or antibiotic/antimycotic.

In vivo efferocytosis was determined by collecting a skin biopsy from mice at day 5 post infection. Skin biopsy section was dissociated and processed for flow cytometry staining: surface staining for F4/80 followed by fixation and permeabilization for intracellular Ly6G staining. Macrophages were gated on and analyzed for Ly6G, indicating efferocytosis. Efferocytosis index was calculated by multiplying the percent of efferocytosis macrophages by the MFI normalized to the total number of macrophages.

Immunofluorescence staining

Cells were cultured in 8-well chamber slides. Lipid raft staining was done using Vybrant AlexaFluor-488 lipid raft labeling kit (Thermo) on live peritoneal macrophages. Cells were incubated with AF488 labeled cholera toxin B (CTB) subunit, which binds to ganglioside G_{M1} that is found in lipid rafts. Cells were then labeled with an antibody to CTB which crosslinks the labeled lipid rafts to localize to areas on the plasma membrane. Following labeling, cells were fixed in 4% PFA for 15 minutes followed by washes with PBS. Slides were blocked with 3%

BSA for 1-2 hours at room temperature. Primary antibodies (against CD36 and SIRPα) were incubated at 1:100 for overnight at 4°C. Secondary antibodies (anti-mouse or anti-rabbit AlexaFlour-647) were incubated at 1:200 for 1 hour at room temperature. Samples were mounted with the nuclear dye 4',6-diamidino-2-phenylindole (DAPI) antifade and sealed with a coverslip. Slides were visualized and pictures acquired on Nikon Eclipse Ci with filters for DAPI, GFP, and Texas Red and camera Nikon Ds-Qi2.

Proximity ligation assay was done using Duolink PLA kit (Sigma) on bone marrow neutrophils cultured in 8-well chambered cell culture slides (Corning). Neutrophils were pretreated with 10μM BLT1 antagonist U-75302 or 10nM LTB_4. Neutrophils were co-cultured with GFP-MRSA at MOI 50:1 for 3 hours followed by inflammasome activation with 1μM nigericin for 1 hour. Cells were fixed with 4% formaldehyde for 10 minutes and washed with PBS. Slides were blocked with 3% bovine serum albumin (BSA) for 1 hour. Primary antibody incubation using Adipogen antibodies for NLRP3/NALP3 (NACHT, LRR and PYD domains-containing protein 3) (Cryo-2) mouse antibody (1:200 dilution) and ASC (apoptosis-associated speck-like protein containing a carboxy-terminal CARD) (AL177) rabbit antibody (1:200 dilution) in blocking buffer for 2 hours at room temperature. Proximity ligation assay (PLA) staining protocol followed Duolink (Sigma) kit instructions. Slides were allowed to dry before mounting cells with ProLong Gold Antifade Mountant with DAPI (Thermo Fisher Scientific) and with a coverglass. Slides were visualized and pictures acquired on Nikon Eclipse Ci with filters for DAPI, GFP, and Texas Red and camera Nikon Ds-Qi2.

Statistical analysis

Data analysis was performed in GraphPad Prism software (San Diego). Statistical test used are listed in the figure legends. Briefly, Student's t-test was used to compare two experimental groups. One-way ANOVA followed by Tukey multiple comparison correction was used to compare three or more groups. Two-way ANOVA with repeated measured followed by Tukey multiple comparison correction was used to compare infection areas over time between two or more mouse groups. P values < 0.05 were considered significant.

RESULTS

Part I - LTB_4 is a necessary mediator to control MRSA skin infection

LTB_4 promotes bacterial clearance

LTB_4 has been shown to be an important molecule for neutrophil chemotaxis and to promote phagocytes to engulf and kill various types of pathogens [53, 96-101, 103]. We first determined whether MRSA skin infection induced LTB_4 production and responses. MRSA skin infection in C57BL/6 (WT) mice induced expression of both *Alox5* and *Ltb4r1*, genes for 5-LO and BLT1, respectively **(Figure 6A)**. This correlated with higher production of LTB_4 in the skin during MRSA skin infection **(Figure 6B).**

To test the hypothesis that LTB_4 is an important mediator in controlling MRSA skin infections, genetic and pharmacological inhibition of BLT1 was used. Both *Ltb4r1*$^{-/-}$ mice and WT mice treated daily with the BLT1 antagonist U-75302

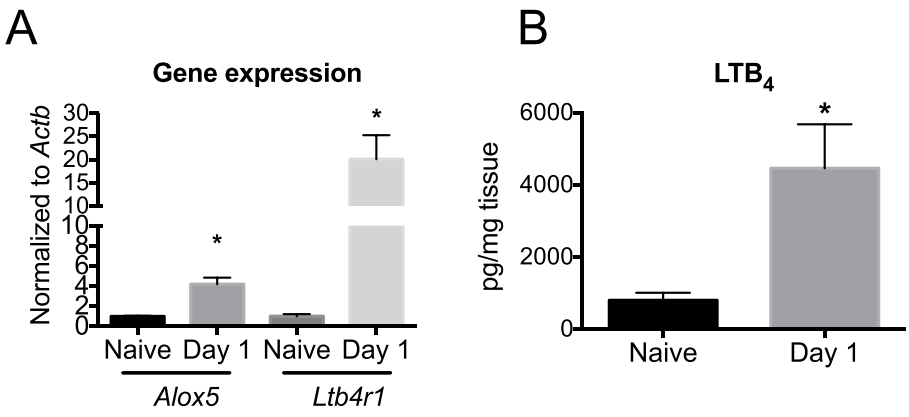

Figure 6. MRSA infection induces LTB_4 production. A-B) WT mice were infected subcutaneously with MRSA ($3x10^6$ CFU). **A)** qRT-PCR for mRNA expression of *Alox5* and *Ltb4r1* from naive skin and day 1 post MRSA skin infection. **B)** LTB_4 EIA from skin biopsy homogenates collected from naive skin and at day 1 post infection. Data are mean ± SEM from 3-6 mice from 2-3 experiments. *$p < 0.05$ (Student's t-test).

had larger infected areas compared to WT mice treated with vehicle control **(Figure 7A).** Bacterial burden measured in the skin at day 1 and day 9 post MRSA skin infection were much higher in *Ltb4r1*$^{-/-}$ and WT mice treated with U-

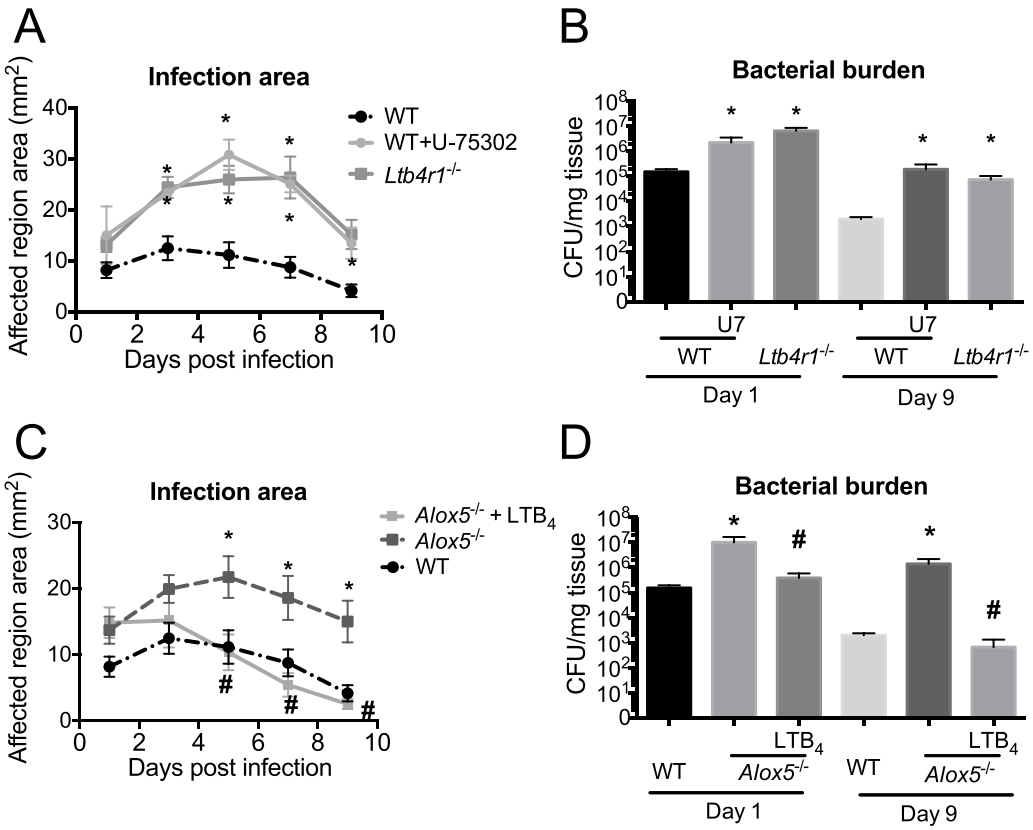

Figure 7. LTB_4 is an important mediator for controlling MRSA skin infection. A-B) WT and *Ltb4r1*$^{-/-}$ mice were infected subcutaneously with MRSA (3x10^6 CFU). WT mice were treated daily with topical 0.001% BLT1 antagonist U-75302 (U7). **A)** Infection areas were measured every other day for 9 days. **B)** Bacterial CFUs normalized to tissue weight were measured at days 1 and 9 post infection**. C-D)** WT and *Alox5*$^{-/-}$ mice were infected subcutaneously with MRSA (3x10^6 CFU). *Alox5*$^{-/-}$ mice were treated daily with topical 3.37x10^{-6}% LTB_4 ointment. **C)** Infection areas were measured every other day for 9 days. **D)** Bacterial CFUs normalized to tissue weight were measured at days 1 and 9 post infection. Data are mean ± SEM from 5-13 mice from 2-3 experiments. **A** and **C)** *p < 0.05 vs. WT, #p < 0.05 vs. *Alox5*$^{-/-}$ (Two-way ANOVA followed by Tukey multiple comparison correction). **B** and **D)** *p < 0.05 vs. WT, #p < 0.05 vs. *Alox5*$^{-/-}$ (One-way ANOVA followed by Tukey multiple comparison correction).

75302 compared to WT mice treated with vehicle control **(Figure 7B)**. To further determine the contribution of LTB_4 in MRSA skin infection, an add-back experiment was performed. To do this, leukotriene deficient *Alox5*$^{-/-}$ mice were infected with MRSA and treated daily with topical ointments containing LTB_4 or vehicle control. *Alox5*$^{-/-}$ mice had larger infection areas compared to WT mice, which was similar to observations with *Ltb4r1*$^{-/-}$ mice. 5-LO deficient mice treated daily with topical LTB_4 ointment had a reduction in infection area, which was restored to levels seen in WT mice **(Figure 7C)**. *Alox5*$^{-/-}$ mice also had higher bacterial burdens in the skin at day 1 and day 9 post infection and *Alox5*$^{-/-}$ mice treated with LTB_4 ointment restored bacterial clearance **(Figure 7D)**. Taken together, LTB_4 is produced during MRSA skin infection and LTB_4 actions mediated through BLT1 activation are needed to eliminate infection through controlling infection area size and bacterial burden.

LTB_4 promotes abscess architecture

MRSA skin infection is characterized by neutrophil recruitment and abscess formation. Since LTB_4 is a known chemoattractant, histology analyses were performed to determine whether increased infection areas could be due to differences in immune cell populations. H&E sections from biopsies collected at day 1 post MRSA skin infection revealed no significant impairments in cell recruitment in *Ltb4r1*$^{-/-}$ or *Alox5*$^{-/-}$ mice compared to WT mice. However, the organization and structure of the abscesses were noticeably different **(Figure 8A)**. Cells recruited to the skin of WT mice developed an abscess architecture

surrounded by a fibrous capsule. Infection in *Ltb4r1*$^{-/-}$ and *Alox5*$^{-/-}$ mice did not induce a well-structured abscess and developed a smaller fibrous layer around the abscess compared to WT mice. Treating *Alox5*$^{-/-}$ mice with topical LTB_4 ointment restored abscess structuring and increased fibrous layer thickness surrounding the abscess **(Figure 8B)**. These data suggest that during MRSA skin infection, LTB_4 is dispensable for cell recruitment; however, LTB_4 is needed for optimal abscess architecture organization.

Innate immune cells, such as neutrophils and macrophages, have major roles in controlling *S. aureus* skin infection [164, 165]. Others have shown that neutrophils are the most abundant cell type recruited to the skin early during infection and the majority of the cells in the abscess are neutrophils [166].

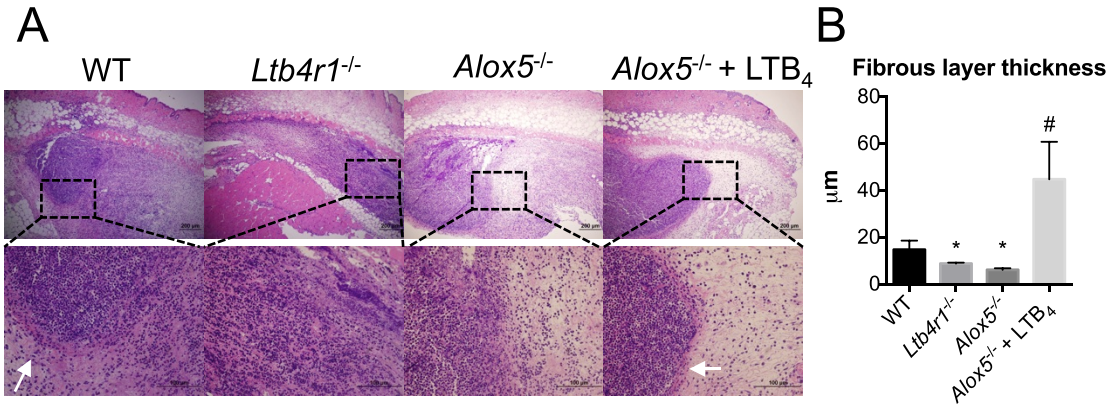

Figure 8. LTB_4 promotes abscess architecture. A-B) WT, *Ltb4r1*$^{-/-}$, and *Alox5*$^{-/-}$ mice were infected subcutaneously with MRSA ($3x10^6$ CFU). *Alox5*$^{-/-}$ mice were treated with topical $3.37x10^{-6}$% LTB_4 ointment. **A)** H&E images of skin biopsy sections collected at day 1 post infection. Top panels show 4X and bottom panels show 40X magnification. Images are representative of 4-5 mice from 1 experiment. **B)** Thickness of the fibrous layer surrounding the abscess visible on H&E stains at day 1 post infection. Quantification performed with ImageJ software as described in the "Materials and methods". Data represent mean ± SEM from 3-4 mice from 1 experiment. *$p < 0.05$ vs. WT, #$p < 0.05$ vs. *Alox5*$^{-/-}$ (One-way ANOVA followed by Tukey multiple comparison correction). White arrows indicate fibrous layer surrounding abscess.

Macrophages have been shown to interact around the abscess [167] and perivascular macrophages are important for neutrophil extravasation [165]. To determine where these cell types are located in the skin during MRSA skin

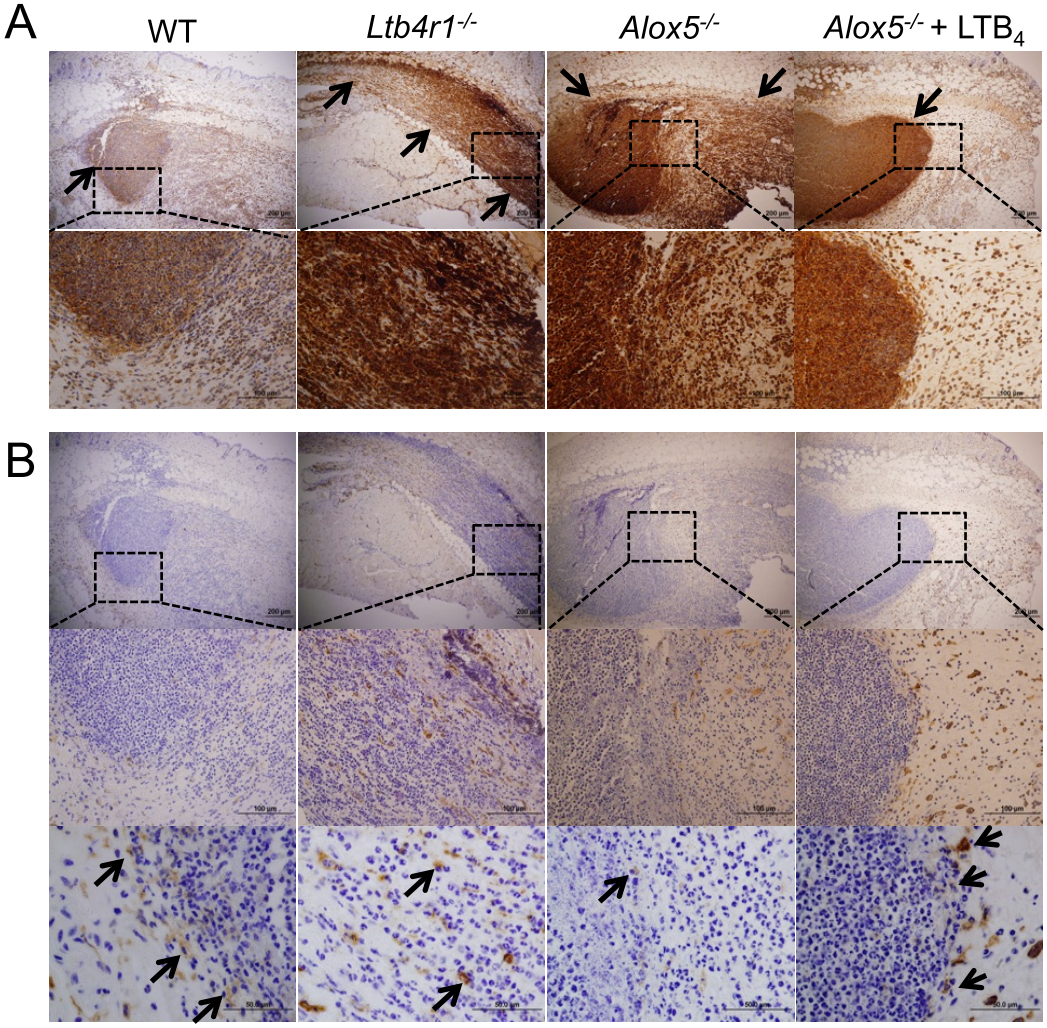

Figure 9. Macrophage and neutrophil interactions with abscess structure. **A-B)** WT, *Ltb4r1*$^{-/-}$, and *Alox5*$^{-/-}$ mice were infected subcutaneously with MRSA (3x10^{6} CFU). *Alox5*$^{-/-}$ mice were treated with topical 3.37x10^{-6}% LTB_4 ointment. Skin biopsies were collected at day 1 post infection. **A)** IHC for neutrophils (Ly6C/G) shown in brown and counterstain shown in blue. Top panels show 4X and bottom panels show 40X magnification. **B)** IHC for macrophages (F4/80) shown in brown and counterstain shown in blue. Top panels show 4X, middle panels show 40X, and bottom panels show 100X magnification. Images are representative of 4-5 mice from 1 experiment. Black arrows indicate cells.

infection, biopsy sections were used for immunohistochemistry (IHC) to detect neutrophils (Ly6G/C antibody) and macrophages (F4/80 antibody). WT, *Ltb4r1*$^{-/-}$, and *Alox5*$^{-/-}$ mice all had abundant neutrophil recruitment, indicating no impairment in neutrophil recruitment to the skin. The abscess in WT mice was primarily composed of neutrophils, however, neutrophils from *Ltb4r1*$^{-/-}$ and *Alox5*$^{-/-}$ mice did not cluster into an abscess structure **(Figure 9A)**. Treatment of *Alox5*$^{-/-}$ mice with topical LTB_4 ointment restored neutrophil abscess formation. Macrophages were found in close proximity to the abscess in WT mice day 1 post infection. However, macrophages from both *Ltb4r1*$^{-/-}$ and *Alox5*$^{-/-}$ mice lacked this association. Reduced macrophage interactions with the abscess in *Alox5*$^{-/-}$ were restored when mice were treated with topical LTB_4 ointment **(Figure 9B)**. This suggests that LTB_4 plays a role in promoting abscess architecture and organization likely by mediating interactions between macrophages and neutrophils in the skin.

Since LTB_4 seemed important for mediating organized neutrophil abscess formation and architecture, the next question was how LTB_4 affected neutrophil direction in the skin. In order to observe the dynamics of neutrophil migration in the skin, intravital microscopy imaging was used. Mice expressing GFP in myeloid cells, *Lys*^{EGFP} mice, were infected with MRSA and treated with an ointment containing no active ingredient, LTB_4, or the BLT1 antagonist U-75302. At day 1 post MRSA skin infection, mice were prepared for two-photon microscopy and an area near the abscess was imaged for 30 minutes.

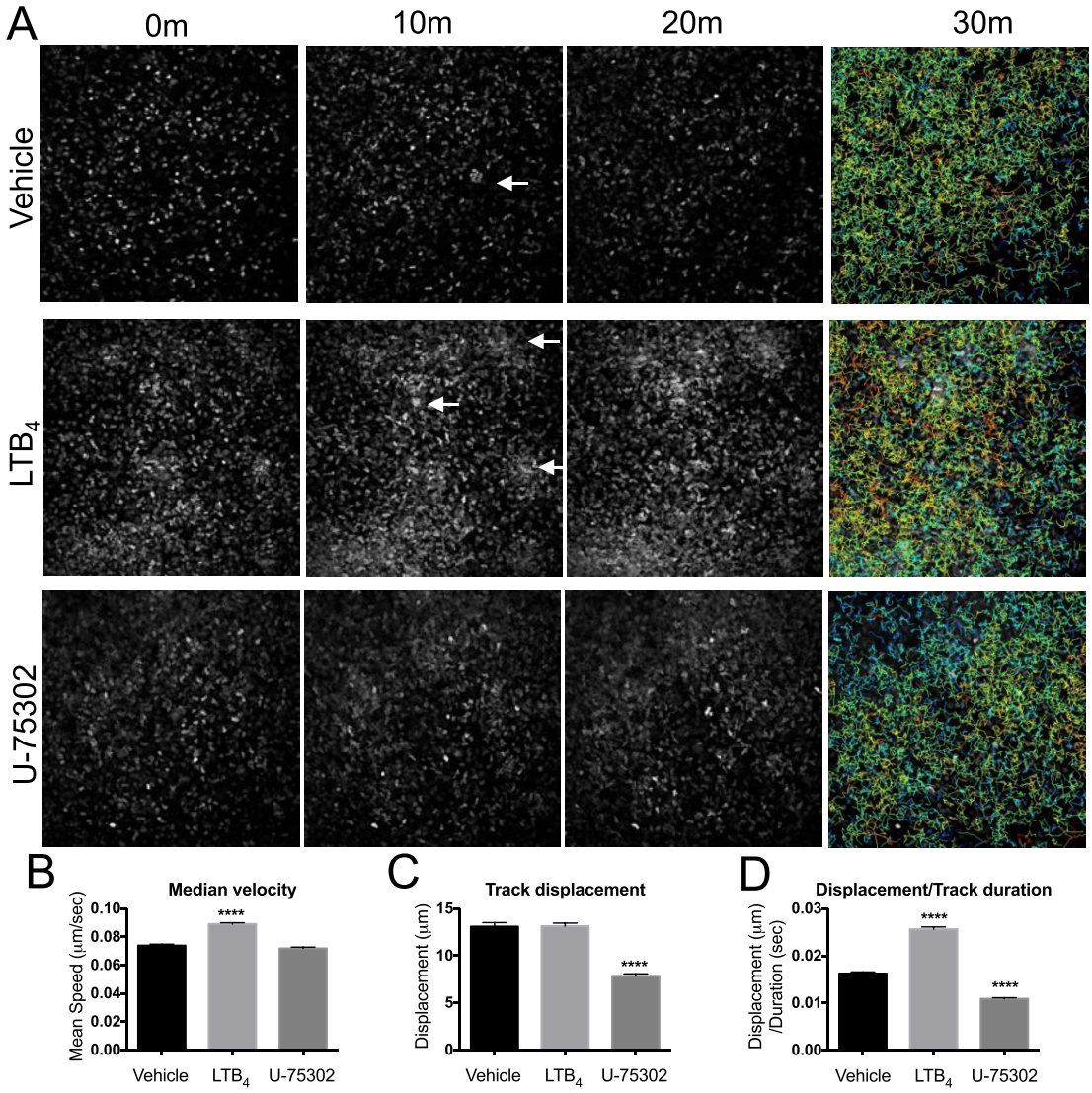

Figure 10. LTB_4 provides neutrophil direction. A-D) *Lys*^{EGFP} mice were infected subcutaneously with MRSA ($3x10^6$ CFU) and treated with ointments containing $3.37x10^{-6}$% LTB_4, 0.001% BLT1 antagonist (U-75302), or vehicle-control. At day 1 post infection, mice were imaged by two-photon intravital microscopy for 30 minutes as described in the "Materials and methods". **A)** Still frames of intravital imaging movies taken at 0, 10, 20, and 30 minutes. 30 minute frames include track paths of individual cells. The color of path indicates heat map of median velocity (red=fast, blue=slow). **B)** Median velocity of GFP^+ cells. **C)** Track displacement of GFP^+ cells. **D)** Ratio of displacement/track duration. Track paths and quantifications were measured by FIJI (ImageJ) TrackMate plugin software as described in the "Materials and methods". Data are mean ± SEM of at least 1000 GFP^+ cells representative of 3-4 mice from 2-3 experiments. ****$p < 0.0001$ vs. vehicle (One-way ANOVA followed by Tukey multiple comparison correction). White arrows indicate swarming.

Although all myeloid cells express GFP in this mouse model, it has been reported that neutrophils have brighter GFP signal than other myeloid cells [153], which was also identifiable in these experiments. Neutrophils in the skin of mice treated with vehicle-ointment (control) formed swarm-like clusters **(Figure 10A)**. While neutrophils in the skin of mice treated with topical LTB_4 ointment formed more swarm-like clusters than vehicle-treated mice, BLT1 antagonist treatment severely blunted these neutrophil accumulations. Additionally, although BLT1 antagonist treatment did not affect velocity, neutrophil median velocity was increased when mice were treated with LTB_4 **(Figure 10B)**. Displacement values (the vector of distance from starting point A to ending point B) were similar between LTB_4 treatment and control mice; however, displacement values were significantly reduced in mice treated with BLT1 antagonist **(Figure 10C)**. The ratio of displacement to duration could be used to estimate directionality, indicating how far cells travel within a given time. Neutrophils that traveled a further distance away from the starting point in a given duration would have a greater ratio number than neutrophils that did not travel as far within a given duration. The ratio of displacement/duration was increased with LTB_4 and decreased with BLT1 antagonist treatment compared to vehicle-control mice **(Figure 10D)**. This suggested that neutrophils in LTB_4 treated mice had a more directed migration whereas BLT1 antagonist treated mice had impaired migration, which recapitulated the observations seen in the movies.

Since LTB_4 improved neutrophil direction in the skin and promoted abscess formation, the location of LTB_4 in the skin during infection was next evaluated.

WT skin biopsy sections from naive and day 1 post MRSA skin infection were processed for MALDI analysis. The MALDI detectors at the time of imaging were not calibrated for high sensitivity detection of LTB_4 or other leukotrienes due to difficulties with reliably detecting charged molecules [168] . However, arachidonic acid (AA) could be reliably detected. MALDI imaging revealed high abundance of

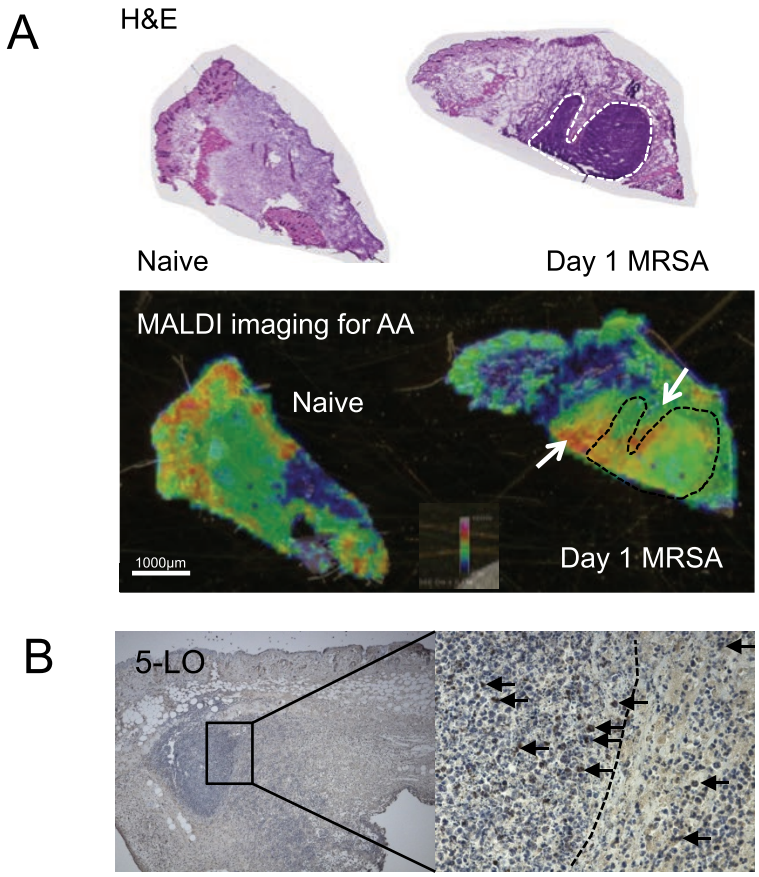

Figure 11. Arachidonic acid and 5-LO are found in close proximity to the abscess. A-B) WT mice were infected subcutaneously with MRSA ($3x10^6$ CFU) and biopsies were collected from naive skin and at day 1 post infection. **A)** Top panel: H&E images. Bottom panel: MALDI images for AA (red for high abundance and blue for low abundance). Images are representative of 2-3 mice from 1 experiment. Dotted lines indicate abscess edge. White arrows indicate high AA abundance. **B)** IHC on day 1 post infection for 5-LO. Left panel shows 4X and right panel shows 40X magnification. 5-LO shown in brown and counterstain in blue. Data are representative of 2-3 mice from 1 experiment. Black arrows indicate 5-LO^+ cells.

AA surrounding the abscess of WT mice infected with MRSA **(Figure 11A)**. Since macrophages were also found in close proximity to the abscess, it is likely that macrophages and possibly other cell types near the periphery of the abscess are contributing to LTB_4 production. It is also possible that LTB_4 and other AA products are major players in promoting abscess architecture during MRSA skin infections.

Since AA was found in high abundance surrounding the abscess, we next stained biopsy sections from naive and day 1 post MRSA skin infection for 5-LO by IHC. There was a high abundance of 5-LO^+ cells near the abscess periphery **(Figure 11B)**. Taken together, LTB_4, as well as other 5-LO products, are likely found in high abundance surrounding the abscess, which likely promotes neutrophil direction to develop a well-structured abscess.

MRSA killing involves LTB_4-mediated NADPH oxidase activity

Mice deficient in 5-LO and BLT1 had higher bacterial burden compared to WT mice **(Figure 7)**, and high bacterial burdens seemed to correlate with impaired abscess structure. We then decided to determine the mechanism by which LTB_4 enhances MRSA antibacterial functions in the skin. First IHC for gram stains were analyzed to determine where bacteria were located in the skin during infection. MRSA were located within neutrophils located inside the abscess in the skin of WT mice **(Figure 12)**. *Ltb4r1*$^{-/-}$ and *Alox5*$^{-/-}$ mice had many clusters of extracellular MRSA colonies throughout the skin. Treating *Alox5*$^{-/-}$ mice with topical LTB_4 ointment restored phagocytosis of bacteria. This suggests

that LTB_4 was necessary for phagocytosis of MRSA and abscess formation, both of which are necessary for effective bacterial clearance.

LTB_4 has been shown to be important in reactive oxygen species (ROS) generation, which is a major mechanism utilized by phagocytes to kill bacteria [169]. In order to test whether LTB_4 is involved in NADPH-oxidase mediated killing of MRSA in vivo, two models were utilized; a genetic knockout model (*Cybb*$^{-/-}$) that lacks the membrane-bound subunit, gp91^{phox}, of the NADPH oxidase and a pharmacological model to inhibit NADPH oxidase activity with apocynin treatment. Mice deficient in gp91^{phox} and WT mice treated with apocynin had significantly larger infection areas compared to WT mice at day 1

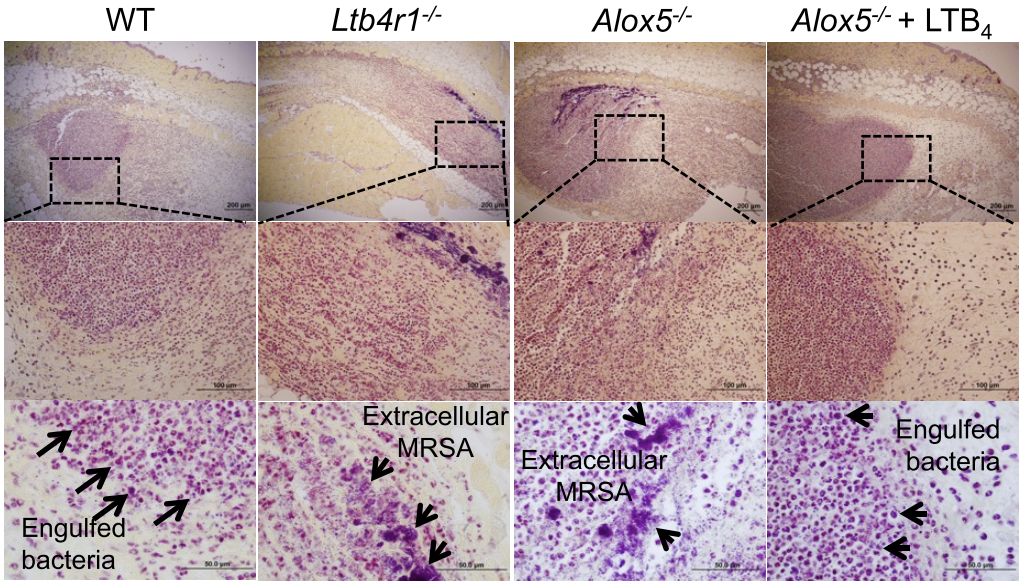

Figure 12. LTB_4 promotes bacterial containment. WT, *Ltb4r1*$^{-/-}$, and *Alox5*$^{-/-}$ mice were infected subcutaneously with MRSA ($3x10^6$ CFU). *Alox5*$^{-/-}$ mice were treated daily with topical $3.37x10^{-6}$% LTB_4 ointment. Gram staining (MRSA stained purple) of skin biopsy sections collected at day 1 post infection. Top panels show 4X, middle panels show 40X, and bottom panels show 100X magnification. Images are representative of 3-5 mice from 1 experiment. Arrows indicate MRSA.

post MRSA skin infection **(Figure 13A)**. Larger infection areas in *Cybb*$^{-/-}$ mice and apocynin-treated mice were correlated with higher bacterial burdens

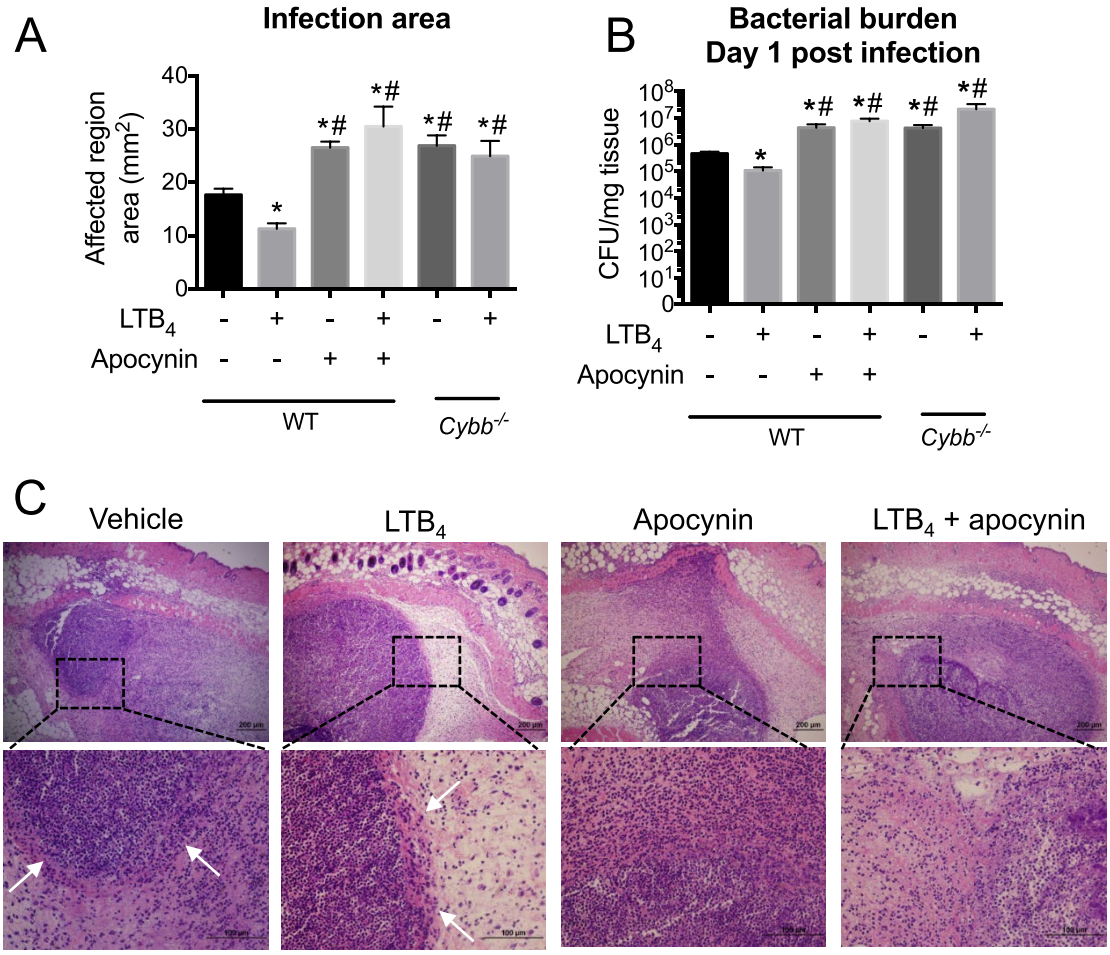

Figure 13. LTB$_4$ promotes NADPH oxidase-mediated killing of MRSA. A-B) WT and *Cybb*$^{-/-}$ mice were infected subcutaneously with MRSA (3x10^6 CFU). WT mice were treated with topical ointments containing 3.37x10^{-6}% LTB$_4$, 16.6% apocynin, or 3.37x10^{-6}% LTB$_4$ + 16.6% apocynin, or vehicle-control. *Cybb*$^{-/-}$ mice were treated with topical ointments containing 3.37x10^{-6}% LTB$_4$ or vehicle control. **A)** Infection areas measured at day 1 post infection. **B)** Bacteria CFUs normalized to tissue weight measured at day 1 post infection. **C)** H&E images of day 1 post infection from WT mice treated with topical ointments containing 3.37x10^{-6}% LTB$_4$, 16.6% apocynin, or 3.37x10^{-6}% LTB$_4$ + 16.6% apocynin, or vehicle-control. Top panels show 4X and bottom panels show 40X magnification. Images are representative of 5-8 mice from 2 experiment. Data are mean ± SEM of 8-15 mice from 2-3 experiments. *p < 0.05 vs. WT treated with vehicle and #p < 0.05 vs. WT treated with LTB$_4$ ointment (One way ANOVA followed by Tukey multiple comparison correction). Arrows indicate abscess edge.

compared to WT mice **(Figure 13B)**. Additionally, topical LTB_4 ointment reduced infection areas and improved bacterial clearance in WT mice but not in *Cybb*$^{-/-}$ or apocynin-treated mice. H&E analysis of tissue biopsy sections taken at day 1 post MRSA skin infection revealed that treating mice with apocynin disrupted abscess architecture, which impaired effective bacterial containment and clearance **(Figure 13C)**. This shows that NADPH-oxidase activity is necessary for MRSA killing and that topical LTB_4 treatment did not revert MRSA killing with NADPH-oxidase deficiency. Also, this suggests that abscess architecture may also be mediated through a ROS-dependent process.

LTB_4/BLT1 promotes IL-1β production

LTB_4 is an important molecule involved in the production of cytokines and other inflammatory mediators [66, 67]. A custom multiplex assay was created to measure multiple inflammatory mediators simultaneously in skin biopsy homogenates. Skin biopsy samples from WT and *Ltb4r1*$^{-/-}$ mice collected from naive uninfected skin, day 1 and day 9 post MRSA infection revealed that several inflammatory mediators are decreased in *Ltb4r1*$^{-/-}$ mice during infection compared to WT mice **(Figure 14A)**. Importantly, day 1 post infection, *Ltb4r1*$^{-/-}$ had lower expression of IL-1β **(Figure 14B)**, which is important for abscess formation during *S. aureus* skin infection [170]. Additionally, chemokines such as CXCL2 **(Figure 14C)** were enhanced in *Ltb4r1*$^{-/-}$ at day 1 post infection and there was no difference in ICAM1 expression **(Figure 14D)**. Since CXCL2 and ICAM1 are important for neutrophil recruitment, observing no impairments in neutrophil

recruitment in H&E stains **(Figure 8A)**, this suggests that LTB_4 is dispensable for neutrophil recruitment but is necessary for immune responses at the site of infection by mediating production of various inflammatory mediators.

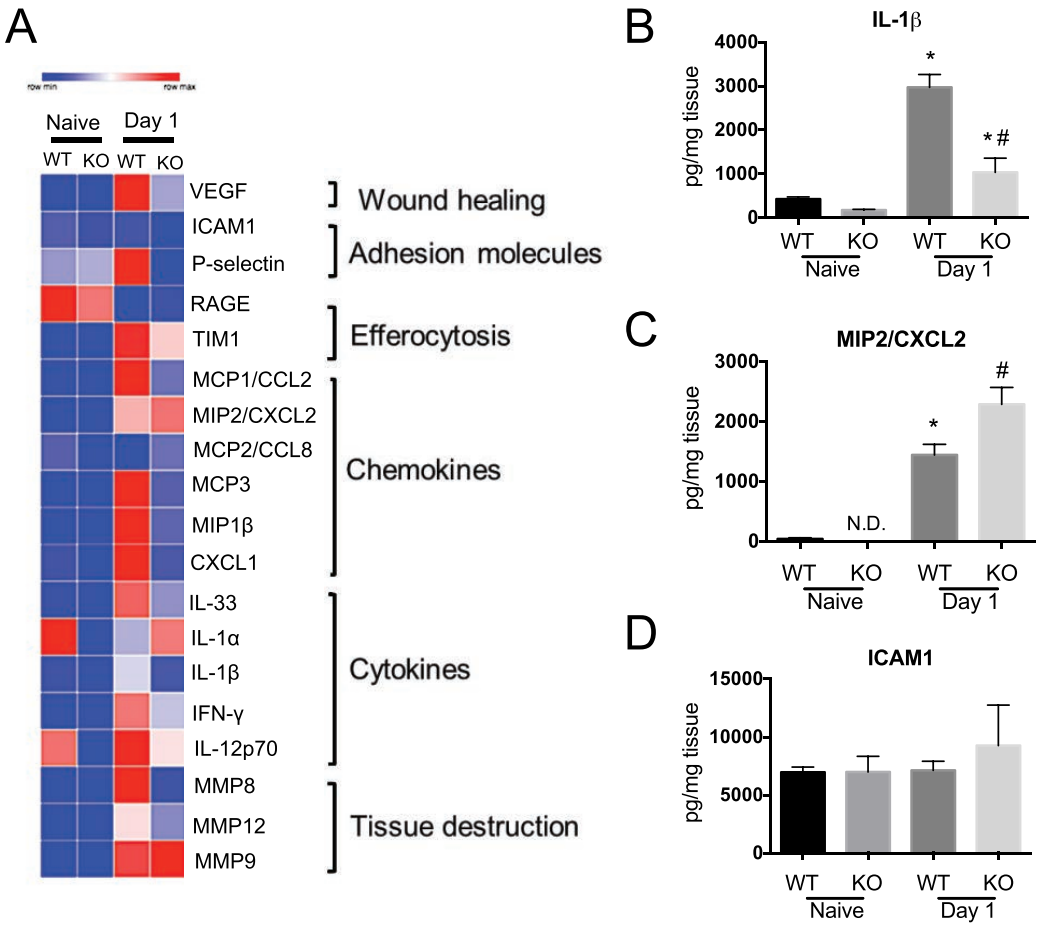

Figure 14. LTB_4 drives expression of inflammatory mediators. A-D) WT and *Ltb4r1*$^{-/-}$ (KO) mice were infected subcutaneously with MRSA ($3x10^6$ CFU). Biopsies were collected from naive skin and at day 1 post infection. **A)** Heatmap of analytes measured in skin biopsy homogenates. Heatmap created using GraphPad Prism software. **B)** Graph of IL-1β from heatmap. **C)** Graph of MIP2/ CXCL2 from heatmap. **D)** Graph of ICAM1 from heatmap. Data are mean ± SEM of 3-10 mice from 2-4 experiments. *$p < 0.05$ vs. naive, #$p < 0.05$ vs. infected WT (One-way ANOVA followed by Tukey multiple comparison correction). N.D. indicates not detected.

Following up on the multiplex assay finding that *Ltb4r1*$^{-/-}$ mice had low IL-1β in the skin **(Figure 14B)**, and that LTB_4 has been shown to regulate IL-1β production in other disease settings such as arthritis [171], the role of LTB_4 in controlling IL-1β in MRSA skin infection was next evaluated. IL-1β is produced as

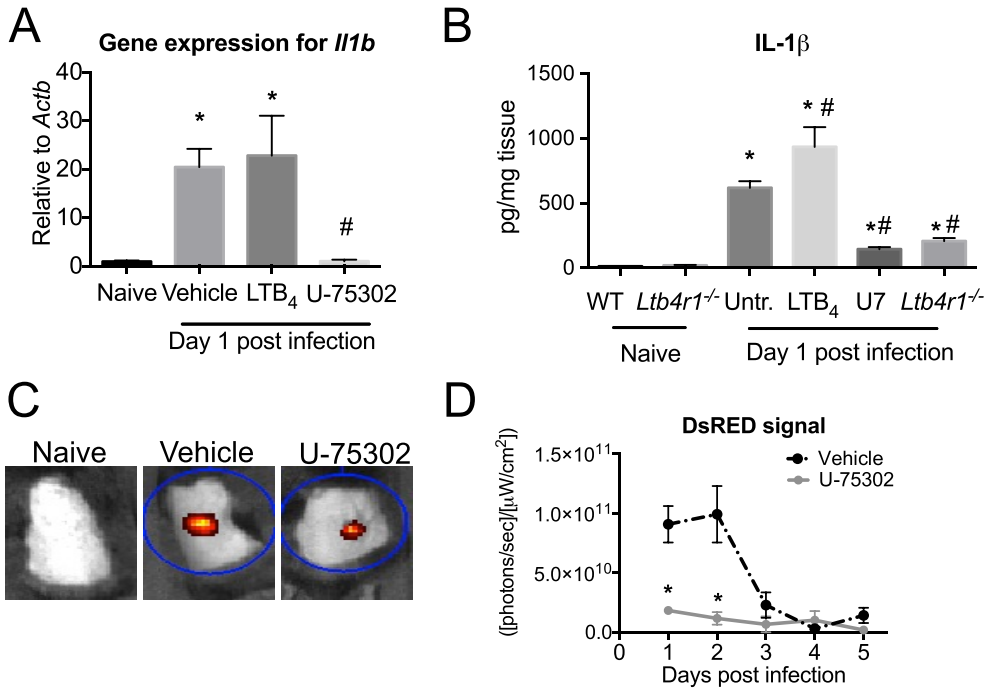

Figure 15. LTB_4 is necessary for IL-1β production. A) WT mice were infected subcutaneously with MRSA ($3x10^6$ CFU). WT mice were treated daily with topical ointments containing $3.37x10^{-6}$% LTB_4, 0.001% BLT1 antagonist U-75302, or vehicle. Gene expression for *Il1b* from naive skin or day 1 post infection. **B)** ELISA for IL-1β from biopsies collected from mice described in **A** and also naive skin and day 1 post MRSA infection from *Ltb4r1*$^{-/-}$ mice. **C-D)** pIL1DsRED mice were infected subcutaneously with MRSA ($3x10^6$ CFU) and treated daily with topical ointments containing 0.001% BLT1 antagonist (U-75302) or vehicle. **C)** Images of naive or day 1 infected pIL1DsRED mice scanned for DsRED fluorescence by IVIS as described in the "Materials and methods". Images are representative of 8-12 mice from 2-3 experiments. **D)** DsRED fluorescence intensity measured daily for five days post infection. Data are mean ± SEM of 3-10 mice from 2-4 experiments. **A** and **B)** *p < 0.05 vs. naive, #p < 0.05 vs. Day 1 WT treated with vehicle (One-way ANOVA with Tukey multiple comparison correction). **D)** *p < 0.05 vs. WT treated with vehicle (Two-way ANOVA followed by Tukey multiple comparison correction).

a pro-cytokine, which requires maturation [121]. MRSA skin infection induced expression of *Il1b* **(Figure 15A)**. MRSA-infected mice treated with LTB_4 ointment did not significantly alter *Il1b* expression, however BLT1 antagonist U-75302 treatment blunted *Il1b* expression during MRSA skin infection. ELISA data confirmed that IL-1β is produced in the skin of mice during MRSA skin infection and that LTB_4 treatment increased levels of IL-1β **(Figure 15B)**. Increased levels of IL-1β despite no differences in gene expression suggest that LTB_4 may be involved in promoting IL-1β processing. BLT1 antagonist treatment and mice deficient in BLT1 had lower levels of IL-1β at day 1 post MRSA skin infection compared to WT mice. To determine whether LTB_4 influences the kinetics of IL-1β during MRSA skin infection, we employed the IL-1β reporter mouse pIL1DsRED [151] using IVIS in vivo imaging technology. The pIL1DsRED mice were infected with MRSA and treated with a topical ointment containing BLT1 antagonist U-75032 or vehicle control. Mice were imaged by IVIS for DsRed signal every day post infection for 5 days **(Figure 15C)**. Signal of DsRed, was highest at days 1 and 2 post infection and decreased by day 3 of infection **(Figure 15D)**. This suggests that IL-1β is expressed early during MRSA skin infection. BLT1 antagonist treatment had minimal expression of DsRed at all points measured during infection suggesting that LTB_4 was important for *Il1b* expression during MRSA skin infection.

Next, we aimed to identify which cells produced IL-1β during MRSA skin infection. The pIL1DsRED mice were infected with MRSA and treated with or without BLT1 antagonist U-75302. BLT1 antagonist treatment did not alter the

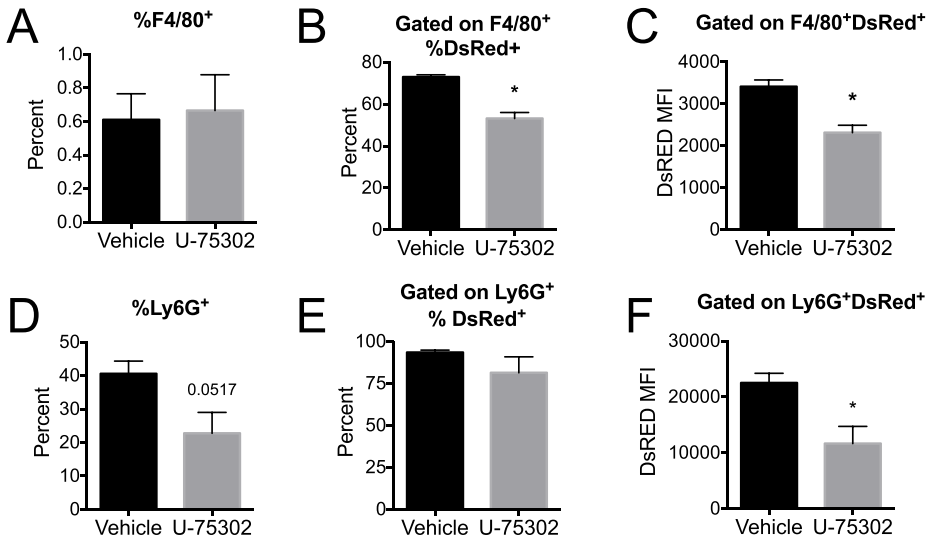

Figure 16. LTB_4/BLT1 promotes IL-1β expression in the skin. A-F) pIL1DsRED mice were infected subcutaneously with MRSA ($3x10^6$ CFU) and treated daily with topical ointments containing 0.001% BLT1 antagonist (U-75302) or vehicle. Skin biopsies were collected at day 1 post infection and processed for flow cytometry analysis as described in the "Materials and methods". **A)** Percentage of macrophages (F4/80). **B)** Percentage of $F4/80^+$ macrophages expressing DsRed and **C)** DsRed MFI of cells from **B. D)** Percentage of neutrophils (Ly6G). **E)** Percentage of $Ly6G^+$ neutrophils expressing DsRed and **F)** DsRed MFI of cells from **E.** Data are mean ± SEM of 3 mice from 2 experiments. *$p < 0.05$ (Student's t-test).

percent of macrophages in the skin during MRSA skin infection **(Figure 16A)**, however the percent of macrophages expressing *Il1b* (DsRed) was significantly lower than macrophages in the skin of untreated mice **(Figure 16B)**. Not only was the percent of $F4/80^+$ macrophages expressing DsRed was reduced with BLT1 antagonist treatment, but also the mean fluorescence intensity (MFI) of DsRed was reduced in cells expressing DsRed **(Figure 16C).** The percent of $Ly6G^+$ neutrophils was reduced in the skin of mice treated with BLT1 antagonist **(Figure 16D)**. The percent of $DsRed^+$ neutrophils was not significantly reduced but the MFI of DsRed was lower in mice treated with BLT1 antagonist **(Figure 16E-F)**.

Although LTB_4/BLT1 was necessary for mature IL-1β production and since topical treatment with LTB_4 did not enhance expression of *Il1b*, the next step was to evaluate whether LTB_4 controlled IL-1β processing through inflammasome activity. To determine inflammasome assembly, neutrophils were imaged by

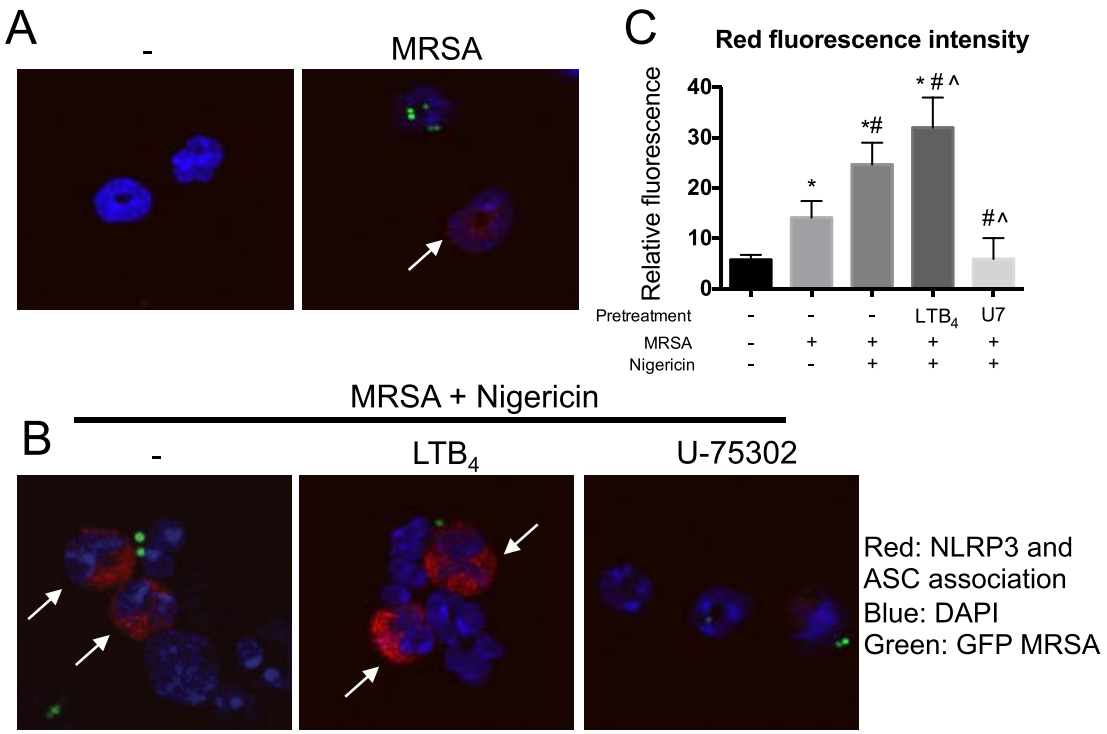

Figure 17. LTB_4 enhances inflammasome assembly. A-C) Bone marrow neutrophils were challenged or not with GFP-expressing MRSA followed by inflammasome activation with nigericin for PLA staining as described in the "Materials and methods". GFP-MRSA shown in green, nuclear DAPI stain shown in blue, and PLA staining for NLRP3 and ASC association shown in red. **A)** Bone marrow neutrophils challenged or not with GFP-MRSA. **B)** Bone marrow neutrophils cultured with GFP-MRSA were pretreated with 10nM LTB_4 or 10μM BLT1 antagonist U-75302 and treated with 1μM nigericin as described in the "Materials and methods". Images are 100X magnification and are representative from neutrophils from 2-3 mice from 1 experiment. **C)** Quantification of red fluorescence intensity from images in **A** and **B** measured by ImageJ analysis as described in the "Materials and methods". Data are mean ± SEM from at least 3-10 neutrophils counted from 2-3 mice from 1 experiment. *$p < 0.05$ vs. cells only, #$p < 0.05$ vs. MRSA only, ^$p < 0.05$ vs. MRSA + nigericin (One-way ANOVA followed by Tukey multiple comparison correction). White arrows indicate NLRP3 and ASC association shown as red fluorescence.

fluorescence microscopy to determine associations of NLRP3 and ASC using PLA. Close proximity of these proteins resulted in red fluorescence. Neutrophils from WT mice were cultured with GFP-expressing MRSA for 3 hours followed by inflammasome activation with nigericin for 1 hour. Neutrophils with no treatment did not show interactions between NLRP3 and ASC **(Figure 17A)**. Neutrophils co-cultured with MRSA induced minimal, but significant, inflammasome assembly. Inflammasome-activated (with nigericin treatment) neutrophils showed significantly higher inflammasome assembly compared to cells only, and LTB_4 treatment further promoted inflammasome assembly. BLT1 antagonist U-75302 treatment inhibited inflammasome assembly **(Figure 17B-C)**. These results suggest that LTB_4/BLT1 is important for *Il1b* expression and that LTB_4 may be an important mediator in regulating inflammasome assembly and activation allowing for mature IL-1β production.

Macrophages are critical for LTB_4 production

Although neutrophils are a major cell type recruited to the skin during MRSA skin infection, macrophages were observed surrounding the neutrophil abscess. Perivascular macrophages have been shown to be important for neutrophil recruitment to the skin [165]. The role of resident macrophages in the skin was during MRSA infection was next evaluated. MMDTR mice were used to investigate this role. MMDTR mice are $Csf1r^{LsL\text{-}DTR\text{-}mCherry}$ mice crossed with $LysM^{cre}$ [152] and are described in more detail in the “Materials and Methods”. Macrophage depletion was confirmed by two methods. The first method was to

scan the mice for mCherry fluorescence by IVIS in vivo imaging. MMDTR mice treated with DT to deplete macrophages reduced mCherry fluorescence in both naive (uninfected) skin and at day 1 post MRSA skin infection **(Figure 18A)**. The second method to confirm macrophage depletion in the skin was to take a biopsy punch at day 1 post MRSA skin infection, dissociated to generate single cells, and detected mCherry by flow cytometry. MMDTR mice treated with DT resulted in lower % mCherry^{+} cells in the skin compared to the PBS vehicle control **(Figure 18B).**

After confirming that the macrophage depletion method was successful, MMDTR mice were treated with DT or PBS-vehicle and infected with MRSA in

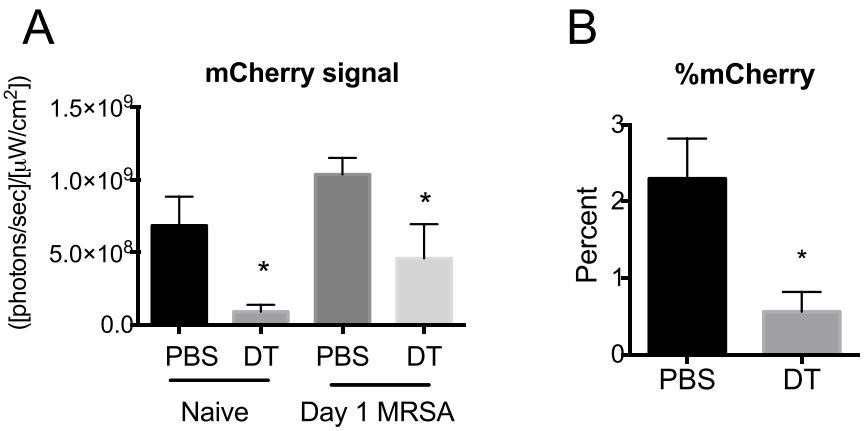

Figure 18. MMDTR mice macrophage depletion. A-B) MMDTR mice were treated with DT to deplete monocytes/macrophages or treated with PBS-vehicle as described in the "Materials and methods". **A)** MMDTR mice treated with DT and PBS were infected subcutaneously with MRSA ($3x10^6$ CFU). Naive and MRSA-infected mice were scanned by IVIS to measure mCherry fluorescence. **B)** Skin biopsies were collected at day 1 post infection and processed for flow cytometry analysis as described in the "Materials and methods". Percent of mCherry^{+} cells in the skin of MMDTR mice treated with PBS or DT. Data are mean ± SEM of 3-8 mice from 1-2 experiments. **A)** *$p < 0.05$ vs. PBS-treated MMDTR mice (One-way ANOVA followed by Tukey multiple comparison correction). **B)** *$p < 0.05$ (Student's t-test).

order to determine the role of macrophages in the immune response to MRSA skin infection. Immunofluorescence was performed on skin biopsy sections taken at day 1 post MRSA skin infection from MMDTR mice treated with PBS-vehicle or

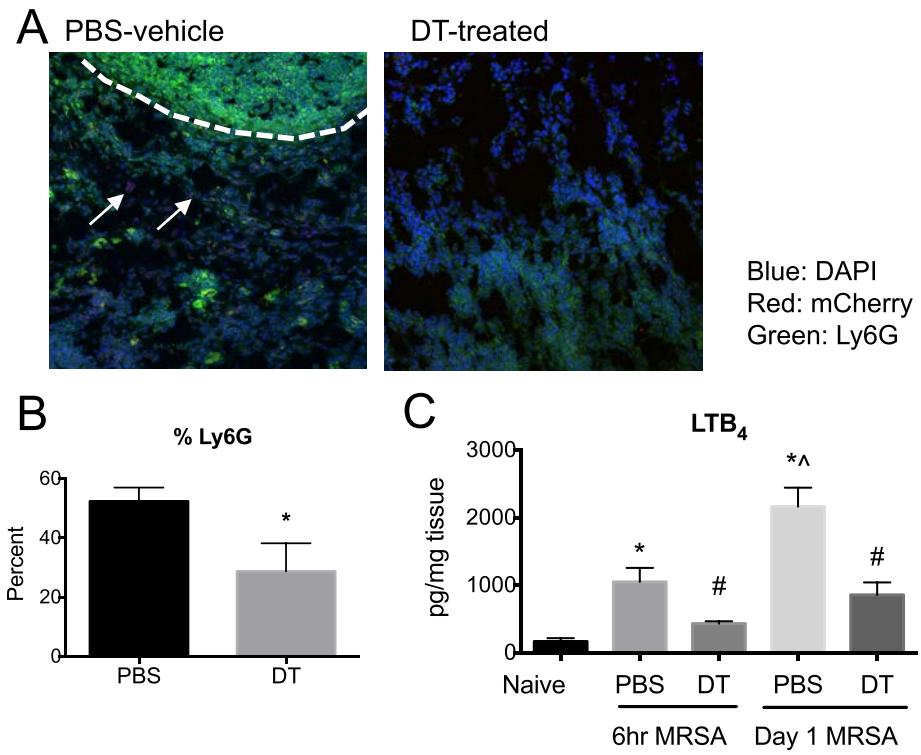

Figure 19. Macrophages are necessary for host defense during MRSA skin infection. A-C) MMDTR mice were treated with DT to deplete monocytes/ macrophages or treated with PBS-vehicle as described in the "Materials and methods". MMDTR mice treated with DT and PBS were infected subcutaneously with MRSA ($3x10^6$ CFU). **A)** IF of biopsy skin sections collected at day 1 post infection for nuclear DAPI stain (blue), mCherry macrophages (red), and Ly6G-AF488 neutrophils (green). Images are 20X magnification and representative of 3-5 mice from 1 experiment. **B)** Flow cytometry analysis of biopsies collected at day 1 post MRSA skin infection from PBS and DT-treated MMDTR mice. Percentage of $Ly6G^+$ neutrophils in the skin. **C)** LTB_4 EIA on skin biopsy homogenates collected from naive skin, 6 hours and day 1 post infection. Data are mean ± SEM of 3-8 mice from 2-3 experiments. **B)** *$p < 0.05$ (Student's t-test) **C**. *$p < 0.05$ vs. naive, #$p < 0.05$ vs. PBS-treated, ^$p < 0.05$ vs. PBS-treated MMDTR at 6 hours post infection (One-way ANOVA followed by Tukey multiple comparison correction). White arrows indicate $mCherry^+$ macrophages. White dotted lines indicate abscess edge.

DT. PBS-treated MMDTR showed abundant neutrophil recruitment and abscess formation, shown as Ly6G-AlexaFluor-488 (Ly6G-AF488) green staining, whereas DT-treated mice had fewer neutrophils and the neutrophils present in the skin failed to develop into an abscess **(Figure 19A)**. Macrophages (mCherry) shown in red were found nearby the neutrophilic abscess in PBS mice, but were not present in DT-treated mice. Since fewer neutrophils were observed by immunofluorescence staining in macrophage-depleted mice, this finding was confirmed by flow cytometry. MMDTR mice treated with DT had fewer neutrophils in the skin at day 1 post MRSA skin infection compared to PBS treated MMDTR mice **(Figure 19B)**. This suggests that macrophages are necessary for neutrophil recruitment and for promoting abscess architecture. Since our data show that LTB_4 is an important mediator involved in controlling MRSA skin infection, LTB_4 was measured in the skin from MMDTR mice 6 hours and day 1 post infection. Macrophage depletion resulted in lower production of LTB_4 compared to PBS-treated mice **(Figure 19C)**, demonstrating that macrophages were an important player in promoting LTB_4 production.

In order to determine whether a lack of LTB_4 in macrophage depleted mice was contributing to poor host defense, DT-treated MMDTR mice were treated with a topical ointment containing LTB_4. Macrophage depletion resulted in larger infection area compared to control mice, but topical LTB_4 treatment on macrophage-depleted mice reduced infection area size **(Figure 20A)**. Macrophage depletion resulted in higher bacterial burdens in the skin, which was reduced when MMDTR mice were treated with LTB_4 **(Figure 20B)**. Topical LTB_4

ointment application on PBS-vehicle control treated mice during MRSA skin infection had minimal effects. These data suggest that macrophages play a major

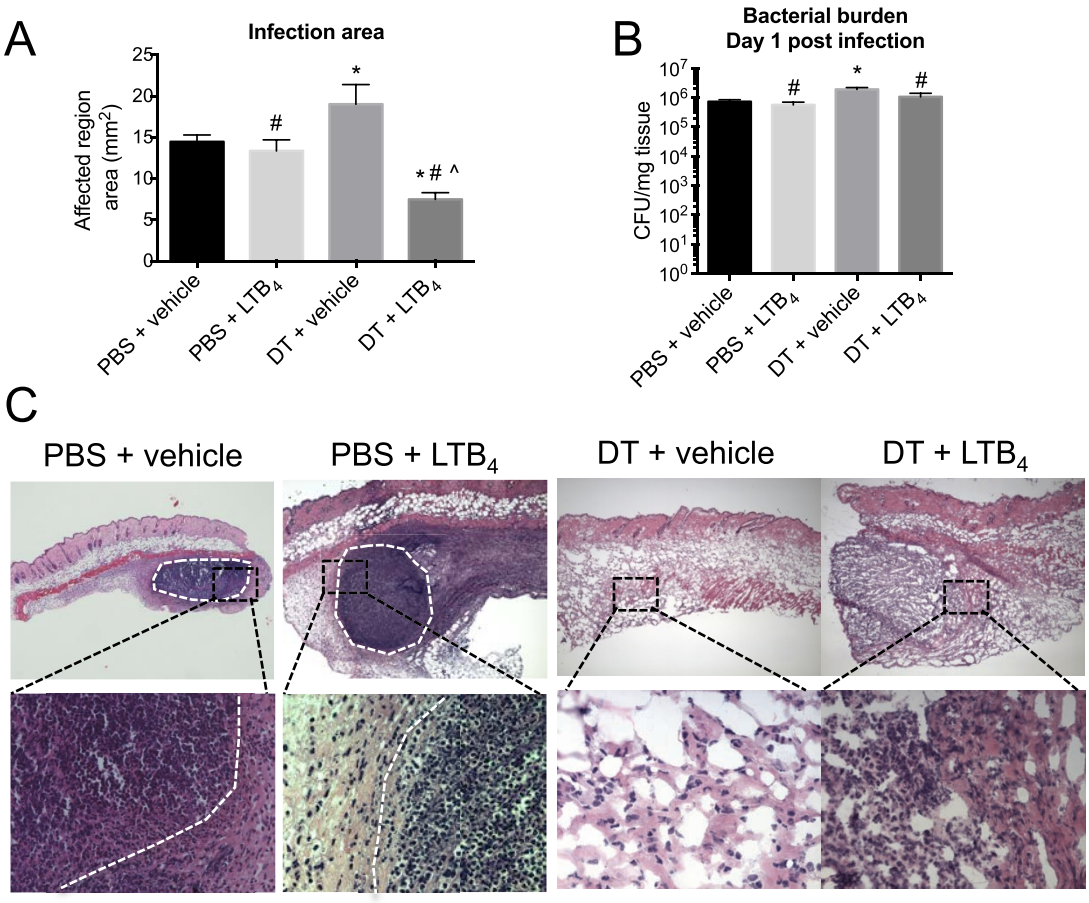

Figure 20. LTB_4 treatment partially restores host defense in MMDTR mice. A-C) MMDTR mice were treated with DT to deplete monocytes/ macrophages or treated with PBS-vehicle as described in the "Materials and methods". PBS and DT-treated MMDTR mice were infected subcutaneously with MRSA ($3x10^6$ CFU) and treated with topical ointments containing $3.37x10^{-6}$% LTB_4 ointment or vehicle. **A)** Infection areas measured at day 1 post infection. **B)** Bacterial CFUs normalized to tissue weight were measured at day 1 post infection. **C)** H&E images. Top panels show 4X and bottom panels show 40X magnification. Images are representative of 4-5 mice from 1 experiment. Data are mean ± SEM of 4-8 mice from 1-2 experiments. *$p < 0.05$ vs. PBS-treated MMDTR treated with vehicle, #$p < 0.05$ vs. DT-treated MMDTR treated with vehicle, ^$p < 0.05$ vs. PBS-treated MMDTR treated with LTB_4 (One-way ANOVA followed by Tukey multiple comparison correction). Dotted lines indicate abscess edge.

role in the immune response during MRSA skin infection by promoting LTB_4 production. Additionally, histology sections taken at day 1 post infection revealed that macrophage-depleted mice did not develop an abscess structure, but topical LTB_4 treatment give to DT-treated mice partially restored neutrophil aggregate formation (**Figure 20C)**. This suggests that LTB_4 and macrophages, possibility

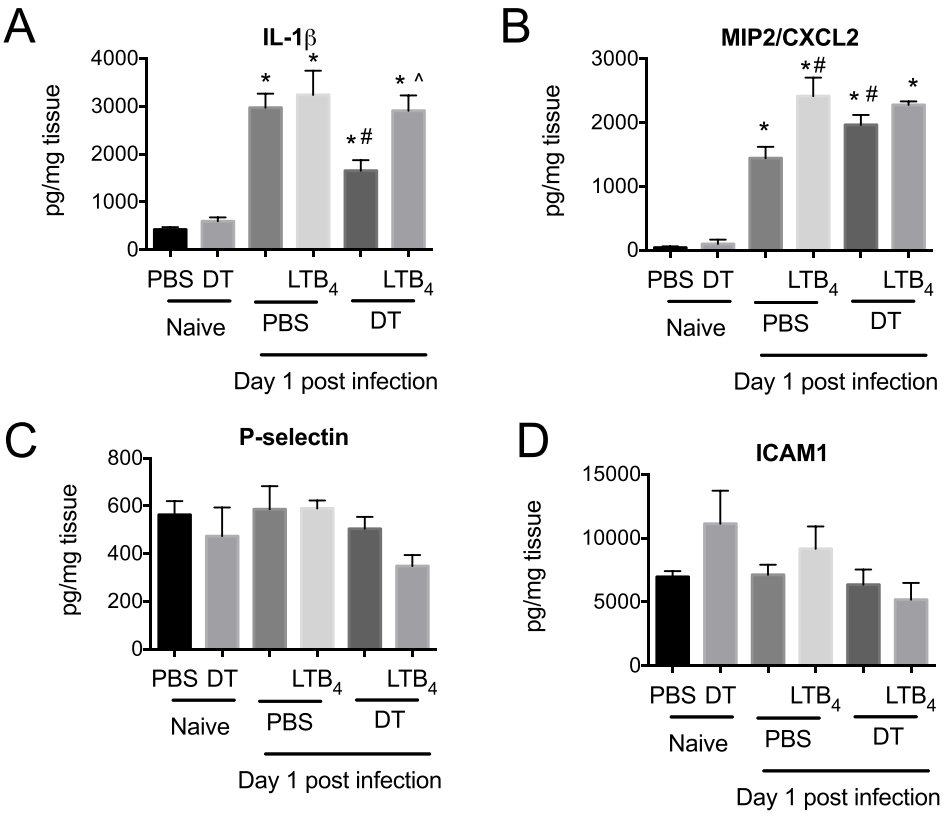

Figure 21. Cytokine and chemokine expression in MMDTR mice. A-D) MMDTR mice were treated with DT to deplete monocytes/macrophages or treated with PBS-vehicle as described in the "Materials and methods". PBS and DT-treated MMDTR mice were infected subcutaneously with MRSA ($3x10^6$ CFU) and treated with topical ointments containing $3.37x10^{-6}$% LTB_4 ointment or vehicle. Biopsies were collected from naive skin or day 1 post infection and used to detect multiple analytes by multiplex assay. **A)** IL-1β. **B)** MIP2/CXCL2. **C)** P-selectin. **D)** ICAM1. Data are mean ± SEM of 3-10 mice from 2-4 experiments. *$p < 0.05$ vs. naive, #$p < 0.05$ vs. infected PBS-treated MMDTR treated with vehicle, ^$p > 0.05$ vs. DT-treated MMDTR treated with vehicle. (One-way ANOVA followed by Tukey multiple comparison correction).

along with other factors, are needed for orchestrating abscess formation during MRSA skin infection.

The next question was whether macrophage depletion affected chemokine and cytokine production. Multiplex assays were conducted on skin biopsy homogenates from PBS-vehicle and DT-treated MMDTR mice that were treated with or without topical LTB_4 ointment. Macrophage depletion reduced the levels of IL-1β at day 1 post infection, which was restored with topical LTB_4 treatment **(Figure 21A)**. Expression of neutrophil chemotactic molecules (CXCL2, P-selectin, and ICAM1) was either unchanged or expressed at higher levels in macrophage-depleted mice **(Figure 21B-D)**. Since macrophages were important for neutrophil recruitment as determined by H&E analysis, but expression of cytokines, chemokines, and adhesion molecules were not all downregulated, this suggests that neutrophils may be capable of recruiting to the site of infection. This suggests other signals provided by macrophages, such as LTB_4, or having direct contact with macrophages is necessary for recruitment and abscess formation.

Macrophage depletion resulted in lower LTB_4 production and reduced neutrophil recruitment. Neutrophils are also capable of producing LTB_4 at the site of injury [81]. In order to determine the role and contribution of neutrophils during MRSA skin infection, WT mice were treated with αLy6G (clone 1A8) depleting antibody or IgG control prior to MRSA skin infection. Infection areas were measured at day 1 post infection, and mice depleted of neutrophils had larger infection areas compared to IgG-controls **(Figure 22A)**. Biopsies were taken at 6

hours and day 1 after infection to measure LTB_4 in the skin. Neutrophil depletion resulted in lower LTB_4 in the skin, but did not completely eliminate production **(Figure 22B)**. To confirm neutrophil depletion, H&E stains were prepared from biopsies. Mice treated with IgG control antibody had abundant cell recruitment

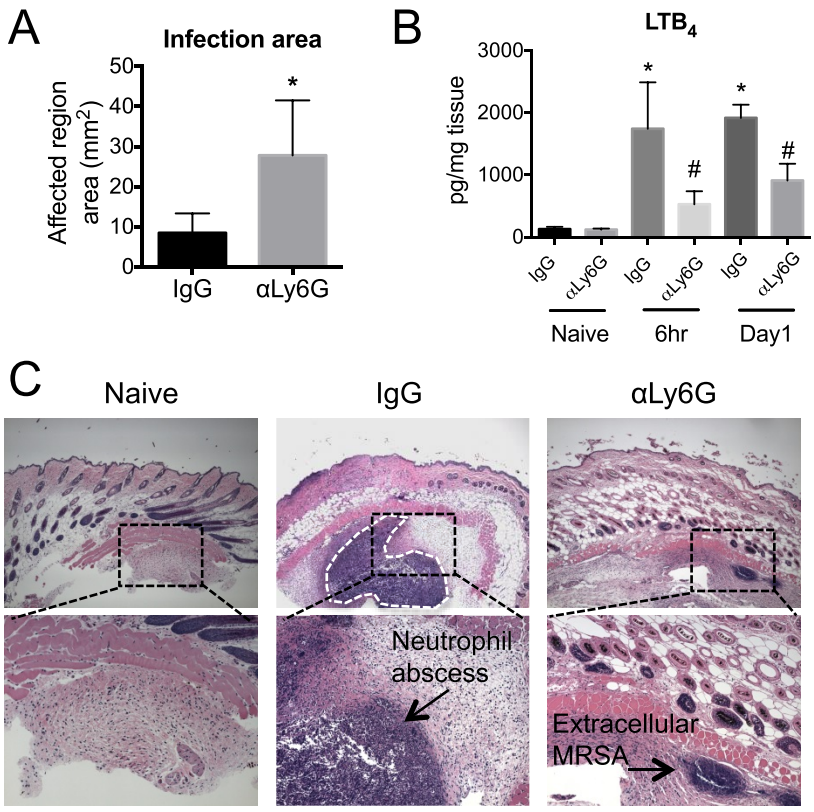

Figure 22. Neutrophils contribute to LTB_4 production. A-C) WT mice were treated with 200µg of Ly6G (clone 1A8) or IgG control 18 hours prior to subcutaneous MRSA skin infection ($3x10^6$ CFU) as described in the "Materials and methods". **A)** Infection area of IgG-treated and αLy6G-treated mice measured at day 1 post infection. **B)** LTB_4 EIA on skin biopsy homogenates collected from naive, 6 hour and day 1 post infection. **C)** H&E images of skin biopsy sections at day 1 post infection. Top panels show 4X and bottom panels show 40X magnification. Images are representative of 4-5 mice from 1 experiment. Data are mean ± SEM of 4-5 mice from 1 experiment. **A)** *$p < 0.05$ (Student's t-test) **B)** *$p < 0.05$ vs. naive, #$p < 0.05$ vs. IgG-treated comparing the same time point (One-way ANOVA followed by Tukey multiple comparison correction). Dotted line indicates abscess edge. Arrows indicate abscess or extracellular MRSA as indicated.

and abscess formation but mice treated with αLy6G antibody had drastically fewer cells in the skin **(Figure 22C)**. Additionally, pockets of extracellular bacteria were observed in neutrophil-depleted mice. These data suggest that macrophages and neutrophils are contributing to LTB_4 production in the skin during infection. However, since other cell types can produce LTB_4, more experiments are needed to elucidate the contribution from specific cell types during MRSA skin infection. Nonetheless, since LTB_4 treatment did not fully restore macrophage-depleted mice, this demonstrates the importance of the interaction between macrophages and neutrophils that require LTB_4.

LTB_4 has therapeutic potential for treating MRSA skin infections

Due to the beneficial role of LTB_4 mediating neutrophil abscess architecture and promoting NADPH-oxidase mediated killing of MRSA, the next question was whether LTB_4 has therapeutic potential for treating MRSA skin infections. Therefore, we further pursued our studies using an antibiotic that is commonly used to treat gram-positive bacterial infections.

Vancomycin (1%) was emulsified in an ointment and used to treat mice infected with MRSA. Vancomycin is used as an intravenous therapy [172] with limited skin penetration. Topical vancomycin preparation had no significant effect on infection area **(Figure 23A)**. LTB_4 ointments had a slight improvement in reducing infection area, and the combination ointment with LTB_4 and vancomycin had no effect relative to LTB_4 ointment alone. Mupirocin (2%) is a topical ointment antibiotic that is used to treat minor skin infections [172]. Mice treated

with 2% mupirocin ointments were very effective at eliminating the MRSA skin infection **(Figure 23B)**. As observed before, LTB_4 ointment slightly reduced infection area, but due to the potency of 2% mupirocin, it was not possible to determine whether combination ointment with 2% mupirocin and LTB_4 had synergistic effects.

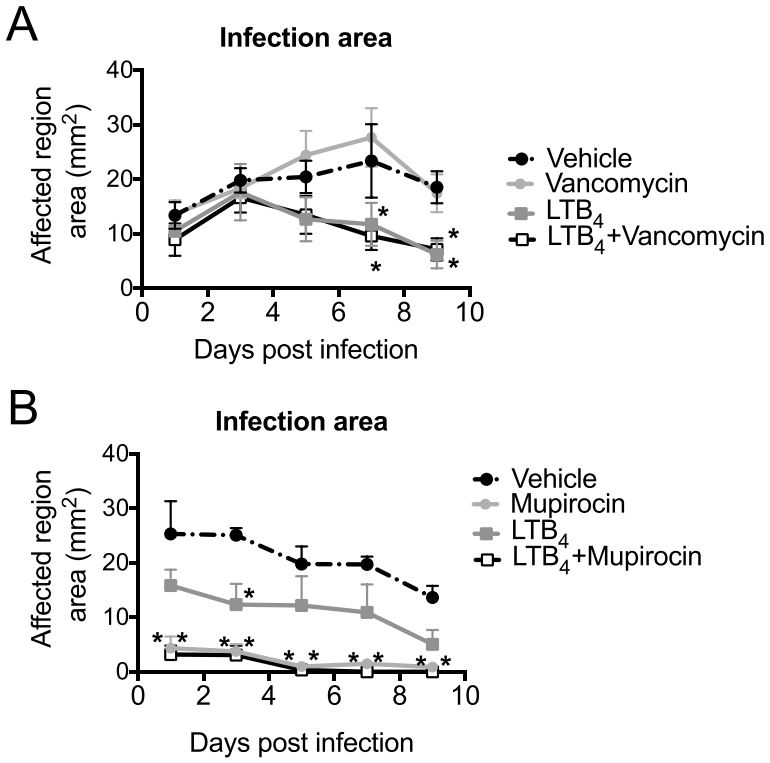

Figure 23. LTB_4 and antibiotic treatments. A) WT mice were infected subcutaneously with MRSA ($3x10^6$ CFU) and treated daily with topical ointments containing 1% vancomycin, $3.37x10^{-6}$% LTB_4, 1% vancomycin + $3.37x10^{-6}$% LTB_4 combination, or vehicle. Infection areas were measured every other day for 9 days post infection. **B)** WT mice were infected subcutaneously with MRSA ($3x10^6$ CFU) and treated daily with topical ointments containing 2% mupirocin, $3.37x10^{-6}$% LTB_4, 2% mupirocin + $3.37x10^{-6}$% LTB_4 combination, or vehicle. Infection areas were measured every other day for 9 days post infection. Data are mean ± SEM of 4-5 mice from 1-2 experiments. *$p < 0.05$ vs. vehicle-control-treated (Two-way ANOVA followed by Tukey multiple comparison correction).

To determine whether mupirocin and LTB_4 function synergistically together, the concentration of mupirocin was reduced from 2% to 0.1%. WT mice were infected with bioluminescent-expressing MRSA and treated with ointments containing no active ingredients, LTB_4 alone, topical antibiotic mupirocin alone, or a combination ointment containing LTB_4 and mupirocin. The use of bioluminescent-expression MRSA allowed for in vivo quantification of bacteria in

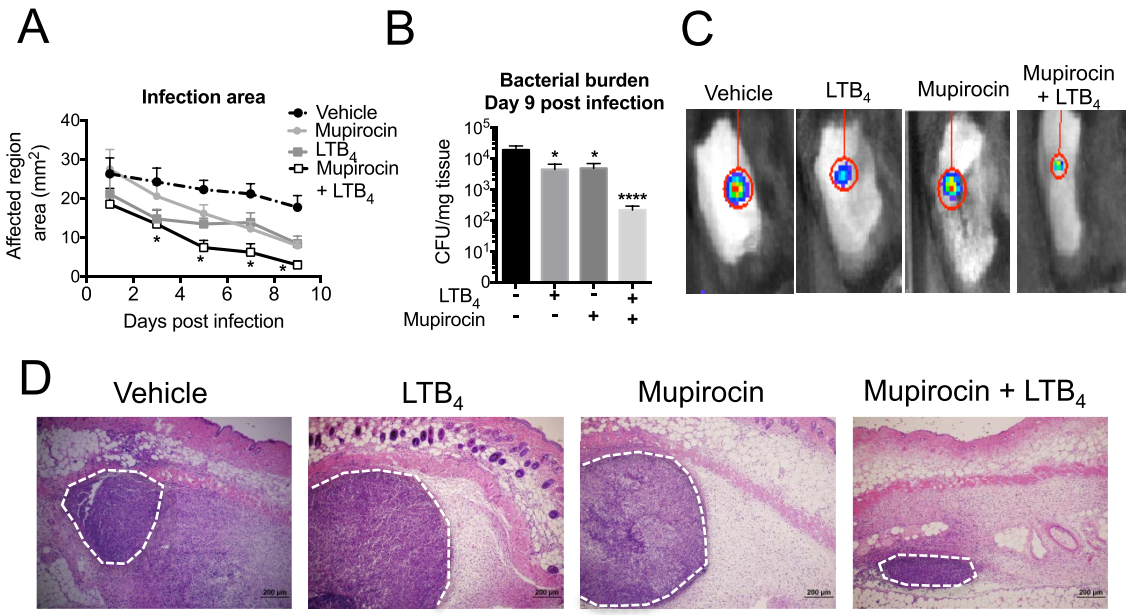

Figure 24. LTB_4 + mupirocin is a potential therapeutic strategy for treating MRSA skin infections. A-C) WT mice were infected subcutaneously with bioluminescent-expressing MRSA ($3x10^6$ CFU) and treated daily with topical ointments containing 0.1% mupirocin, $3.37x10^{-6}$% LTB_4, 0.1% mupirocin + $3.37x10^{-6}$% LTB_4 combination, or vehicle. **A)** Infection areas were measured every other day for 9 days post infection. **B)** Bacterial CFUs normalized to tissue weight measured at day 9 post infection. **C)** BLI of mice scanned by IVIS at day 9 post infection. Images are representative of 5-10 mice from 2 experiments. **D)** H&E images of skin biopsy sections collected at day 1 post infection. Images are 4X magnification and representative of 4-5 mice from 1 experiment. Data are mean ± SEM of 4-5 mice from 1-2 experiments. **A)**$*p < 0.05$ vs. vehicle (Two-way ANOVA followed by Tukey multiple comparison correction). **B)** $*p < 0.05$ vs. vehicle, $****p < 0.001$ vs. vehicle (One-way ANOVA followed by Tukey multiple comparison correction). White dotted lines indicate abscess edge.

the same mouse throughout infection, which aided in determining how effective the ointment treatments were. LTB_4 ointment and mupirocin ointments alone had a slight reduction in infection area compared to WT with no treatment **(Figure 24A)**. The combination ointment containing both LTB_4 and mupirocin greatly reduced infection area and was more effective than the single-agent ointments. The reduction in infection area correlated with a reduction in bacterial burden **(Figure 24B)**. The combination ointment was more successful in promoting bacterial clearance than the single agents alone, which was determined by CFU counts from skin biopsy homogenates and by detecting bioluminescence from bioluminescence-expressing MRSA **(Figure 24C)**. Lastly, H&E sections from biopsies collected at day 1 post MRSA skin infection were evaluated for abscess structure. LTB_4 and mupirocin ointments promoted a defined abscess structure; however the combination ointment developed a smaller, more compact abscess structure **(Figure 24D)**. This suggests that LTB_4 in combination with topical antibiotic mupirocin therapy is a promising strategy to treat MRSA skin infections.

Part II - Aberrant LTB_4 in diabetes drives poor host defense

Diabetic mice have worse skin infection outcome than control mice

People with diabetes are more susceptible to infections [143]. We established a model of MRSA skin infection and diabetes. Male C57BL/6 mice were injected with STZ or vehicle control as described in the "Materials and methods" 30-days prior to MRSA skin infection. STZ-treated mice with blood glucose levels >250mg/dL were considered diabetic. STZ-induced diabetic mice infected subcutaneously with MRSA had significantly larger areas of infection compared to vehicle-control (CT) mice **(Figure 25A-B)**. At day 9 post infection CT mice were mostly healed from the infection, whereas diabetic mice had high bacterial burdens in the skin **(Figure 25C)**.

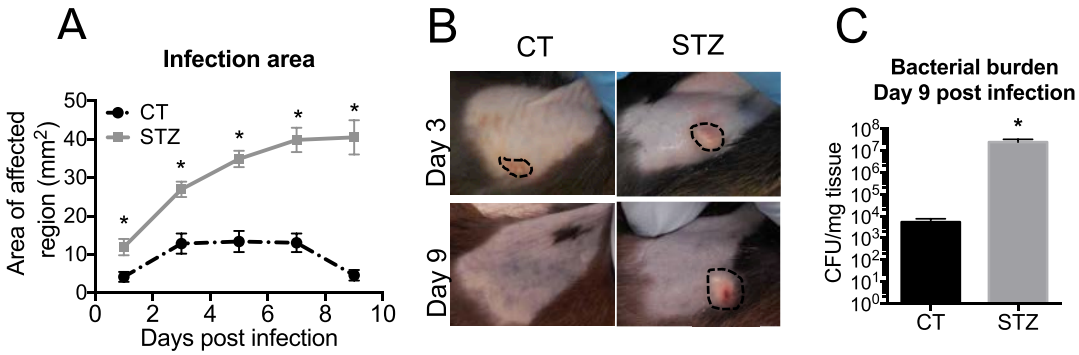

Figure 25. STZ-induced diabetes MRSA infection model. A-C) WT mice were treated with STZ to induce diabetes or treated with vehicle (CT). CT and STZ mice were infected subcutaneously with MRSA ($3x10^6$ CFU). **A)** Infection areas measured every other day for 9 days post infection. **B)** Images of infected areas of CT and STZ mice taken at days 3 and 9 post infection. Images are representative of 10-20 mice from 4-5 experiments. **C)** Bacterial CFUs normalized to tissue weight measured at day 9 post infection. Data are mean ± SEM of 5-10 mice from 2-5 experiments. **A)** *$p < 0.05$ vs. CT (Two-way ANOVA followed by Tukey multiple comparison correction. **C)** *$p < 0.05$ (Student's t-test). Dotted lines outline abscess area.

Another model of T1D was used to confirm experimental findings observed with the STZ-induced diabetes model to address the research goals. Female non-obese diabetic (NOD) mice spontaneously develop T1D at approximately 10-12 weeks of age. Diabetic NOD mice were diabetic (blood glucose >250mg/dL) for no longer than 2 weeks prior to infection. Diabetic NOD (dbNOD) mice had significantly larger infection areas that worsened throughout the course of infection compared to nondiabetic NOD mice (ctNOD) **(Figure 26A-B)**. At day 9 post MRSA infection, dbNOD mice had higher bacterial burdens compared to ctNOD mice **(Figure 26C).** Since the NOD genetic background is known to have impaired innate and adaptive immune functions [173-175], the majority of experiments to address the research goals were accomplished using the STZ-induced diabetes model.

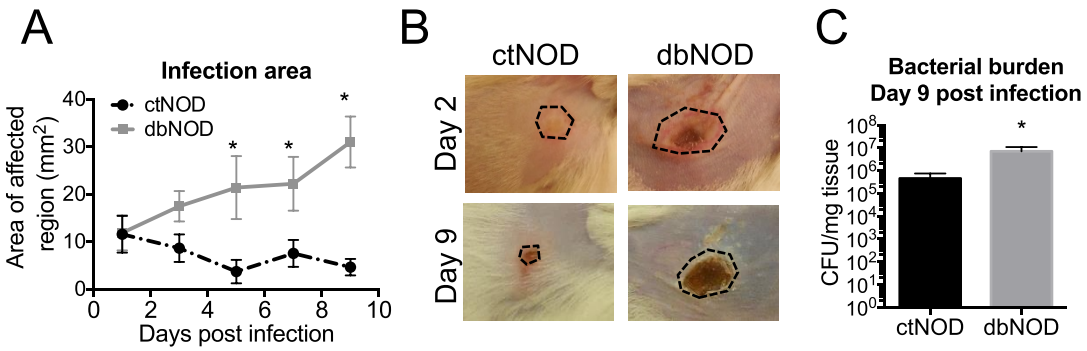

Figure 26. NOD MRSA infection model. A-C) Diabetic (dbNOD) and nondiabetic (ctNOD) mice as described in the "Materials and methods" were infected subcutaneously with MRSA ($3x10^6$ CFU). **A)** Infection areas measured every other day for 9 days post infection. **B)** Images of infected areas of ctNOD and dbNOD mice taken at days 2 and 9 post infection. Images are representative of 10-15 mice from 2-4 experiments. **C)** Bacterial CFUs normalized to tissue weight measured at day 9 post infection. Data are mean ± SEM of 3-6 mice from 2-3 experiments. **A)** *$p < 0.05$ vs. ctNOD (Two-way ANOVA followed by Tukey multiple comparison correction). **C)** *$p < 0.05$ (Student's t-test). Dotted lines outline infection area.

We aimed next to identify the components involved in the poor host defense associated with diabetes. We initially asked whether the poor skin infection outcome could be due to an altered inflammatory response or generation of antimicrobial effector mechanisms. To determine whether there were factors affecting host response, diabetic and nondiabetic mice were

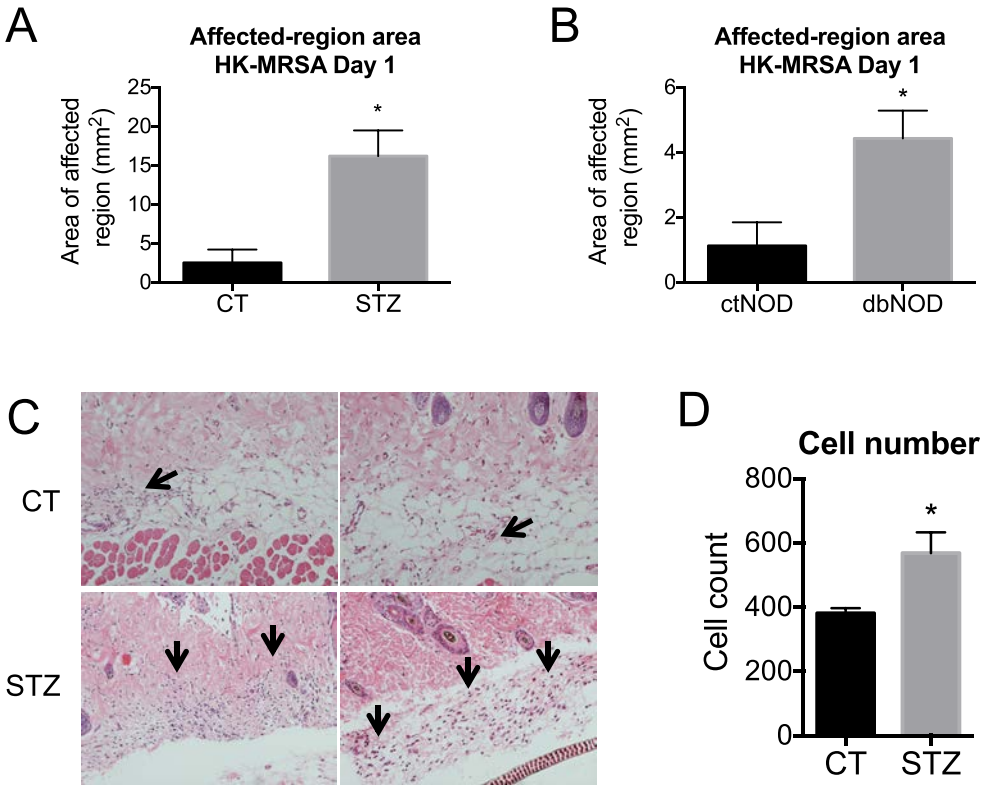

Figure 27. Heat-killed MRSA induces more inflammation in diabetic mice. **A)** CT and STZ mice were injected subcutaneously with HK-MRSA ($3x10^6$) and affected-region areas were measured at day 1 post injection. **B)** ctNOD and dbNOD mice were injected subcutaneously with HK-MRSA ($3x10^6$) and affected-region areas were measured at day 1 post injection. **C)** H&E images from CT and STZ mice described in **A.** Images show 10X magnification and are representative of 3-5 mice from 1-2 experiments. **D)** Cell number quantification from H&E images described in **C.** Quantification performed in ImageJ software as described in the "Materials and methods". Arrows indicate cell recruitment. Data are mean ± SEM of 4-6 mice from 1-2 experiments. *$p < 0.05$ (Student's t-test).

infected with $3x10^6$ heat-killed MRSA (HK-MRSA) to evaluate host activation and inflammation in the absence of bacterial growth. In both STZ-diabetic **(Figure 27A)** and NOD-diabetic mice **(Figure 27B)**, HK-MRSA induced more inflammation compared to their respective nondiabetic controls. Additionally, we observed more cell recruitment to the skin of STZ diabetic mice compared to nondiabetic controls **(Figure 27C-D)**. Since larger affected-regions and more cell recruitment were observed in the skin of diabetic mice, this suggests that there are intrinsic differences in immune cell activation that could lead to poor disease outcome during an active infection.

High LTB_4 production in the skin of diabetic mice

Previous research in our laboratory has shown that diabetic mice have high serum levels of LTB_4, which correlates with overwhelming inflammation and

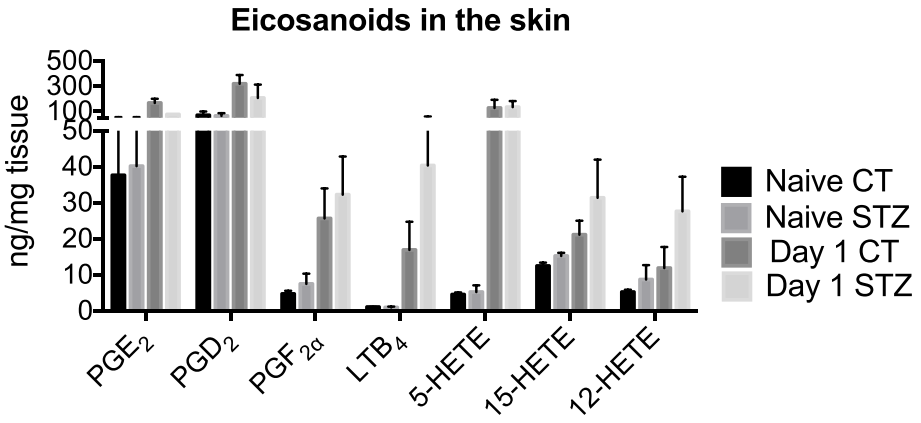

Figure 28. Mass spectrometry of eicosanoids in the skin. CT and STZ mice were infected subcutaneously with MRSA ($3x10^6$ CFU). Skin biopsies were collected from naive skin and at day 1 post infection. Skin biopsy sections were processed to measure eicosanoids by LC-MS as described in the "Materials and methods". Data are mean ± SEM of 2-4 mice from 1 experiment.

increased mortality during a model of polymicrobial sepsis [61]. Whether LTB_4 is implicated in poor host defense during MRSA skin infections is unknown. First, we wanted to identify the major eicosanoids in the skin of diabetic and nondiabetic mice during MRSA skin infection. A panel of the main eicosanoids produced during inflammation was detected by mass-spectrometry **(Figure 28)**. Levels of PGE_2 were seemingly lower in diabetic mice at day 1 post infection, which recapitulated previous findings [176]. Very low levels of LTB_4 levels were detected in naive skin from both diabetic and nondiabetic mice. However, MRSA skin infection induced LTB_4 production, which was exaggerated in the skin of MRSA-infected diabetic mice. Other lipoxygenase metabolites 15-HETE and 12-HETE were also elevated in diabetic mice infected with MRSA, while no differences were seen in 5-HETE levels. This suggests that there may be a

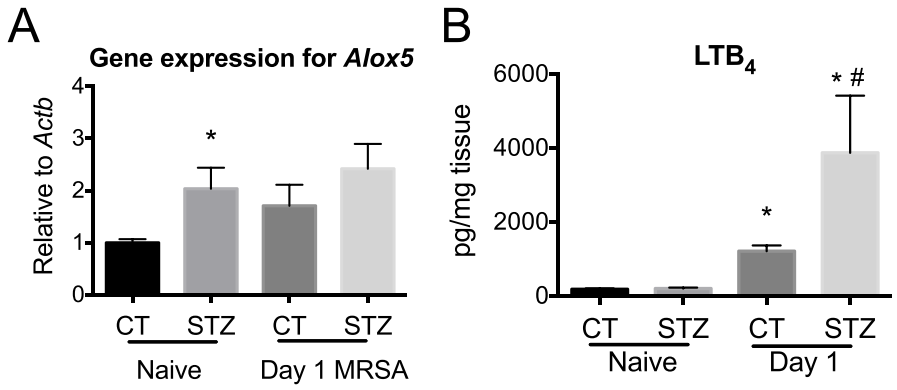

Figure 29. Diabetic mice produce more LTB_4 in the skin during MRSA infection. A-B) CT and STZ mice were infected subcutaneously with MRSA ($3x10^6$ CFU). **A)** Skin biopsies collected from naive skin or at day 1 post infection were analyzed for mRNA expression of *Alox5*. **B)** Skin biopsies homogenates from naive skin or at day 1 post infection were used to measured LTB_4 by EIA. Data are mean ± SEM of 4-10 mice from 2-4 experiments. **A)** *p < 0.05 vs. naive CT (One-way ANOVA followed by Tukey multiple comparison correction. **B)** *p < 0.05 vs. naive, #p < 0.05 vs. infected CT. (One-way ANOVA followed by Tukey multiple comparison correction).

skewing towards some lipoxygenase products, including LTB_4, in the skin of diabetic mice during MRSA skin infection.

We then determined the expression of *Alox5* in naive and day 1 infected skin from CT and STZ mice. There was higher expression of *Alox5* in the skin of diabetic mice, even in the absence of infection **(Figure 29A)**. Although MS analysis showed elevated levels of LTB_4 in the skin, these data were confirmed using EIA. Little LTB_4 was detected in naive skin from both CT and STZ mice. Upon MRSA skin infection, LTB_4 production was elevated in the skin but diabetic mice produced significantly more LTB_4 than CT mice **(Figure 29B)**. These data demonstrate that diabetic mice produce exaggerated levels of LTB_4 in the skin during MRSA infection independent of exaggerated 5-LO expression. This suggests that the activation of various LT synthesis enzymes may be altered in diabetic mice during MRSA skin infection compared to nondiabetic mice.

Uncontrolled BLT1 actions drive poor host defense in diabetic mice

Since LTB_4 can signal through one of two receptors, BLT1 and BLT2, the expression of these receptors was investigated. Expression of *Ltb4r1* was higher in the skin of diabetic mice at day 1 post infection **(Figure 30A**). No differences were observed in expression of *Ltb4r2* between diabetic and nondiabetic mice **(Figure 30B)**. Receptor expression of BLT1 and BLT2 was also confirmed determined by mean fluorescence intensity (MFI) measured by flow cytometry analysis on skin biopsy sections in naive, and days 1, 3, 9 post infection. MFI of BLT1 was higher in the skin of diabetic mice than nondiabetic mice at all time

points measured **(Figure 30C)**. MFI of BLT2 in naive skin was similar between CT and STZ mice, however the MFI of BLT2 during infection was higher in the skin of diabetic mice at day 1 post infection **(Figure 30D)**.

Next, we determined whether genetic deletion of BLT1 or leukotriene production was able to influence host defense to MRSA skin infection in diabetic

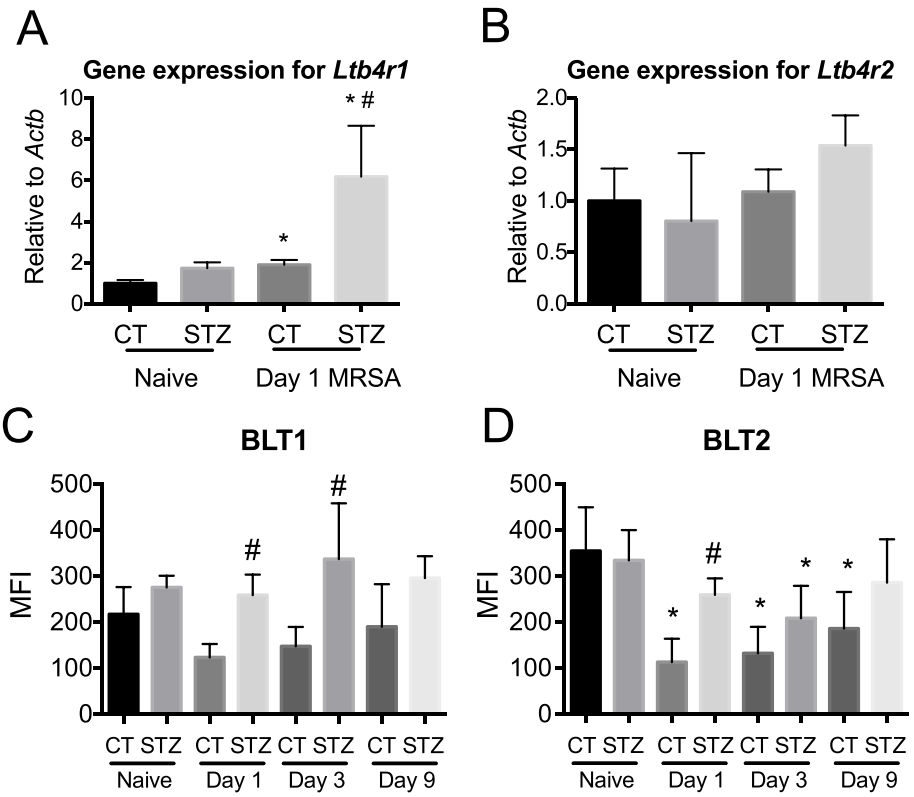

Figure 30. BLT1 and BLT2 MFI in the skin. A-D) CT and STZ mice were infected subcutaneously with MRSA ($3x10^6$ CFU). **A)** Skin biopsies collected from naive skin or at day 1 post infection were analyzed for mRNA expression of *Ltb4r1*. **B)** Skin biopsies collected from naive skin or at day 1 post infection were analyzed for mRNA expression of *Ltb4r2*. **C)** Skin biopsies collected from naive skin and at days 1, 3, and 9 post infection were processed for flow cytometry as described in the "Materials and methods". MFI of cells for BLT1. **D)** Skin biopsies processed for flow cytometry as described in **C** to measure MFI for BLT2. Data are mean ± SEM of 3-8 mice from 1-3 experiments. *$p < 0.05$ vs. naive, #$p < 0.05$ vs. CT compared to the same time point (One-way ANOVA followed by Tukey multiple comparison correction).

mice. Mice deficient in BLT1 (*Ltb4r1*$^{-/-}$) and leukotriene-deficient mice (*Alox5*$^{-/-}$) were induced diabetic with STZ and infected with MRSA. Both *Alox5*$^{-/-}$ and *Ltb4r1*$^{-/-}$ mice were more resistant to developing hyperglycemia after STZ treatment compared to WT. Both knockout strains received more STZ injections, as described in the "Materials and methods" to elevate blood glucose levels to similar levels observed in WT mice treated with STZ **(Figure 31A)**. This allowed for better comparison of the effects of 5-LO and BLT1 deficiencies during hyperglycemia. STZ-diabetic mice deficient in BLT1 and 5-LO products were better protected from MRSA skin infection than WT STZ mice as determined by smaller infection areas **(Figure 31B)** and reduced bacterial burdens **(Figure**

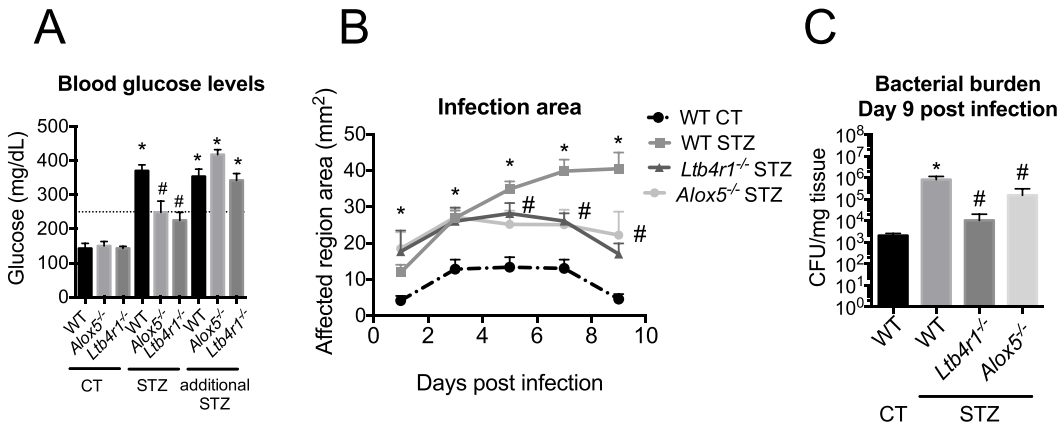

Figure 31. Genetic knockout of BLT1 or 5-LO improves host defense in diabetic mice. A-C) STZ was used to induce diabetes in WT, *Alox5*$^{-/-}$, and *Ltb4r1*$^{-/-}$ mice as described in the "Materials and methods". WT CT, WT STZ, *Alox5*$^{-/-}$ STZ, and *Ltb4r1*$^{-/-}$ STZ mice were infected subcutaneously with MRSA ($3x10^6$ CFU). **A)** Blood glucose levels in nondiabetic mice (CT), after STZ injection, and after additional STZ injections in knockout mice as described in the "Materials and methods". **B)** Infection areas measured every other day for 9 days post infection. **C)** Bacterial CFUs normalized to tissue weight measured at day 9 post infection. Data are mean ± SEM of 5-10 mice from 1 experiment. **A** and **C)** *p < 0.05 vs. nondiabetic CT, #p < 0.05 vs. WT STZ. (One-way ANOVA followed by Tukey multiple comparison correction). **B)** *p < 0.05 vs. WT CT, #p < 0.05 vs. WT STZ.

31C). Taken together, diabetic mice had poor host defense indicated by larger infection areas and higher bacterial burdens, which was partially restored with genetic BLT1 or 5-LO deficiency.

In order to determine which LTB_4 receptor may be contributing to poor host defense, diabetic mice were infected with MRSA and treated daily with topical ointments containing antagonists for BLT1 (U-75302) or BLT2 (LY255283). Infection areas of STZ-diabetic mice treated with BLT1 antagonist, but not BLT2 antagonist, were smaller than untreated STZ mice **(Figure 32A).** Additionally, diabetic mice treated with BLT1 antagonist had lower bacterial burdens in the skin at day 9 post infection **(Figure 32B)**, suggesting that BLT2 is

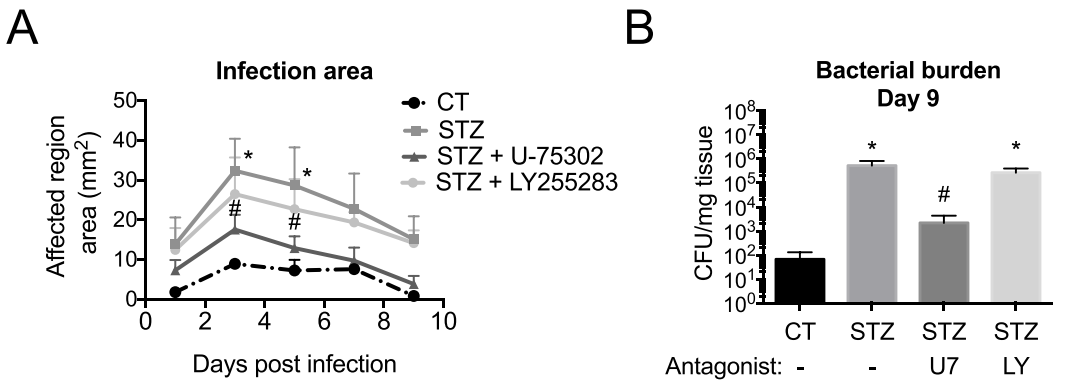

Figure 32. BLT1 or BLT2 antagonist treatment. A-B) CT and STZ mice were infected subcutaneously with MRSA ($3x10^6$ CFU). STZ mice were treated daily with topical ointments containing 0.001% BLT1 antagonist (U-75302), 0.001% BLT2 antagonist (LY255283), or vehicle. **A)** Infection areas measured every other day for 9 days post infection. **B)** Bacterial CFUs normalized to tissue weight measured at day 9 post infection. U-75302 (U7) and LY255283 (LY). Data are mean ± SEM of 4-6 mice from 2 experiments. **A)** *p < 0.05 vs. CT, #p < 0.05 vs. STZ-treated mice treated with vehicle ointment (Two-way ANOVA followed by Tukey multiple comparison correction. **B)** **p < 0.05 vs. CT, #p < 0.05 vs. STZ-treated mice treated with vehicle ointment (One-way ANOVA followed by Tukey multiple comparison correction).

not involved in poor host defense in diabetic mice. Notably, BLT2 is a low affinity receptor for LTB_4. Other agonists (such as 12-HHT and 12-HETE) have higher

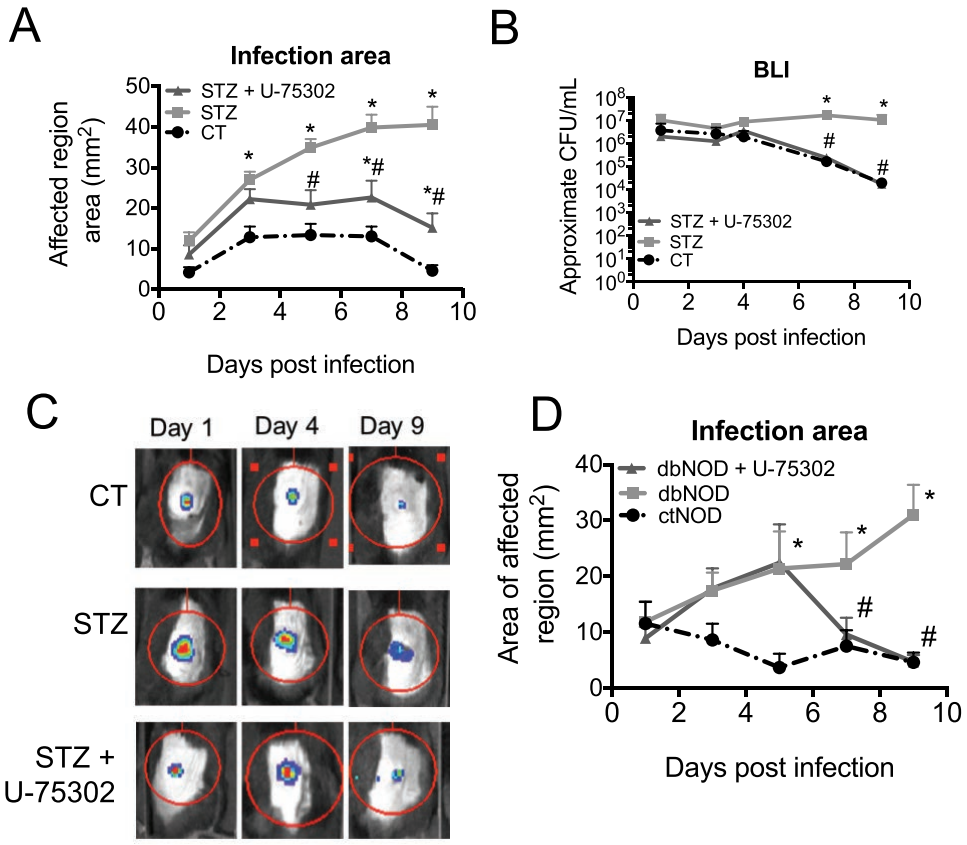

Figure 33. BLT1 antagonist improves host defense in diabetic mice. A-C) CT and STZ mice were infected subcutaneously with bioluminescent-expressing MRSA ($3x10^6$ CFU). STZ mice were treated daily with topical ointments containing 0.001% BLT1 antagonist (U-75302) or vehicle. **A)** Infection areas were measured every other day for 9 days post infection. **B)** IVIS scans for bioluminescence to quantify bacterial burden in the skin at days 1, 3, 4, 7, and 9 post infection. **C)** Images of mice scanned for BLI at days 1, 4, and 9 post infection. Images are representative to 5-8 mice from 2 experiments. **D)** ctNOD and dbNOD mice were infected subcutaneously with bioluminescent-expressing MRSA ($3x10^6$ CFU). dbNOD mice were treated daily with topical ointments containing 0.001% BLT1 antagonist (U-75302) or vehicle. Infection areas were measured every other day for 9 days post infection. Data are mean ± SEM of 5-10 mice from 2-5 experiments. **A** and **B)** *$p < 0.05$ vs. CT, #$p < 0.05$ vs. STZ-treated mice treated with vehicle (Two-way ANOVA followed by Tukey multiple comparison correction). **D)** *$p < 0.05$ vs. ctNOD, #$p < 0.05$ vs. dbNOD mice treated with vehicle (Two-way ANOVA followed by Tukey multiple comparison correction).

affinities for BLT2 than LTB_4, so BLT2 antagonist treatment is not specific for inhibiting LTB_4 actions exclusively. However, BLT2 antagonist treatment did not worsen infection area or disrupt healing in diabetic mice with the dose tested. Therefore, we focused our research effects by studying the role of LTB_4 and BLT1 actions and how this influences host defense in diabetic mice.

To further evaluate the therapeutic potential of blocking BLT1 in the skin of diabetic mice, mice were infected with bioluminescent-expressing MRSA. This allowed for in vivo bioluminescence imaging (BLI) for bacterial burden quantification in the skin throughout the infection in the same animal. Infection areas of diabetic mice treated with BLT1 antagonist U-75302 were smaller than those observed in diabetic mice treated with vehicle-control **(Figure 33A)**. IVIS in vivo imaging revealed that diabetic mice were unable to eliminate bacteria, whereas nondiabetic mice and diabetic mice treated with BLT1 antagonist demonstrated bacterial clearance overtime **(Figure 33B-C)**. To confirm that the BLT1 antagonist U-75302 was effective in restoring host defense in diabetic mice, the same treatment protocol was used in diabetic NOD mice. Similar to diabetic STZ mice, diabetic NOD mice treated with BLT1 antagonist had smaller infection areas compared to diabetic mice receiving no treatment **(Figure 33D)**. These data show that BLT1 antagonist treatment improved host defense of diabetic mice during MRSA skin infection.

Impaired abscess formation in diabetic mice

Alluding to the observations above further studies were done to determine the consequences of aberrant LTB_4 production and the mechanisms by which lack of LTB_4 signaling treatment restored host defense in diabetic mice. Since nondiabetic mice infected with MRSA showed neutrophil recruitment and abscess formation, the next question was whether enhanced levels of LTB_4 affected phagocyte recruitment and abscess formation in diabetic mice. Nondiabetic mice developed an abscess and although diabetic mice had significantly more cell recruitment than CT mice, there was no well-defined abscess structure **(Figure 34)**. Diabetic mice treated with BLT1 antagonist U-75302 partially restored abscess formation.

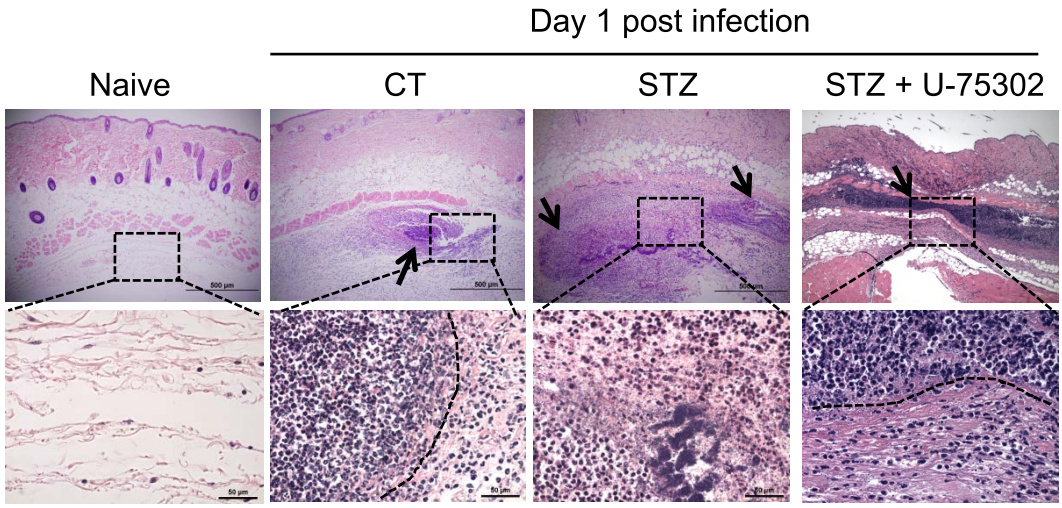

Figure 34. Uncontrolled cell recruitment to the skin of diabetic mice during MRSA infection. CT and STZ mice were infected subcutaneously with MRSA ($3x10^6$ CFU). STZ mice were treated with topical ointments containing 0.001% BLT1 antagonist (U-75302) or vehicle. H&E images of skin biopsy sections collected from naive skin and at day 1 post infection. Top panels show 4X and bottom panels show 40X magnification. Images are representative of 3-5 mice from 2-4 experiments. Dotted lines outline abscess edge. Black arrows indicate cell recruitment.

The abscess is composed of live and dead neutrophils, bacteria, and contained by the formation of a fibrous capsule that is composed of fibrin and collagen fibers [128, 177]. On H&E stains, an eosinophilic fibrous staining was

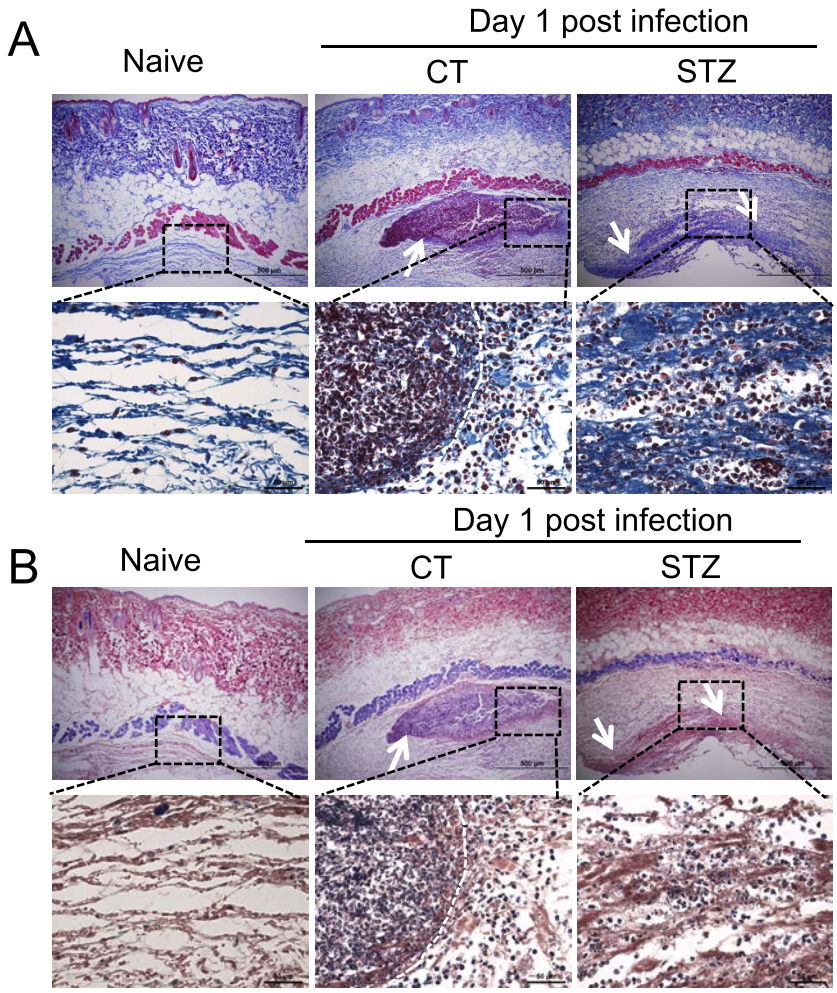

Figure 35. Irregular collagen deposition in the skin of diabetic mice. A-B) CT and STZ mice were infected subcutaneously with MRSA ($3x10^6$ CFU). STZ mice were treated with topical ointments containing 0.001% BLT1 antagonist (U-75302) or vehicle. Biopsies were collected from naive skin and at day 1 post infection and processed for histology staining as described in the "Materials and methods". **A)** Masson's trichrome blue stain to detect collagen shown in blue. **B)** PTAH stain of skin biopsy sections to detect fibrin shown in blue and collagen shown in pink. Top panels show 4X and bottom panels show 40X magnification. All images are representative of 3-5 mice from 2-4 experiments. Dotted lines outline abscess edge. Arrows indicate cell recruitment. White arrows and dotted lines show abscess edge.

observed surrounding the abscess of CT mice, which was not apparent in STZ mice. We next determined whether diabetic mice were unable to produce fibrin/collagen during infection, which may impair abscess formation. Histology sections were stained with Masson's trichrome blue **(Figure 35A)** and PTAH **(Figure 35B)** stains. Masson's trichrome blue stains collagen in blue. PTAH stain labels fibrin in blue/black and collagen in pink. The fibrous capsule in CT mice at day 1 post MRSA skin infection appeared to be composed primarily of collagen. There was irregular collagen deposition observed in the skin of diabetic mice at day 1 post MRSA skin infection. Although fibrin was reported to be a major component of the abscess capsule [128] , minimal fibrin staining was observed in the skin of MRSA-infected mice. However, more staining is required to differentiate the types of collagen and fibrin to determine the exact composition of the abscess in the skin during MRSA skin infection. Nonetheless, the irregular deposition of these fibrous molecules in the skin of diabetic mice may be associated with poor abscess formation.

Next, we evaluated what mediators were altered in the skin of diabetic mice and whether BLT1 antagonist treatment influenced the production of these mediators. To do this, skin biopsy homogenates were tested in a multiplex assay to detect multiple analytes at once **(Figure 36A)**. Expression of the adhesion molecule ICAM1 **(Figure 36B)** was enhanced, while CXCL2 **(Figure 36C)** and receptor for advanced glycation end-products (RAGE) **(Figure 36D)** were downregulated in the skin of diabetic mice at day 1 post infection. These are potent inflammatory mediators influencing host defense through activating

macrophages and promoting neutrophil migration towards the site of infection. Expression of IL-1β was trending to be lower in the skin of diabetic mice but was not different between diabetic and nondiabetic mice in the skin during infection at day 1 post infection **(Figure 36E).** STZ-diabetic mice treated with BLT1 antagonist restored expression profiles (e.g. decreasing expression of ICAM1 and RAGE) of many of these mediators to levels observed in CT nondiabetic mice.

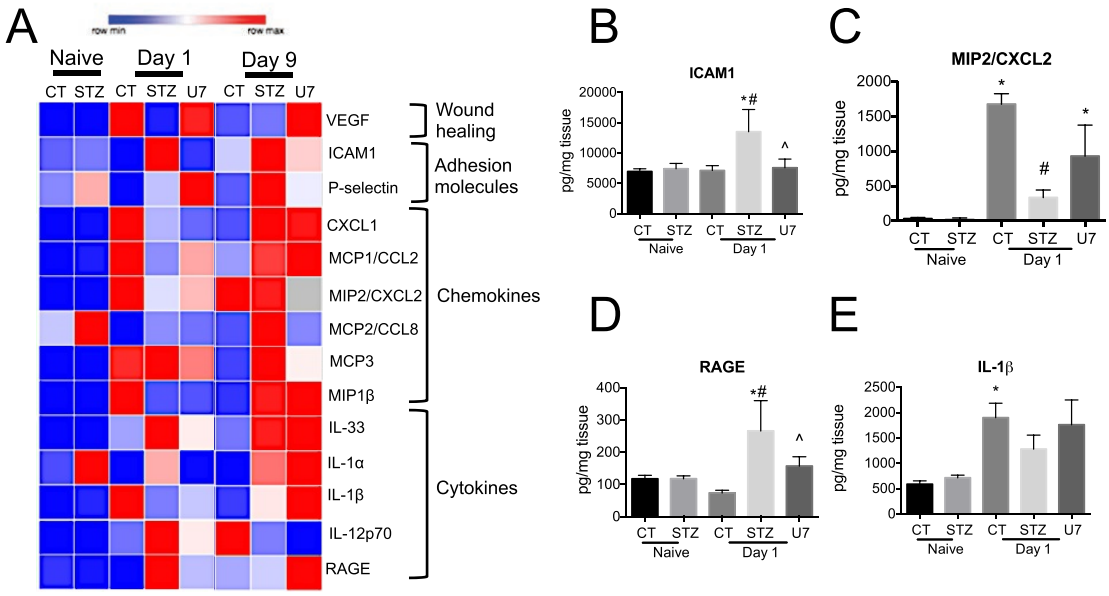

Figure 36. Altered cytokine and chemokine generation in diabetic mice. A-E) CT and STZ mice were infected subcutaneously with MRSA ($3x10^6$ CFU). STZ mice were treated daily with topical ointments containing 0.001% BLT1 antagonist U-75302 (U7) or vehicle. **A)** Heatmap of analytes measured in skin biopsy homogenates taken from naive skin and at days 1 and 9 post infection. Heatmap created in GraphPad Prism software. **B)** ICAM1 from heatmap. **C)** MIP2/CXCL2 from heatmap. **D)** RAGE from heatmap. **E)** IL-1β from heatmap. Data are mean ± SEM of 3-8 mice from 2-4 experiments. *p < 0.05 vs. naive, #p < 0.05 vs. infected CT, ^p < 0.05 vs. infected STZ mice treated with vehicle ointment (One-way ANOVA followed by Tukey multiple comparison correction). N.D. not detected.

Although LTB_4-dependent IL-1β production is necessary for MRSA clearance in homeostasis **(Figure 15)**, a role for IL-1β in the skin of diabetic mice during MRSA skin infection was not obvious. Initially, we infected diabetic and nondiabetic IL-1β reporter mice (pIL1DsRED) with MRSA and examined IL-1β-

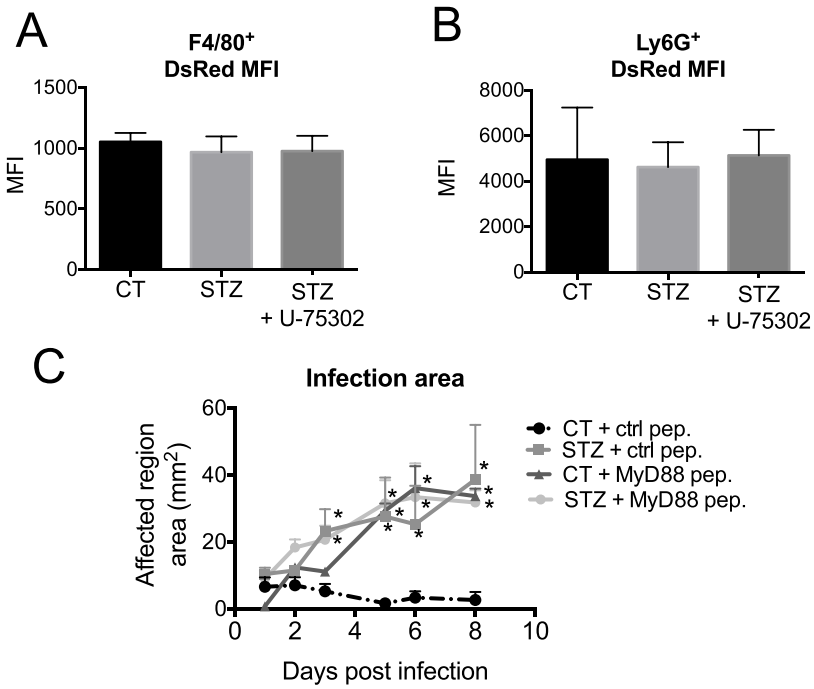

Figure 37. IL-1β likely does not contribute to poor host defense in diabetic mice during MRSA skin infection. A-B) CT and STZ pIL1DsRED mice were infected subcutaneously with MRSA ($3x10^6$ CFU). STZ mice were treated daily with topical ointments containing 0.001% BLT1 antagonist (U-75302) or vehicle. Skin biopsies were collected at day 1 post infection and processed for flow cytometry analysis as described in the "Materials and methods". **A)** MFI of DsRED in $F4/80^+$ macrophages in the skin of pIL1DsRED mice. **B)** MFI of DsRED in $Ly6G^+$ neutrophils in the skin at day 1 post MRSA skin infection. **C)** CT and STZ pIL1DsRED mice were infected subcutaneously with MRSA ($3x10^6$ CFU). CT and STZ mice were treated daily with topical ointments containing 0.033% MyD88-blocking peptide (pep.) or equivalent concentration of non-targeting control peptide (ctrl pep). Data are mean ± SEM of 3-8 mice from 1-2 experiments. *$p < 0.05$ vs. CT treated with control peptide. (Two-way ANOVA followed by Tukey multiple comparison correction).

producing cells. No significant differences were observed in DsRED MFI in macrophages or neutrophils in the skin at day 1 post infection between CT and STZ mice **(Figure 37A-B)**. Another approach to determine the contribution of IL-1β signaling in the skin was through pharmacological inhibition of MyD88, an adaptor required for IL1R signaling. Diabetic and nondiabetic mice were treated daily with a topical ointment containing MyD88 blocking peptides or non-targeting control peptides during MRSA skin infection. Nondiabetic control mice treated with the MyD88 peptide had worse infection compared to control peptide. However, diabetic mice treated with the MyD88 peptide had no significant effect on infection area compared to diabetic mice treated with the control peptide **(Figure 37C)**. Although MyD88 blocking peptide prevents signaling of other TLR and IL1 receptor family members, and since diabetic mice were unchanged, it suggests that other mediators may play a more significant role in poor host defense. Importantly, while IL-1β may play a significant role in abscess formation during MRSA skin infection in nondiabetic mice, IL-1β in the skin of diabetic mice is not deficient and that other mechanisms are involved in poor host defense in diabetic mice.

Uncontrolled neutrophil and macrophage responses

The next step was to determine how abundant LTB_4 levels in the skin of diabetic mice altered the dynamics of cell migration during MRSA skin infection. To do this, MRSA-infected diabetic and nondiabetic mice with GFP-expressing myeloid cells (Lys^{EGFP}) were used for intravital microscopy. Diabetic mice were

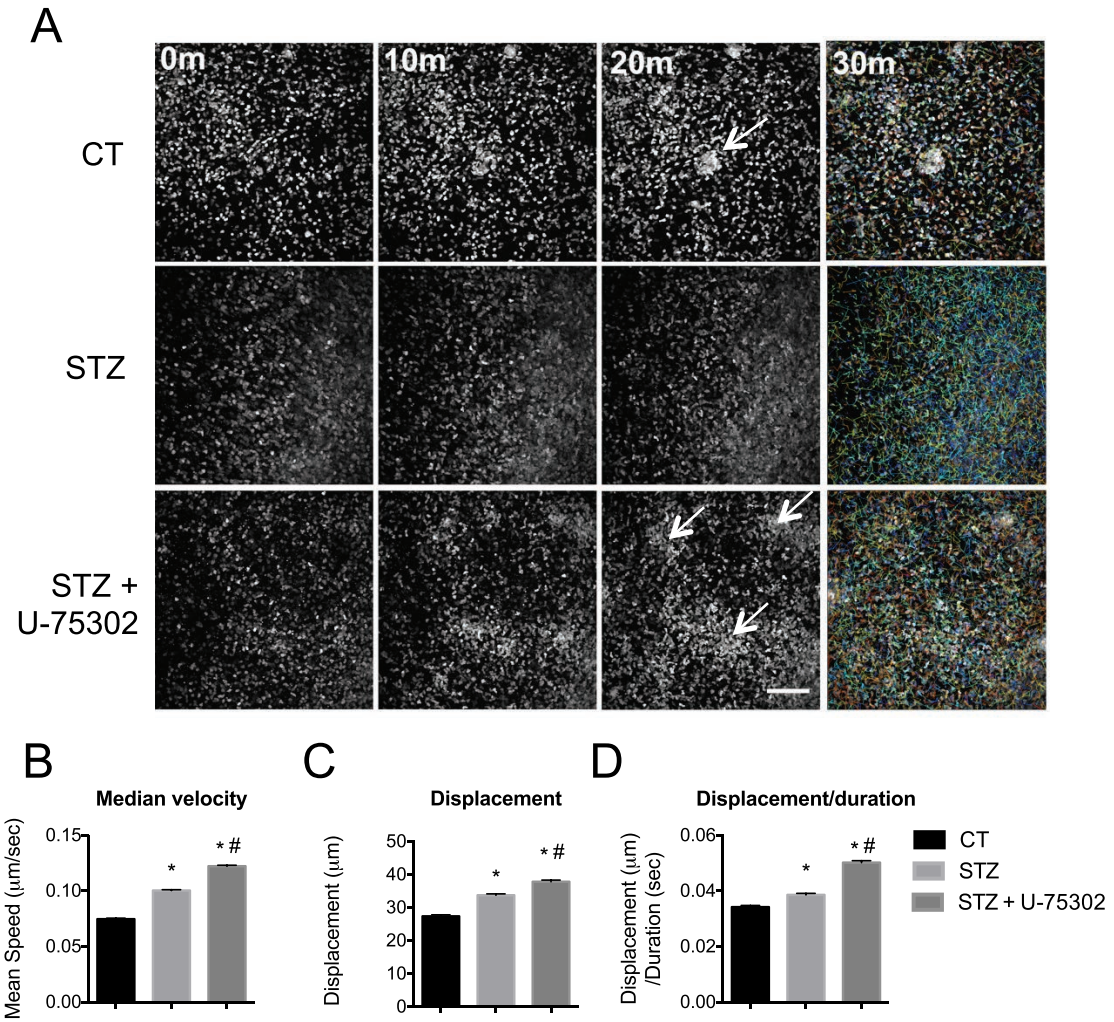

Figure 38. Neutrophils in diabetic mice have impaired direction. A-D) CT and STZ *Lys*^{EGFP} mice were infected subcutaneously with MRSA (3x10^6 CFU). STZ mice were treated daily with topical ointments containing 0.001% BLT1 antagonist (U-75302) or vehicle. At day 1 post infection, mice were imaged by two-photon intravital microscopy for 30 minutes as described in the "Materials and methods". **A)** Still frames of intravital imaging movies taken at 0, 10, 20, and 30 minutes. 30 minute frames include track paths of individual cells. The color of path indicates heat map of median velocity (red=fast, blue=slow). **B)** Median velocity of GFP$^+$ cells. **C)** Track displacement of GFP$^+$ cells. **D)** Ratio of displacement/track duration. Track paths and quantifications were measured by FIJI (ImageJ) TrackMate plugin software as described in the "Materials and methods". Data are mean ± SEM of 1000+ GFP$^+$ cells representative of 3-4 mice from 2-4 experiments. *p < 0.0001 vs. CT, #p < 0.0001 relative to STZ-treated mice treated with vehicle ointment (One-way ANOVA followed by Tukey multiple comparison correction). White arrows indicate swarming.

treated with or without a topical ointment containing BLT1 antagonist U-75302. Infection areas in skin flaps of anesthetized mice were imaged by intravital microscopy for 30 minutes **(Figure 38A)**. Neutrophils in CT mice formed swarm-like accumulations, whereas neutrophils in diabetic mice showed faster speed and lacked apparent direction **(Figure 38B)**. Neutrophils in diabetic mice treated with BLT1 antagonist treatment surprisingly had even faster speed than diabetic neutrophils and the swarm-like accumulations were restored. Also, the displacement of neutrophils was longer in neutrophils from diabetic mice and BLT1 antagonist further increased displacement values **(Figure 38C)**. The ratio of displacement to duration revealed that neutrophils from diabetic mice treated with BLT1 antagonist was higher indicating more directed migration than neutrophils in diabetic mice **(Figure 38D)**. Since the multiplex assay revealed that BLT1 antagonist restored many of the chemokine and cytokine profile during MRSA skin infection, it is likely that blocking BLT1 allowed for neutrophils to better sense the other chemoattractant gradients in the skin to improve abscess formation.

Next, we decided to investigate whether the diabetic milieu influenced the localization of neutrophils and macrophages in the infected skin. IHC slides stained for a neutrophil marker (Ly6G/C) revealed little to no neutrophils in the skin of naive mice. At day 1 post MRSA skin infection, we detected a great abundance of neutrophils, which were organized within an abscess in the skin of nondiabetic mice **(Figure 39A)**. Similar to what H&E slides revealed, diabetic mice had a greater abundance of neutrophils, but lacked organized abscess

structure. However, BLT1 antagonist treatment both limited the recruitment of neutrophils and correlated with concentrated neutrophil accumulation in areas

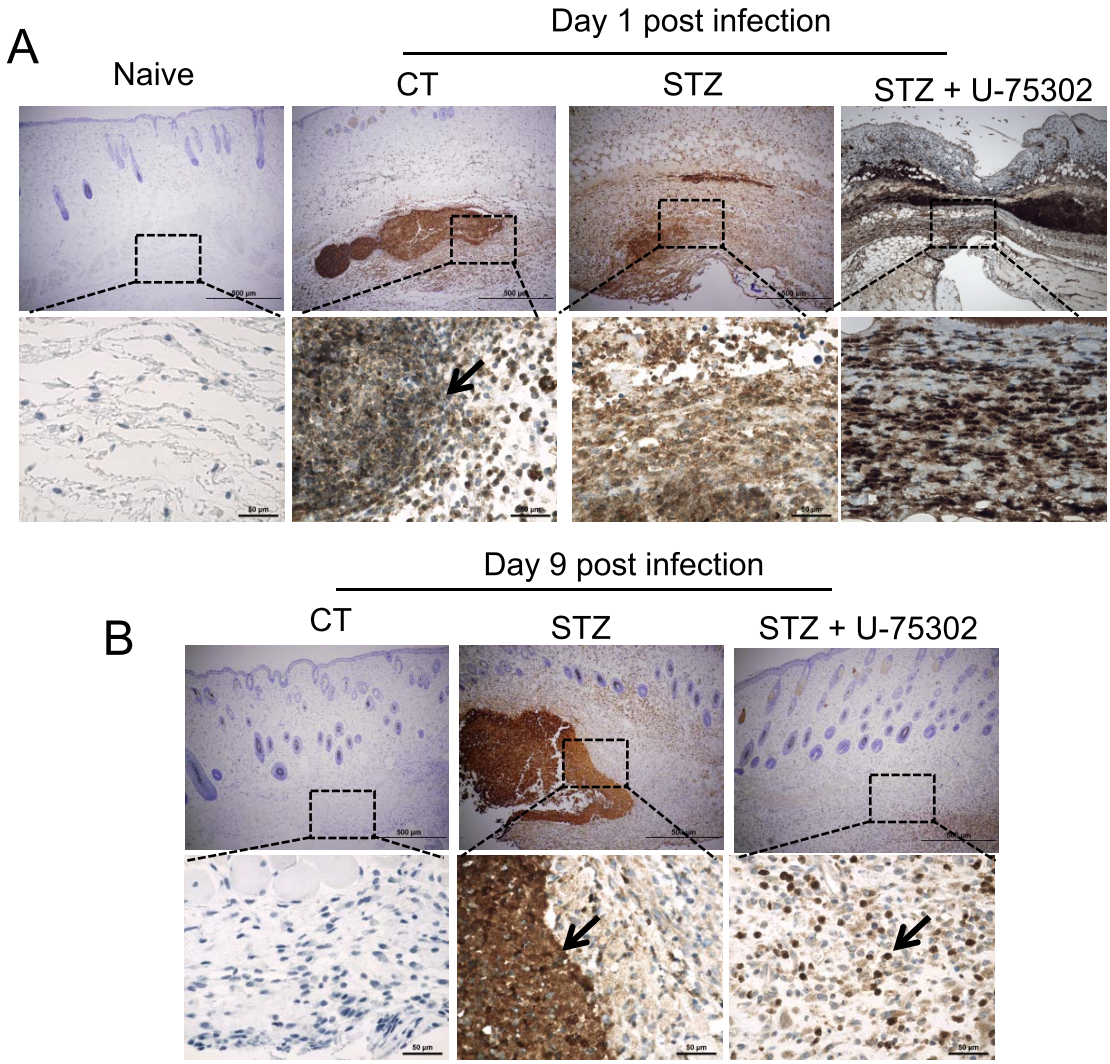

Figure 39. Uncontrolled neutrophil recruitment and poor organization in the skin of diabetic mice during infection. A-B) CT and STZ mice were infected subcutaneously with MRSA ($3x10^6$ CFU). STZ mice were treated with topical ointments containing 0.001% BLT1 antagonist (U-75302) or vehicle. Biopsies were collected from naive skin and at day 1 post infection and processed for IHC staining for neutrophils (Ly6C/G) as described in the "Materials and methods". Neutrophils are shown in brown with counterstain in blue. **A)** Naive and day 1 post infection. **B)** Day 9 post infection. Top panels show 4X and bottom panels show 40X magnification. All images are representative of 3-5 mice from 2-4 experiments. Top panels show 4X. Bottom panels show 40X magnification. Representative of 3-5 mice from 2-4 experiments. Arrows indicate neutrophils.

near the infection in the skin. At day 9 post infection, whereas few numbers of neutrophils were in the skin of nondiabetic mice, diabetic mice still had a notable

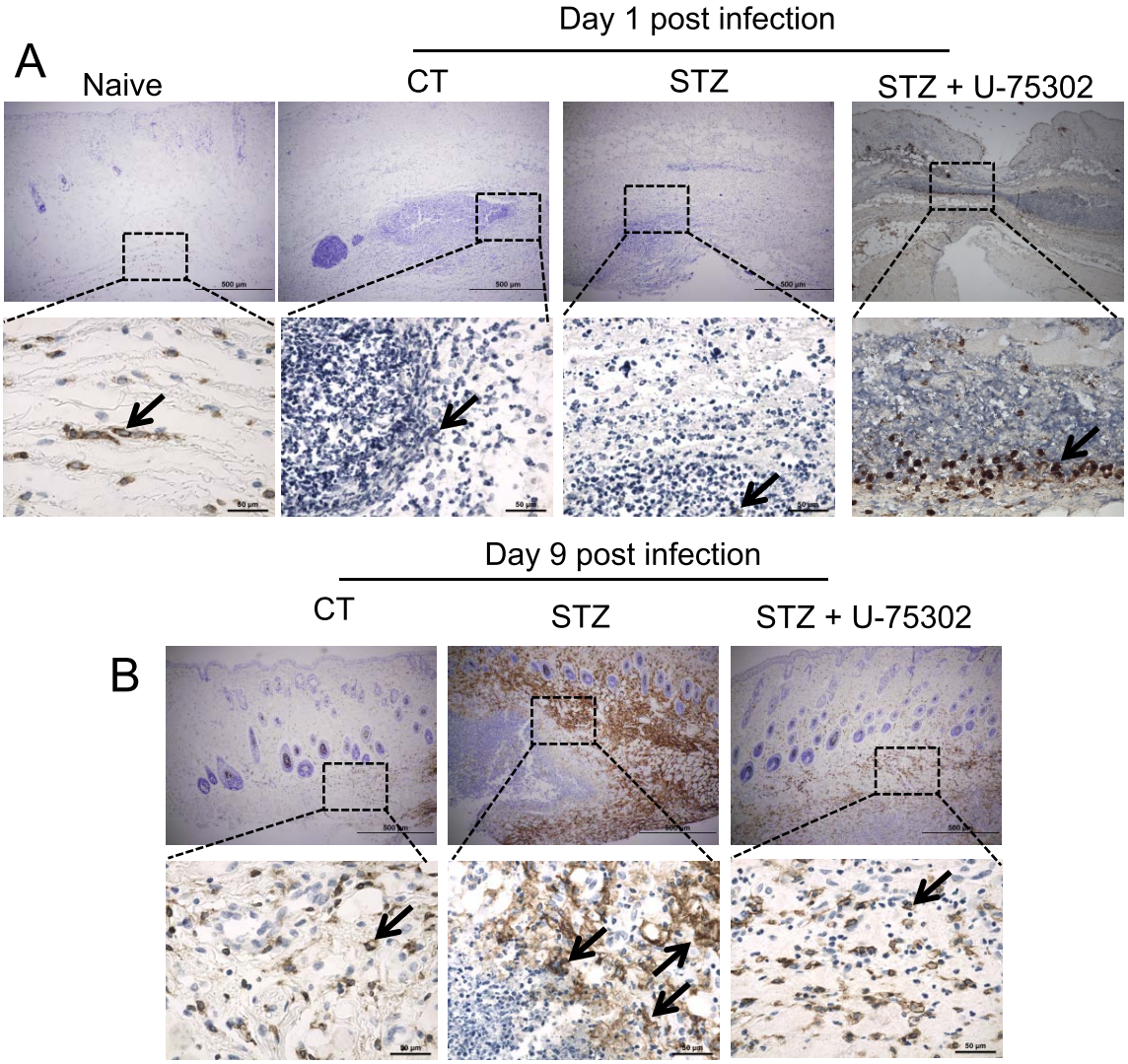

Figure 40. Impaired macrophage interactions with the abscess. A-B) CT and STZ mice were infected subcutaneously with MRSA ($3x10^6$ CFU). STZ mice were treated with topical ointments containing 0.001% BLT1 antagonist (U-75302) or vehicle. Biopsies were collected from naive skin and at day 1 post infection and processed for IHC staining for macrophages (F4/80) as described in the “Materials and methods”. Macrophages are shown in brown with counterstain in blue. **A)** Naive and day 1 post infection. **B)** Day 9 post infection. Top panels show 4X and bottom panels show 40X magnification. All images are representative of 3-5 mice from 2-4 experiments. Top panels show 4X. Bottom panels show 40X magnification. Representative of 3-5 mice from 2-4 experiments. Arrows indicate macrophages.

abundance of neutrophils in the skin, which was reduced with BLT1 antagonist treatment **(Figure 39B)**.

Macrophages associated around the periphery of the neutrophil abscess in nondiabetic mice. IHC staining for F4/80 revealed that macrophages were located in the skin at the various time points after infection. A population of tissue-resident macrophages was observed in the skin of naive skin. At day 1 post MRSA skin infection, macrophages in control mice were found along the periphery of the abscess and in diabetic mice, macrophages were found at more distant locations **(Figure 40A)**. BLT1 antagonist treatment restored the interactions of macrophages with the neutrophil aggregates. At day 9 post MRSA skin infection, control mice had relatively more macrophages present in the skin compared to naive skin, likely promoting tissue remodeling and repair after infection **(Figure 40B)**. Interestingly, there were more macrophages in the skin of diabetic mice at day 9 post infection compared to control mice, which was greatly reduced with BLT1 antagonist treatment.

Macrophages in diabetic mice are detrimental to host defense

In order to better understand the role of skin-resident macrophages during MRSA skin infection in diabetic mice, macrophages were depleted prior to infection using MMDTR mice. Diabetic and nondiabetic MMDTR were treated with diphtheria toxin (DT) or PBS-vehicle control. Initially, we performed immunofluorescence to determine whether macrophages influence neutrophil migration to the site of infection. Immunofluorescence sections from skin biopsy

samples collected at 6 hours post infection revealed more robust neutrophil recruitment to the skin in diabetic MMDTR mice when compared to nondiabetic mice, as shown by Ly6G-antibody (red fluorescence) **(Figure 41)**. However, diabetic DT-treated MMDTR mice had a marked decrease in neutrophil recruitment to the skin.

At 2 days post infection, diabetic MMDTR mice had significantly larger infection area compared to nondiabetic MMDTR mice **(Figure 42A)**. However, DT-treated diabetic MMDTR mice showed reduced infection areas compared to PBS-vehicle-treated diabetic MMDTR mice, which also correlated with reduced bacterial burden **(Figure 42B).** Flow cytometry analysis of skin biopsies collected at day 1 post infection confirmed similar observations that DT-treatment reduced the numbers of $Ly6G^+$ neutrophils in the skin as observed at 6 hours post infection **(Figure 42C).** Macrophage depletion also reduced the levels of LTB_4 in

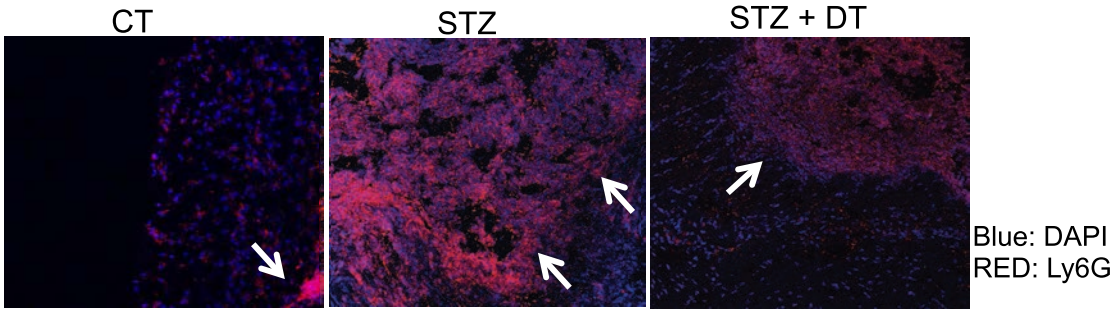

Figure 41. Macrophage depletion limits neutrophil recruitment. MMDTR were treated with STZ to induce diabetes as described in the “Materials and methods”. STZ MMDTR mice were treated with DT prior to subcutaneous MRSA skin infection ($3x10^6$ CFU) as described in the “Materials and methods”. Skin biopsy sections were collected at 6 hours post infection and sectioned for immunofluorescence staining for neutrophils (Ly6G-AlexaFluor 594) shown in red and counterstained with DAPI shown in blue. Images show 20X magnification and are representative of 3-4 mice from 1-2 experiments. Arrows indicate neutrophils.

the skin, suggesting that macrophages are either a significant source of LTB_4 or that they are needed to promote the production of LTB_4 **(Figure 42D).**

Next, we determined whether macrophage depletion altered production of inflammatory mediators in the skin with a multiplex assay. Similar to the results seen in the multiplex assay with diabetic mice treated with BLT1 antagonist,

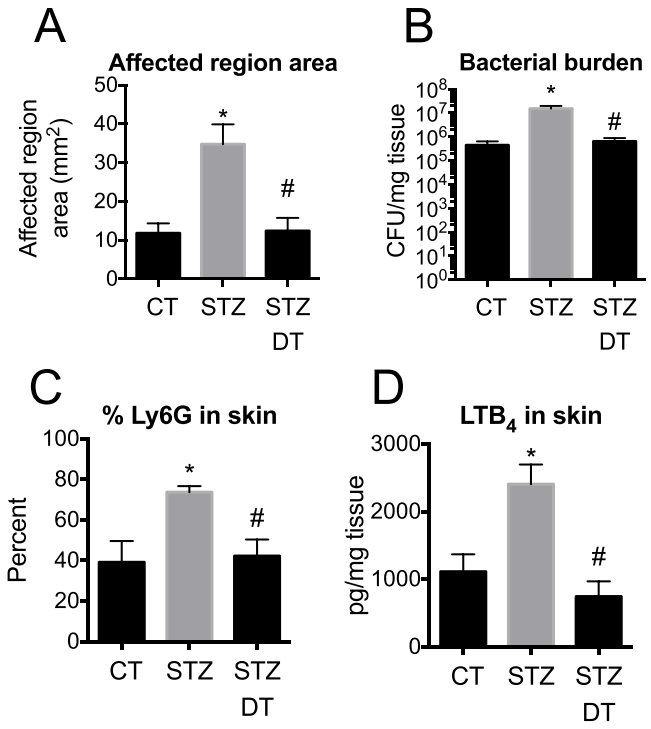

Figure 42. Macrophage depletion improves host defense in diabetic mice. A-D) MMDTR were treated with STZ to induce diabetes as described in the "Materials and methods". STZ MMDTR mice were treated with DT prior to subcutaneous MRSA skin infection ($3x10^6$ CFU) as described in the "Materials and methods". **A)** Infection area measured at day 2 post infection. **B)** Bacterial CFUs normalized to tissue weight measured at day 2 post infection. **C)** Skin biopsies collected at day 2 post infection were processed for flow cytometry analysis as described in the "Materials and methods" and analyzed for percent of $Ly6G^+$ neutrophils. **D)** LTB_4 measured by EIA from skin biopsy homogenates collected at day 2 post infection. Data are mean ± SEM of 3-9 mice from 1-2 experiments. *$p < 0.05$ vs. infected CT, #$p < 0.05$ vs. infected STZ (One-way ANOVA followed by Tukey multiple comparison correction).

macrophage depletion in diabetic MMDTR mice restored the expression of many of the chemokines and cytokines to levels similar to nondiabetic mice. Depleting macrophages in diabetic mice resulted in lowered expression of CXCL2 **(Figure 43A)**, however levels of P-selectin **(Figure 43B)** were unchanged. Also, expression of MMP8 was elevated in diabetic mice but reduced in diabetic mice without macrophages **(Figure 43C)**. Expression of monocyte chemoattractant

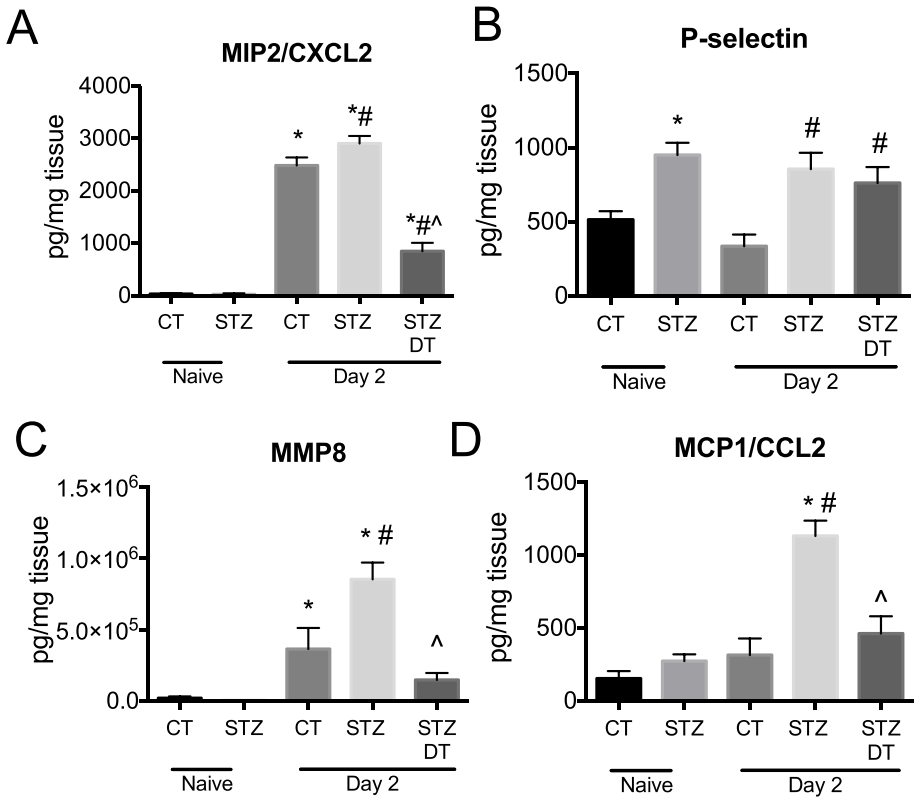

Figure 43. Macrophage depletion dampens inflammation. A-D) MMDTR were treated with STZ to induce diabetes as described in the “Materials and methods”. STZ MMDTR mice were treated with DT prior to subcutaneous MRSA skin infection ($3x10^6$ CFU) as described in the “Materials and methods”. Skin biopsies were collected at from naive skin and at day 2 post infection. Multiplex assays were performed on skin biopsy homogenates. **A)** MIP2/ CXCL2. **B)** P-selectin. **C)** MMP8. **D)** MCP1/CCL2. Data are mean ± SEM of 3-7 mice from 1-2 experiments. *$p < 0.05$ vs. naive, #$p < 0.05$ vs. infected CT, ^$p < 0.05$ vs. infected STZ (One-way ANOVA followed by Tukey multiple comparison correction).

CCL2 was highly expressed in the skin of diabetic mice but was reduced when macrophages were depleted **(Figure 43D)**. This suggests that macrophages in the skin of diabetic mice produce inflammatory mediators that promote exaggerated LTB_4 production and subsequently overwhelming inflammation and poor host defense.

Uncontrolled cell death and poor cell clearance in diabetic mice

S. aureus skin infections are known to induce cell death [128]. Neutrophil recruitment and cell death are typical events that occur during infection or injury. If apoptotic cells are not cleared effectively, they become necrotic and produce DAMPs that elicit more inflammation. Here, we are hypothesizing that either exaggerated cell death or poor clearance of dead cells leads to secretion of DAMPs that further enhance inflammation. Histology sections from skin biopsies from MRSA-infected diabetic and nondiabetic mice were stained by TUNEL assay to visualize dead cells in the skin **(Figure 44A)**. Very few cells in naive skin were apoptotic. At day 1 post infection there were increased levels of apoptotic cells in the skin of nondiabetic mice but were much higher in the diabetic mice. At day 9 post infection, there were few apoptotic cells in the skin of nondiabetic mice, the inflammatory process was resolved and the dead cells properly eliminated. However, diabetic mice still had great numbers of apoptotic cells in the skin, which was reduced with topical BLT1 antagonist treatment.

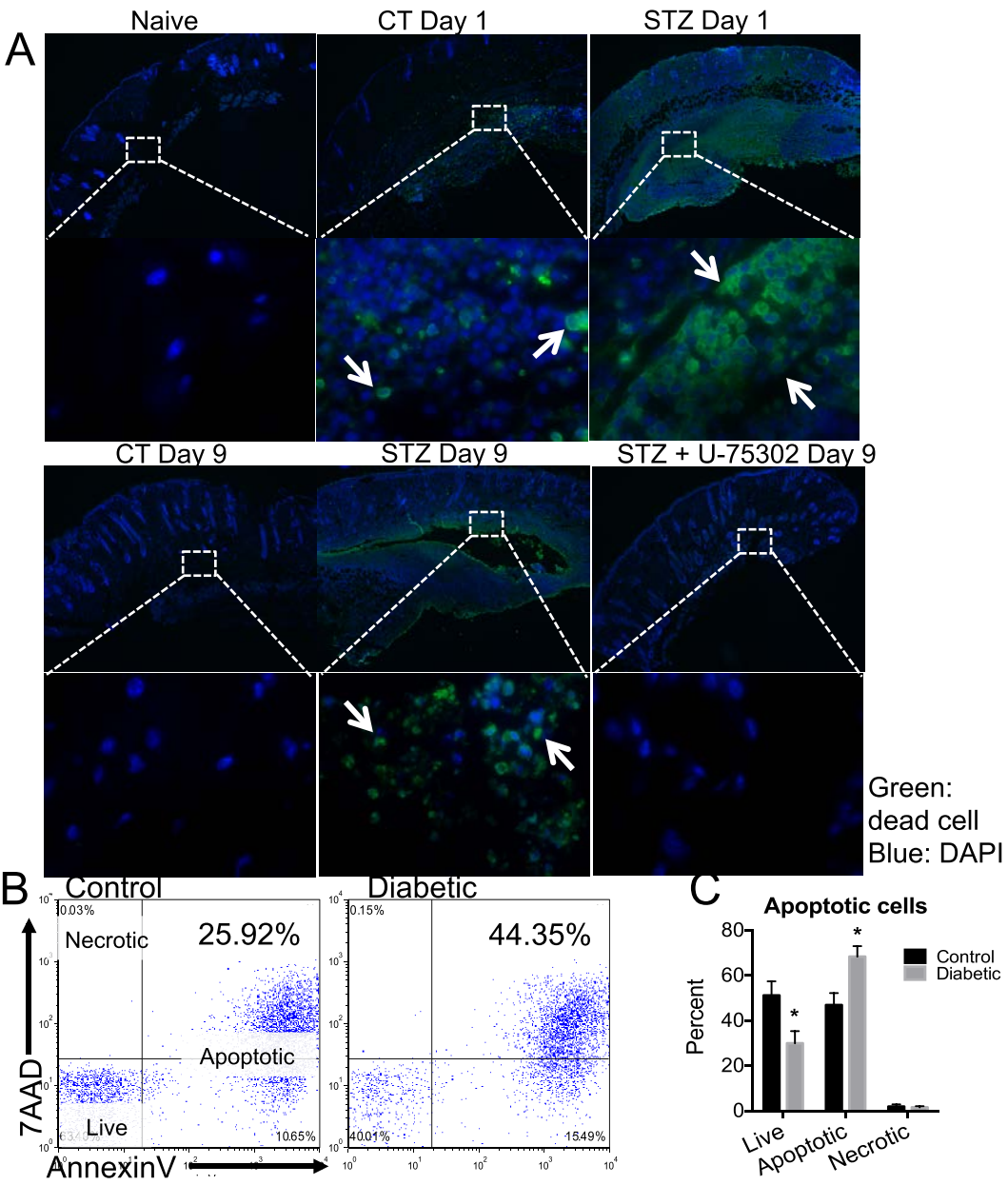

Figure 44. Uncontrolled cell death in diabetic mice. A-C) CT and STZ mice were infected subcutaneously with MRSA ($3x10^6$ CFU) and STZ mice were treated daily with 0.001% BLT1 antagonist U-75302 ointment. **A)** Skin biopsy sections were collected from naive skin and at days 1 and 9 post infection. TUNEL staining to label apoptotic cells in FITC (shown in green) with DAPI counterstain as described in the "Materials and methods". Top panels show 4X and bottom panels show 100X magnification and are representative of 3-5 mice from 1-2 experiments. **B)** Skin biopsy sections were processed for flow cytometry as described in the "Materials and methods". Dot plots showing 7AAD and AnnexinV. **C)** Quantification of percentages from data described in **B.** Data are mean ± SEM of 3-5 mice from 2-3 experiments. *$p < 0.05$ (Student's t-test). White arrows show apoptotic cells.

Flow cytometry analysis measuring markers of apoptosis, 7AAD and AnnexinV, in dissociated skin biopsy samples taken day 1 post infection revealed a higher percentage of apoptotic cells from the skin of diabetic mice compared to nondiabetic mice **(Figure 44B-C).** The persistence of dead cells in the skin of diabetic mice during MRSA skin infection may promote a constant inflammatory signal leading to prolonged inflammation and poor host defense mechanisms.

Since high burdens of dead cells were observed in the skin of diabetic mice, this could be resultant from high cell recruitment or impaired clearance of dead cells. *S. aureus* has been shown to upregulate expression of the "don't eat me" marker CD47 on human neutrophils, inhibiting apoptotic cell clearance [156]. Following the hypothesis that macrophages from diabetic mice have impaired efferocytosis of IACs, expression of signal-regulatory protein alpha (SIRPα), and the receptor for CD47 was measured. Compared to resident peritoneal

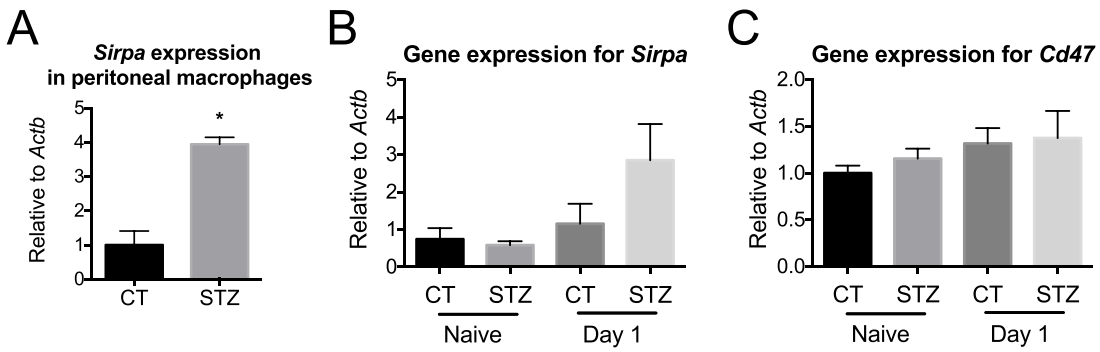

Figure 45. Macrophages from diabetic mice have high expression of *Sirpa.* A) Gene expression for *Sirpa* from peritoneal macrophages isolated from CT and STZ mice. **B)** CT and STZ mice were infected subcutaneously with MRSA ($3x10^6$ CFU). Gene expression for *Sirpa* from skin biopsy sections collected from naive skin and at day 1 post infection. **C)** Gene expression for *Cd47* from skin biopsy sections described in **B.** Data are mean ± SEM of 3-5 mice from 1-3 experiments. *$p < 0.05$ (Student's t-test).

macrophages from nondiabetic mice, macrophages from diabetic mice had higher expression of *Sirpa* **(Figure 45A)**. Expression of *Sirpa* was also higher the skin of diabetic mice during infection compared to nondiabetic mice **(Figure 45B).** SIRPα binds to the "don't eat me" marker CD47. Expression of *Cd47* was not significantly different between diabetic and nondiabetic mice in naive or day 1 post MRSA skin infection **(Figure 45C).** This may suggest that high apoptotic cell burden in diabetic mice during infection is not determined by CD47 expression.

In order to measure expression of SIRPα in the skin, skin biopsies were collected from naive and days 1, 3, and 9 post infection to detect MFI by flow cytometry. MFI of SIRPα was similar in naive skin from diabetic and nondiabetic mice, however the MFI of SIRPα, but not its ligand CD47 was significantly higher in the skin of diabetic mice during infection **(Figure 46A-B)**. This suggests that the elevated expression of SIRPα in the skin of diabetic mice may be interfering

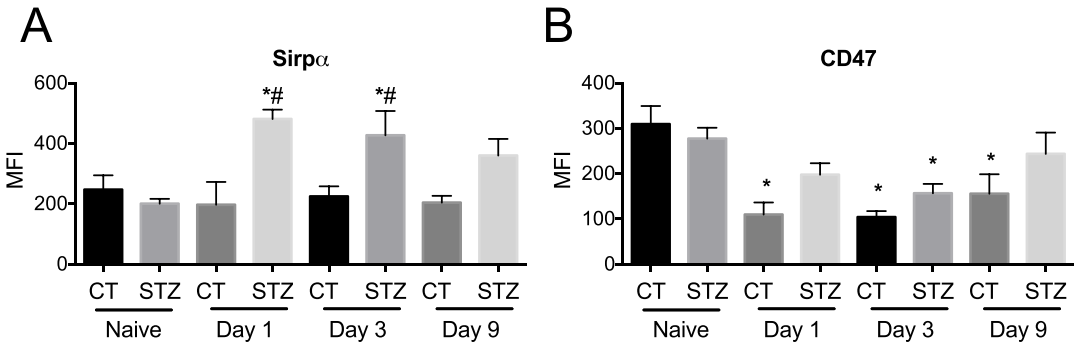

Figure 46. Expression of SIRPα and CD47 in the skin. A-B) CT and STZ mice were infected subcutaneously with MRSA ($3x10^6$ CFU). Skin biopsies were collected from naive skin and at days 1, 3, and 9 post infection and processed for flow cytometry analysis as described in the "Materials and methods". **A)** MFI of cells in the skin for SIRPα**. B)** MFI of cells in the skin for CD47. Data are mean ± SEM of 3-4 mice from 1 experiment. *$p < 0.05$ vs. naive, #$p < 0.05$ relative to infected CT compared to the same time point (One-way ANOVA followed by Tukey multiple comparison correction).

with effective apoptotic cell clearance, leading to high apoptotic cell burden. More experimentation is necessary to determine the contribution of receptor expression by the various cell populations in the skin.

To test whether macrophages from diabetic mice had impaired apoptotic cell clearance, in vitro efferocytosis assays were performed. Peritoneal macrophages from diabetic and nondiabetic mice were cultured with MRSA-infected apoptotic cells (IACs) that were prepared from bone marrow neutrophils isolated from diabetic and nondiabetic mice. Macrophages from nondiabetic mice engulfed similar levels of IACs regardless whether the cells were from diabetic or nondiabetic mice. Similarly macrophages from nondiabetic mice engulfed similar levels of nondiabetic and diabetic sourced IACs **(Figure 47A)**. In order to determine whether impaired efferocytosis occurs in vivo, biopsy sections were collected from diabetic and nondiabetic mice at day 5 post infection. Dissociated biopsy sections were processed for flow cytometry analysis by labeling macrophages with F4/80-PECy7 antibody followed by intracellular staining for Ly6G-AF488. Macrophages were gated on and analyzed for intracellular Ly6G, indicating efferocytosis. There were a higher percentage of macrophages observed in the skin of diabetic mice compared to nondiabetic mice. However, the efferocytosis index was significantly lower in macrophages from diabetic mouse skin compared to control **(Figure 47B)**.

There are reports phagocytic receptors and SIRPα associating with lipid rafts to facilitate or inhibit efferocytosis, respectively [178, 179]. Lipid rafts are subdomains in the plasma membrane. Lipid rafts are thought to enhance the

concentration of signaling molecules, allowing for improved activation and signaling transduction [180]. The next step was to visualize the expression of SIRPα on macrophages and to determine association with lipid rafts. Peritoneal macrophages from diabetic and nondiabetic mice were labeled for lipid rafts

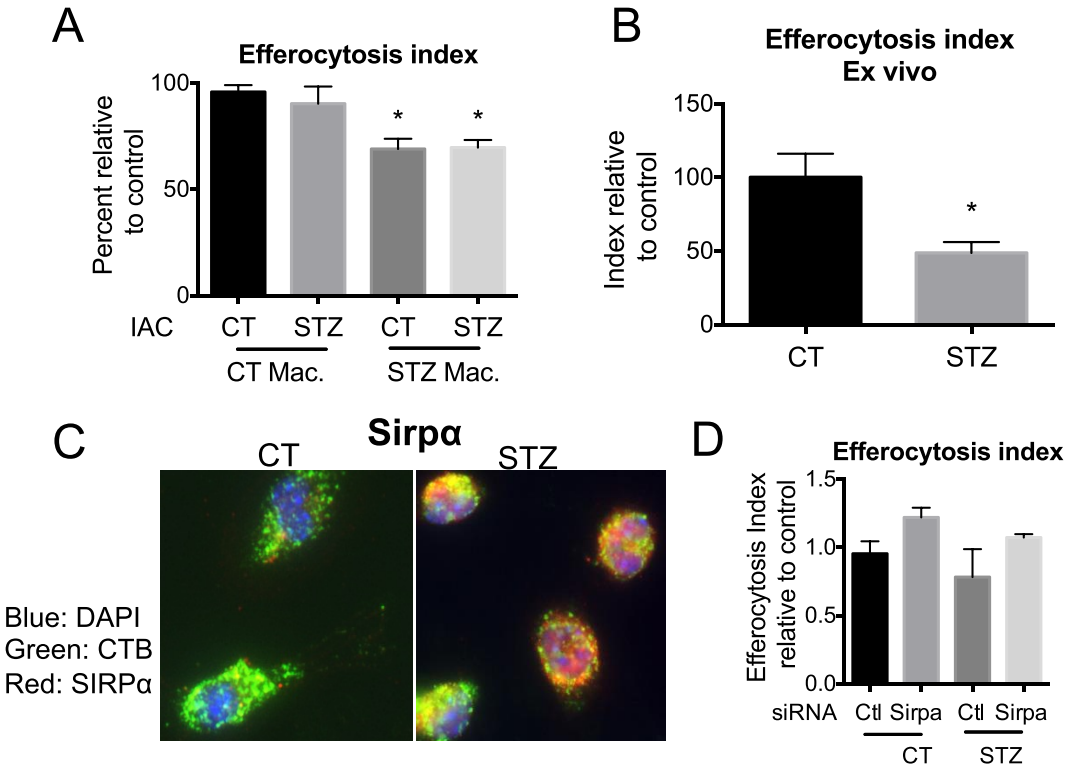

Figure 47. Macrophages from diabetic mice have impaired efferocytosis. **A)** Efferocytosis assay using peritoneal macrophages and IACs isolated from CT and STZ mice as described in the "Materials and methods". **B)** CT and STZ mice were infected subcutaneously with MRSA ($3x10^6$ CFU) and skin biopsies were collected at day 5 post infection. Biopsies were processed for flow cytometry analysis for efferocytosis as described in the "Materials and methods". **C)** Peritoneal macrophages from CT and STZ mice labeled with cholera toxin B (CTB)-AF488 to label lipid rafts, SIRPα-AF594, and counterstained with DAPI. **D)** Efferocytosis assay performed using peritoneal macrophages from CT and STZ mice treated with siRNA to knockdown SIRPα or treated with scrambled control (Ctl) as described in the "Materials and methods". Data are mean ± SEM of 2-5 mice from 1-4 experiments. **A)** *$p < 0.05$ vs. CT co-cultured with the same IAC source (One-way ANOVA followed by Tukey multiple comparison correction). **B)** *$p < 0.05$ (Student's t-test).

using anti-cholera toxin B antibody (green fluorescence) and anti-SIRPα antibody (red fluorescence). Whereas SIRPα was not localized in lipid rafts in macrophages from nondiabetic mice, SIRPα appeared to be in lipid rafts in macrophages from diabetic mice **(Figure 47C)**. This suggests that the expression and cellular location and organization of SIRPα could be playing a major role in the impaired efferocytosis of IACs by macrophages from diabetic mice. To determine whether elevated expression of SIRPα was impairing efferocytosis, macrophages from diabetic and nondiabetic mice were treated with silencing RNA (siRNA) to knockout SIRPα. Treating macrophages with siSirpa showed higher efferocytosis of IACs compared to macrophages treated with scrambled control **(Figure 47D)**. More experimentation is required to determine the contribution of SIRPα and other receptors in poor efferocytosis by macrophages in diabetic mice.

Taken together, macrophages in the skin of diabetic mice were detrimental to infection through promoting excessive LTB_4 production, neutrophil recruitment and cell death, and macrophages had impaired clearance of dead cells, contributing to overwhelming inflammation.

DISCUSSION

Part I - LTB_4 is necessary for host defense

LTB_4 promotes antimicrobial effector functions

LTB_4 promotes phagocytosis and killing of many types of pathogens [53, 95, 97-99, 101, 103]. In vitro assays with bone marrow neutrophils and peritoneal macrophages challenged with LTB_4 did not affect MRSA killing (data not shown). This may be a pathogen-specific effect or possibly that the use of bone marrow neutrophils and peritoneal macrophages are not appropriate cells to model skin infection. Bone marrow neutrophils have a more immature phenotype compared to neutrophils that are recruited to the skin which are in a more active state [181]. Likewise, peritoneal macrophages may not exhibit the same phenotype as macrophages located in other sites [182], such as with the skin. However, in vivo, LTB_4 was necessary to promote bacterial killing in the skin, which is likely mediated through NADPH oxidase activity. LTB_4 has been shown to induce $p47^{phox}$ expression and translocation to the membrane allowing NADPH oxidase assembly in vitro and in vivo [106]. MRSA killing required NADPH oxidase activity and topical LTB_4 application did not restore MRSA killing. Although there are other mechanisms utilized by phagocytes to kill bacteria, such as the production of antimicrobial peptides and RNS. LTB_4 has been shown to induce the production of NO and defensins such as CRAMP in mice and LL37 in human neutrophils [103, 109, 112]. We cannot exclude the role of other antimicrobial molecules during MRSA skin infection that are functioning directly or indirectly of LTB_4 actions.

Enhancing beneficial inflammation is important for promoting antimicrobial effector functions to eliminate infections. However, wound healing is necessary to restore homeostasis to the tissue environment. Eicosanoids are involved in wound healing mechanisms [183]. BLT2 signaling mediated through 12-HHT and 12-HETE have been shown to promote keratinocyte migration and promote VEGF expression which aid in wound healing [54, 55]. Other eicosanoids that are involved in wound healing include specialized pro-resolving mediators that include lipoxins, resolvins, and protectins [184]. More experimentation is required to elucidate the roles of these various eicosanoids during infection and to determine whether the balance of these mediators is altered in the context of diabetes.

Source of LTB_4 in the skin

Macrophages and neutrophils are major sources of LTB_4 production during inflammatory response [30]. The relative contributions of individual cells in LTB_4 production are not fully understood. The MMDTR approach allows for selective depletion of monocytes and macrophages with diphtheria toxin treatment (DT), which does not deplete other cells such as dendritic cells or neutrophils [152]. DT treatment resulted in lower levels of LTB_4 produced in the skin. Neutrophil depletion with Ly6G (clone IA3) depleting antibodies also resulted in lower LTB_4 levels, suggesting that neutrophils are also an important source. However, the contribution of LTB_4 production by other cell types cannot be ruled out such as the contribution by dendritic cells [185] and other cell types

participating in LTB_4 production by transcellular biosynthesis [32]. Further, experiments depleting both cell types are needed to unveil whether other cell types are indeed required for LTB_4 production during infection. Also, it is likely that LTB_4 is produced from multiple sources and requires several cell populations for abundant production. Perivascular macrophages are important for neutrophil recruitment to the skin during *S. aureus* infection [165]. Circulating neutrophils extravasated in close proximity to perivascular macrophages. We observed that macrophage depletion in MMDTR mice resulted in remarkably fewer $Ly6G^+$ neutrophils in the skin during MRSA skin infection. Since neutrophils also produce LTB_4, it is unclear whether the lack of macrophages leading to poor neutrophil recruitment is the cause of LTB_4 or that macrophages produce a considerable amount of LTB_4 in the skin.

LTB_4 and abscess architecture

MRSA skin infections characteristically develop abscesses [128]. Abscess formation in response to *S. aureus* infection is thought to occur in stages resulting with a central core of live bacteria encased by eosinophilic pseudocapsule surrounded by layers of live and dead neutrophils [186]. However, *S. aureus* abscess might differ dependent on the infected organ formation involves complex sequential regulatory steps that lead to migration of phagocyte, cell death, elimination of dead cells and compartmentalization and there are variances depending on anatomical site. Furthermore, abscesses in the kidneys are fatal without treatment whereas abscesses in the skin are necessary

for effective containment and prevents dissemination [170]. We did not observe dissemination or lethality in our infection model with any genotype or treatment condition. This could be due to the relatively low infection inoculum used in our skin infection model compared to others' ($3x10^6$ vs. $1\text{-}2x10^7$) [187, 188]. Alternatively, there could be other molecules involved in the dissemination of bacteria that are unrelated to LTB_4/BLT1 effects. Future experiments are needed to evaluate the factors involved in bacterial dissemination from a skin infection.

Additionally, macrophages were found in close proximity to the abscess during MRSA skin infection. However, adding back LTB_4 to macrophage-depleted mice partially restored abscess formation by promoting better neutrophil clustering. This suggests that the presence of macrophages in the skin may be necessary for abscess architecture, or that macrophages are the primary source of other chemoattractants that are necessary for abscess formation. Despite this, since macrophage depletion resulted in worse infection outcome, it is likely that macrophages are either the source of LTB_4 or provide the signals required for LTB_4 production and other inflammatory mediators that are necessary for controlling MRSA skin infection. Nonetheless, these results demonstrate an important role of macrophages in orchestrating effective host defense mechanisms during MRSA skin infection.

Before an abscess is formed, neutrophils need to migrate to the site of infection. This requires a series of steps including rolling, adherence, and transmigration [68]. LTB_4 is known to be chemotactic for neutrophils as well as other cell types [75, 189]. Inhibition of the enzyme that produces LTB_4,

leukotriene A_4 hydrolase (LTA4H) with an inhibitor such as bestatin results in less neutrophil recruitment and higher *S. aureus* burden and infection area [137]. However, bestatin is a non-selective inhibitor that also blocks the activity of peptidases. Bestatin has been shown to promote many anti-inflammatory effects, and has implications as use as an anti-inflammatory agent [190]. Therefore, the exact role of LTB_4 in the skin host defense remained to be determined. In different models of inflammatory diseases, such as arthritis, BLT1 is required for neutrophil recruitment to the joints [171] or in a model of spinal-cord injury [67]. However, in a model of tissue injury [81] and in our MRSA skin model there was no initial recruitment impairment in *Ltb4r1*$^{-/-}$ neutrophils to the site of injury. These suggest the molecules required for rolling, adherence, and transmigration are unaffected by LTB_4/BLT1 in MRSA skin infection models. Alternatively, the role of LTB_4/BLT1 in neutrophil recruitment may differ depending on type of inflammatory stimuli and location (such as sterile inflammation of arthritis in the joint vs. infectious pathogen in the skin). However, the ability of *Ltb4r1*$^{-/-}$ neutrophils to be directed to a local point in the skin was inhibited as shown in both our MRSA infection model as well as in a sterile injury model [81], suggesting LTB_4 functions to provide direction. LTB_4 has been shown to act as a signal-relay signal promoting enhanced neutrophil migration towards other chemotactic molecules such as fMLP [78]. In additions, LTB_4 could also participate in a hierarchical role of lipid-cytokine-chemokine, which enhances cytokine production that in turn enhances chemokine-mediated recruitment of neutrophils [171].

IL-1β has been shown to be important for abscess formation [170]. Since BLT1 antagonist treated mice and *Ltb4r1*$^{-/-}$ mice had less IL-1β produced, it is likely that LTB_4 mediates *Il1b* expression and inflammasome activation to promote IL-1β production. IL-1β processing through NLRP3 inflammasome activation requires two signals: 1) TLR activation and gene expression and 2) NLRP3 inflammasome assembly and activation. LTB_4 is known to enhance NFκB activation [60]. Our data also show that LTB_4 promotes inflammasome assembly and activation. BLT1 antagonist treatment blocked the expression of *Il1b* and mature IL-1β levels. PLA on neutrophils activated for inflammasome assembly revealed that LTB_4 promoted more associations of NLRP3 and ASC, whereas BLT1 antagonist inhibited inflammasome assembly. In *S. aureus* skin infection, it is thought that the majority of IL-1β production is mediated through NLRP3 inflammasome activity. MRSA produces toxins, such as α-hemolysin that have been shown to activate NLRP3 [191]. Additionally, proteases produced by neutrophils and bacteria are able to cleave pro-IL-1β into mature IL-1β independently of inflammasome activation [121]. We did not evaluate whether toxins produced by MRSA or proteases were involved in IL-1β processing during skin infection. Our experiments here cannot rule out other non-canonical IL-1β processes or inflammasome activation.

Therapeutic potential of enhancing LTB_4/BLT1 actions

In the era of antibiotic resistant bacteria, a new therapeutic strategy that incorporates host-derived products along with effective antibiotic therapy are

desperately needed. Immunomodulatory therapies to boost host immune functions are potential strategies better treat infections [192]. There are many potential advantages to using LTB_4 in immunotherapeutic protocols, such as: 1) compared with generation of recombinant proteins, LTB_4 can be readily and inexpensively synthesized with a high degree of purity. 2) The short half-life of LTB_4 could provide flexibility and precision in controlling pro-inflammatory actions. 3) LTB_4 administration to humans have been well-tolerated [193, 194], and 4) LTB_4 amplifies initial antimicrobial responses by enhancing bacterial recognition and phagocytosis [60, 104, 106], release of ROS [106, 114], IL-1β levels, and pro-inflammatory responses through MyD88 expression and NFκB activation [106, 114].

Due to these immunostimulatory roles LTB_4 exerts on phagocyte effector functions, targeting LTB_4/BLT1 has a potential for enhancing beneficial inflammation to better control MRSA skin infections. Our data show that LTB_4 and mupirocin combination ointment promoted faster MRSA clearance compared to single agent ointments and no treatment. How LTB_4 and mupirocin function together to promote synergistic activities remains to be determined. Antibiotics have been shown to synergize with antimicrobial peptides, which improves bacterial clearance [195]. Antibiotics may promote other immune activation besides bacterial killing. Likewise, LTB_4 has been shown to induce expression of LL37 [112], which has been shown to improve antibiotic therapy [196]. More research is needed into ointment stability and treatment regime to promote optimal infection control without inducing host damage.

Treatment protocols employing exogenous LTB_4 can be greatly beneficial to patients known to exhibit poor host defense and attenuated LT synthesis such as in malnutrition [197], cigarette smoking [198], vitamin D deficiency [199], HIV infection [200], and bone marrow transplantation [201]. Adding back LTB_4 to immunodeficient patients could potentially restore phagocyte response and favor appropriate host defense. Additionally, small amounts of exogenous LTB_4 treatment are able to boost effector functions in immunocompetent WT mice. In a model of *Streptococcus pneumoniae* lung infections, aerosolized LTB_4 treatment restores host defense mechanisms in *Alox5*$^{-/-}$ mice and enhancing effector functions in WT mice [116]. Intravenous injection of LTB_4 in macaques enhances plasma levels of the antimicrobial peptides α-defensins. Plasma from the treated macaques can neutralize pathogens ex vivo [202]. LTB_4 treatment during influenza virus infection reduces viral titers compared to untreated mice [111]. The reduction in viral titers correlates with enhanced levels of the cathelicidin-related antimicrobial peptide (CRAMP). Neutrophils are a major source of CRAMP so when mice are depleted of neutrophils, exogenous LTB_4 treatment during influenza infection is unable to control viral load [111].

A potential pitfall is that LTB_4 might lead to overwhelming recruitment of neutrophils, which may contribute to tissue injury. Also, the stability and safety of LTB_4 in vivo is a concern, but it has been shown that bronchoscopy instillation of LTB_4 into the airways of normal human subjects elicited a marked influx of neutrophils. Inhalation of LTB_4 proved to be well tolerated and did not cause any

significant adverse effects on blood pressure, pulmonary function, or bronchial responsiveness [193].

The importance of LTB_4 during infections is apparent and exogenous treatment with LTB_4 may be a potential therapeutic strategy. However, high LTB_4 levels during some infections or in chronic inflammatory diseases may need to be blunted to limit inflammation and alternative therapeutic strategies to prevent infection-mediated organ injury are necessary.

Conclusion

To summarize, LTB_4 is induced by MRSA skin infection and is an important mediator for host defense **(Figure 48).** LTB_4 provided direction to neutrophils to develop into an organized abscess structure. Bacterial killing was dependent on LTB_4 mediated NADPH oxidase activity. LTB_4 also promoted IL-1β production, which likely aids in abscess formation. Combination therapy of LTB_4

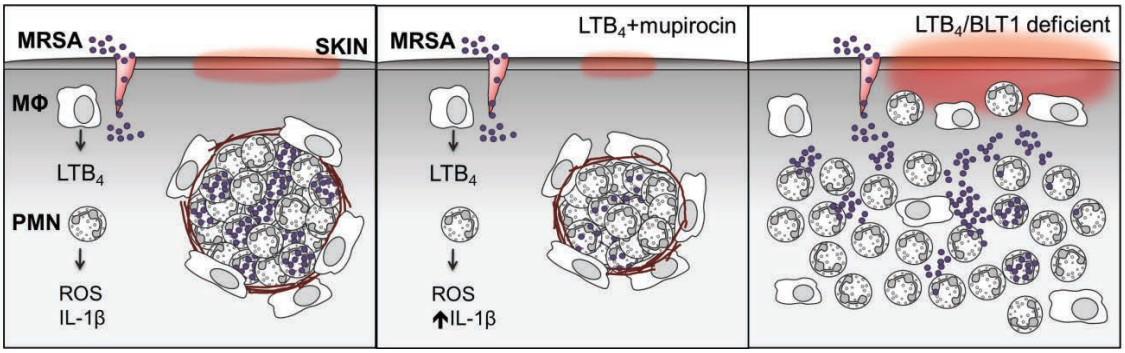

Figure 48. Summary of LTB_4 promoting MRSA skin infection clearance. Left panel: MRSA skin infection requires tissue-resident macrophages for optimal LTB_4 production and neutrophil recruitment. LTB_4 provides direction to neutrophils to contain bacteria and form an abscess surrounded by fibrous collagen. Middle panel: Combination ointment with LTB_4 + topical antibiotic mupirocin is more efficient at eliminating infection. Right panel: Mice lacking LTB_4/BLT1 actions fail to contain bacteria or develop an abscess.

and mupirocin was synergistic for better treating MRSA skin infection. This demonstrates potential for LTB_4 to be used as an immunostimulatory therapy to treat antibiotic-resistant infections.

Part II - LTB_4 complicates host defense in diabetes

Diabetes model

Both people with Type 1 and Type 2 diabetes are more susceptible to infections. One mouse model to study T1D is the NOD mouse, however NOD mice are known to have impaired immune cell activation and functions [173, 174]. These impaired immune functions may drive the minor differences observed between the NOD and STZ models during MRSA skin infection, such as dbNOD mice displaying a more delayed response to MRSA skin infection compared to the kinetics observed in STZ mice. STZ is a model of T1D, in that mice develop hyperglycemia and very low insulin levels [162] however, STZ-treated diabetic mice lack the autoimmune component of T1D. The benefit of utilizing STZ to induce diabetes allowed for comparisons how a diabetic environment alters phagocyte antimicrobial function during MRSA skin infection. Additionally, STZ provided more flexibility in using various transgenic mouse models to study the role of BLT1, macrophages, and use of fluorescent reporter mice that were not all available on the NOD background. Experiments using NOD mice were used to confirm some of the findings.

Unbalanced inflammation driven by LTB_4

High levels of LTB_4 are detrimental for mycobacterial infections in a zebrafish model of infection [137, 139]. Additionally chronic inflammatory diseases are associated with higher levels of inflammatory cytokines and lipid mediators, including LTB_4. Diabetic mice produce high levels of LTB_4 in the

serum and inhibiting leukotriene production during sepsis in diabetic mice improves survival, which is also correlated with a reduction in inflammatory cytokines such as IL-1β [61]. However the role and contribution of IL-1β in the skin of diabetic mice is not yet understood. At day 1 post infection diabetic mice had slightly lower IL-1β than nondiabetic mice. Additionally, MyD88-blocking peptides had no effect on infection outcome in diabetic mice. Blocking MyD88 would also inhibit signaling of other TLRs and IL-1β-family members, this suggests that other mediators are playing a predominate role in driving overwhelming inflammation in the skin of diabetic mice during MRSA skin infection. Future experiments are required to elucidate the role of these other mediators.

The location of LTB_4 in the skin may contribute to poor host defense. Since LTB_4 is a chemotactic molecule, excessive LTB_4 levels may disrupt gradients in the skin, impairing neutrophil migration. Blocking BLT1 in diabetic mice restored neutrophil direction, possibly by altering expression or production of other chemotactic molecules or by allowing neutrophils to detect gradients of other chemokines in the skin. These events may allow for better abscess formation in diabetic mice during MRSA skin infection to improve bacterial containment.

Macrophages in diabetic mice contribute to poor host defense

During MRSA skin infection, macrophages were found in close proximity to the neutrophilic abscess. In naive skin, there were no significant differences in

the levels of LTB_4 produced, or the percentage of macrophages in the skin comparing diabetic and nondiabetic mice. During MRSA skin infection, high LTB_4 levels and dysregulated production of chemokines and cytokines was observed in diabetic mice. This suggests that MRSA skin infection uncontrolled cell activation. Since diabetic mice depleted of macrophages (DT-treated diabetic MMDTR mice) improved host defense, it is likely that macrophages in diabetic skin are promoting overwhelming inflammation. However, whether continuous macrophage depletion throughout the course of infection is beneficial remains to be determined. Since macrophages also have functions in eliminating apoptotic cells, it is likely that macrophage depletion at later stages of infection may interfere with the resolution phase.

Others have reported that macrophages from db/db diabetic (type 2 diabetes model) mice have impaired phagocytosis of apoptotic thymocytes [203] and that ob/ob (type 2 diabetes model) have impaired phagocytosis of apoptotic Jurkat T cells [204]. Although these are models of T2D, which were not investigated in these research goals, these studies support the hypothesis that uncontrolled apoptotic cell burden in the skin of diabetic mice during MRSA skin infection arise due to poor apoptotic cell clearance. Apoptotic cells that fail to be cleared can become necrotic and produce DAMPs, which are inflammatory signals [205]. There are many other receptors important for mediating or inhibiting efferocytosis. BAI1, TIM-4 and MerTK are receptors that recognize phosphatidylserine (PS). [206]. Our data suggest a role of SIRPα in mediating

poor efferocytosis in diabetic mice. However, more research is required to elucidate the roles for other receptors in apoptotic cell clearance.

Additionally, the mechanism of cell death may contribute to the inflammatory milieu. Besides apoptosis, cell death mechanisms include necroptosis (programmed cell necrosis), autophagy, pyroptosis, and caspase-independent cell death [207]. Distinguishing the mode of cell death is challenging [208]. Apoptotic cells can be labeled with TUNEL staining that detects DNA breaks. However, TUNEL staining does not differentiate between apoptosis and necrosis. Additionally, the presence of PS on the surface of cell membranes can be detected with AnnexinV labeling in combination with a cell impermeable DNA dye such as 7AAD. *S. aureus* has been reported to induce necrosis [156], necroptosis [209] and pyroptosis [210]. Although we observed high numbers of dead cells in the skin of diabetic mice during MRSA skin infection, future experiments are required to investigate the mechanism of cell death.

Therapeutic potential of dampening LTB_4/BLT1 actions

Overwhelming production of inflammatory mediators and reactive oxygen species are known to be detrimental to host defense in different models of infection [211-214]. Therapeutic strategies to block the actions of inflammatory mediators could also restore protective host defense mechanisms. It is known that people with diabetes are more susceptible to numerous infections, including systemic, respiratory, and skin infections [143, 145, 215]. Both innate and adaptive immune cells from diabetics have impaired functions including impaired

phagocytosis and killing of pathogens [147, 148]. Macrophages from diabetic mice produce higher levels of LTB_4 than from control mice even under basal conditions [61]. Although seemingly counterintuitive, the mechanism by which people with diabetes are more susceptible to infections may operate in a similar manner to other infections where high levels of LTB_4 are detrimental to host defense [61, 137, 139]. Since LTB_4 is able to enhance IL-1β levels through inflammasome activation [120] and that LTB_4/BLT1 signaling enhances MyD88 and NFκB activities [60], it is possible that blocking LT synthesis or inhibiting BLT1 can prevent overwhelming inflammation.

Diabetic mice are more susceptible to MRSA skin infection than nondiabetic mice. Diabetic mice infected with MRSA have increased LTB_4 production in the skin, which correlates with uncontrolled production of inflammatory mediators and neutrophil migration. Although LTB_4 has therapeutic potential for better controlling MRSA skin infection, excessive LTB_4/BLT1 actions could promote overwhelming inflammation. In the skin during MRSA skin infection, diabetic mice produce higher levels of LTB_4 compared to nondiabetic mice. BLT1 antagonist treatment on diabetic mice dampened inflammation to limit neutrophil recruitment and cell death, restored neutrophil migration and abscess formation, which contributed to better bacterial control.

BLT1 antagonist treatment may be beneficial in various conditions in which chronic inflammation is detrimental. One example is with sepsis, which BLT1 antagonist treatment improved survival [141]. Another example is that BLT1 antagonist treatment prevented insulin resistance in a model of T2D [216].

More research is needed to address how BLT1 antagonist treatment is beneficial and what the mechanisms of action are in various inflammatory conditions.

The effects of BLT1 antagonist treatment on other cell types in the skin may play a role in reducing inflammation during infection. Keratinocytes express BLT1 and since the BLT1 antagonist treatment ointments are applied topically, the treatment may have effects on the keratinocytes. Keratinocytes produce cytokines and antimicrobial peptides [217]. Additionally, keratinocytes from people with diabetes have impaired cell migration and proliferation [218] and treating with the BLT1 antagonist may be altering the inflammatory profile of these cells, even in the absence of infection. More experiments are needed to determine how the BLT1 antagonist is altering the skin.

Although our data demonstrate that exaggerated LTB_4 levels and uncontrolled BLT1 signaling are a driving factor for poor host defense in diabetic mice, we cannot exclude the possibility of other inflammatory mediators involved during MRSA skin infection. BLT1 antagonist treatment clearly improves host defense in diabetic mice, however the same treatment regime in nondiabetic mice exacerbate the infection. The mechanism by which the BLT1 antagonist demonstrates these seemingly counterintuitive effects is not well understood. It is possible that other inflammatory mediators are involved in host defense, which could be differentially produced between diabetic and nondiabetic mice. Future experiments are necessary to determine which cells in the skin are affected by BLT1 antagonism and the consequences of this treatment strategy.

Conclusion

Excessive LTB_4 levels in the skin of diabetic mice promoted overwhelming inflammation leading to poor host defense, which was restored with topical treatment with BLT1 antagonist ointment **(Figure 48).** Skin macrophages were a key player in promoting LTB_4 production in the skin. However, macrophages in diabetic mice were necessary to promote excessive LTB_4 levels in the skin. The relative contribution of LTB_4 production by macrophages or other cells, such as neutrophils, has yet to be determined. In response to infection, there was uncontrolled neutrophil recruitment and poor abscess structure observed in the skin of diabetic mice. Along with uncontrolled neutrophil recruitment, high

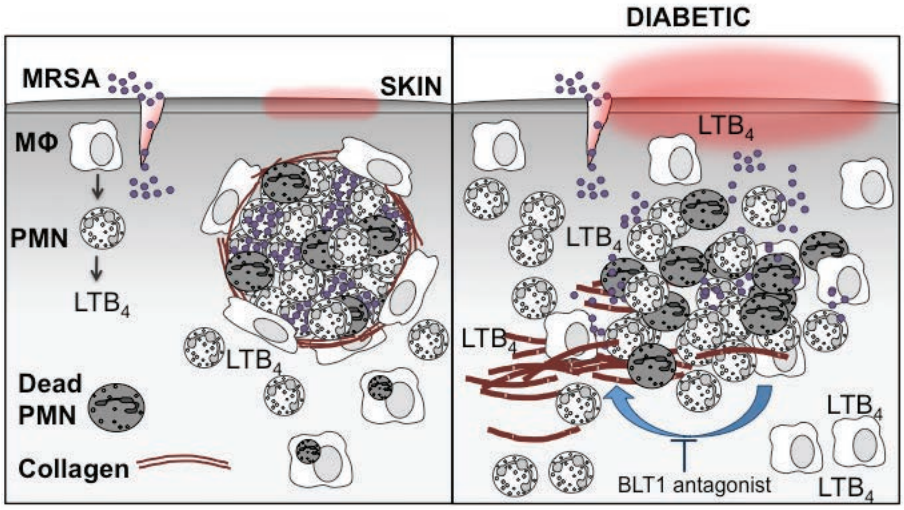

Figure 49. Summary of excessive LTB_4 driving uncontrolled inflammation in diabetic mice during MRSA skin infection. Left panel: MRSA skin infection requires tissue-resident macrophages for optimal LTB_4 production and neutrophil recruitment. LTB_4 provides direction to neutrophils to contain bacteria and form an abscess surrounded by fibrous collagen. Right panel: Macrophages in diabetic mice promote excessive LTB_4 production, overwhelming neutrophil recruitment, irregular collagen deposition, and uncontrolled cell death and bacterial burden. BLT1 antagonist treatment reduces inflammation by breaking continuous overwhelming inflammatory signals.

numbers of dead cells were observed in diabetic mice. The levels of LTB_4 determine infection outcome. In nondiabetic mice, LTB_4 is an important molecule in promoting antibacterial functions to eliminate MRSA. Additionally, combination ointment therapy of LTB_4 and antibiotic mupirocin greatly accelerated the clearance of infection. Conversely, in settings of chronic inflammation such as diabetes, high LTB_4 levels drove overwhelming inflammation and contributed to poor host defense. Dampening inflammation through blocking BLT1 improved host defense. Since the levels of LTB_4 correlated with infection outcome, this highlights the importance of future research into investigating how underlying conditions affect inflammatory mediators. Therefore, targeting LTB_4/BLT1 has therapeutic potential and has the potential for being applicable to other settings of vulnerability or chronic inflammation. For infections, this treatment strategy may be used in combination with antibiotics to better control infections.

FUTURE DIRECTIONS

Part I – Beneficial LTB_4 actions

Role of skin-resident macrophages in MRSA skin infection

Due to the challenge of isolating sufficient macrophages from the skin for in vitro experimentation, it is difficult to study these cells. Also, the use of bone marrow derived macrophages or isolating macrophages from other locations, such as the peritoneum, may not serve as good models for dermal macrophages. Therefore, efforts into generating a skin macrophage cell line by transformation in order to retain more physiological characteristics rather than using macrophages isolated from another anatomical site. These cells will be used to investigate the role of skin-resident macrophages during MRSA skin infection. One strategy is to isolate $F4/80^+$ cells from the skin of WT mice and infect the macrophages with J2 retrovirus. J2 retrovirus carries the v-raf and v-myc oncogenes.

Once the cell line is established, the next step will be to characterize and compare gene expression profiles with AMJ2-C11 (alveolar macrophage cell line available at ATCC) and B6PMCL (C57BL/6 peritoneal macrophage cell line generated in our laboratory). Since these cells were generated with J2 retrovirus but are macrophages isolated from different areas (lung, peritoneal cavity, and skin), this will serve as comparisons. Cells will be stained with Diff-Quik for histological analysis. Single-cell RNA-seq will determine differences in gene expression and also to compare the dermal macrophages to primary dermal macrophages isolated from the skin of healthy mice. Functional analyses such as phagocytosis and cytokine and chemokine production will also be determined.

If the dermal macrophage cell line shows a significantly different macrophage subset profile from the other cell lines, this would become a useful tool in the field to study the biology of skin-resident macrophages.

Producers and responders of LTB_4

LTB_4 is an important molecule for controlling MRSA skin infections. Macrophage depletion resulted in lower LTB_4 levels produced in the skin during MRSA skin infection suggesting that macrophages are a likely source for LTB_4. However, macrophage depletion also significantly reduced neutrophil recruitment to the skin. Since neutrophils are also a source of LTB_4 in the skin [81], it is possible that the reduction of LTB_4 seen in macrophage-depleted mice is the result from fewer neutrophils recruited to the skin. Also, neutrophil depletion with Ly6G antibody treatment also reduced levels of LTB_4, but not completely. It is likely that both macrophages and neutrophils are sources of LTB_4. The goals for this future direction would be to identify which cells are producing LTB_4 and which cells are responding to LTB_4.

The use of MMDTR mice to deplete macrophages and Ly6G antibody to deplete neutrophils will help determine the role of these cells in LTB_4 production. Depleting macrophages and neutrophils in the same animals would eliminate both cell types and would be expected to produce very little LTB_4 in the skin. However, eliminating macrophages and neutrophils during infection brings up the concern that these cells have other functions (phagocytosis and killing of pathogens, and producing other chemokines) that would also be eliminated.

Therefore, generating a *Alox5*^{flox} mouse with CRISPR/CAS9 would be a useful tool to knockout leukotriene production in various cell types by crossing them to various Cre-specific mouse strains: *LysM*^{cre} would eliminate leukotriene production from myeloid cells, Csf1r^{cre} from macrophages, *MRP8*^{cre} from neutrophils, *CD11c*^{cre} from dendritic cells, *Adipoq*^{cre} from adipocytes, *Krt17*^{cre} from keratinocytes, and *Col1a2*^{cre} from fibroblasts. Eliminating 5-LO expression in various cell types would determine which cell types are important for leukotriene production during MRSA skin infection.

Potential problems could be that eliminating 5-LO activity in various cell types may induce compensatory production of leukotrienes by other cells. Additionally, 5-LO deficiency impairs the production of all leukotrienes and other 5-LO metabolites. The role of these other metabolites by individual cell may be overlooked with the proposed *Alox5*^{flox} mouse model. However, another strategy to add back various leukotrienes in ointment form may be utilized to determine whether certain leukotrienes are involved in MRSA skin infection or not. Examples would be to treat *Alox5* knockout or cell-specific knockout mice with topical ointments containing LTB_4 or other leukotrienes such as LTD_4, which has been shown to have antimicrobial defense activities [107].

Another future direction is to determine which cells are responding to LTB_4. The use of the newly generated mouse model *Ltb4r1*$^{LsL\text{-}DsRED\text{-}DTR}$ would be a beneficial tool in studying BLT1 in various cell types during MRSA skin infection. These mice contain a floxed stop codon under the *Ltb4r1* promoter, which is removed with cre recombination to generate DsRed-DTR expression.

The DsRED fluorescent marker will be useful to track the cells. Additionally, treating mice with diphtheria toxin will ablate these cells. The *Ltb4r1*$^{LsL\text{-}DsRED\text{-}DTR}$ mouse model will also be crossed with other Cre-expressing mouse strains: *Csf1r*^{cre} for macrophages, *MRP8*^{cre} for neutrophils, *CD11c*^{cre} for dendritic cells, *Adipoq*^{cre} for adipocytes, *Krt17*^{cre} for keratinocytes, and *Col1a2*^{cre} for fibroblasts. These mice will be used to study the role of BLT1 in various cell types during infection. The DTR allows for the specific deletion of these cells at various times before or during infection in order to evaluate the role of these cells are different stages of the infection.

Abscess formation and resolution

There is great interest in studying the mediators that initiate abscess formation and which mediators regulate and end swarming. Microscale arrays have been developed to study swarming behavior of neutrophils in vitro [219]. This technology will be adapted to study the role of LTB_4 and swarming in response to MRSA. These assays will also be imaged by live-cell imaging techniques in co-culture experiments with macrophages.

In vitro 3D abscesses similar to tumor spheroid-models [220] will supplement the 2D microscale arrays. Neutrophils, macrophages, and MRSA will be embedded in a matrix-gel (such as collagen) and cell migration will be observed. Live-cell imaging will be used with fluorescently labeled macrophages, neutrophils, and fibroblasts to visualize interactions between these cells. Co-culture experiments with various cell types will help determine the roles and

contributions of these cells during MRSA infection. Also, since abscess formation is important for bacterial clearance, these experiments will help address the consequences of poor abscess formation. Additionally, some abscesses can become problematic and require surgical drainage. Experiments investigating the factors involved in abscess formation and resolution may help determine how abscesses become chronic.

Part II – Detrimental LTB_4 actions

Insulin versus hyperglycemia

Mice that were induced to be diabetic with STZ did not have significantly impaired host defense after 10 days (data not shown). However, mice that were diabetic for 30 days prior to MRSA skin infection displayed impaired host defense. Attempts to treat diabetic mice with insulin during the course of MRSA skin infection failed to improve host defense (data not shown). This may suggest that chronic diabetes irreversibly alters immune functions. One strategy will be to treat diabetic mice with insulin and maintain euglycemia for various lengths of time prior to MRSA skin infection. This would determine whether maintaining glucose levels reduce the susceptibility to infection risk. Another strategy is to treat mice with phlorizin to reduce blood glucose levels without altering insulin levels.

Also, investigating T2D models will also help elucidate the role of insulin vs. hyperglycemia. Diabetic NOD mice and STZ-induced diabetic mice, which both have low insulin levels and hyperglycemia, both have worse outcome to MRSA skin infection compared to their nondiabetic controls. T2D models db/db and control db/+ mice will be used to investigate whether type 2 diabetic mice also have worse MRSA skin infection and whether topical BLT1 antagonist would improve host defense. Type 2 diabetic mice will be treated with phlorizin to lower blood glucose levels prior to MRSA skin infection to determine whether the treatment improves host defense.

The goals with this aim are to investigate the impact of insulin and hyperglycemia on host defense during MRSA skin infection and whether the mechanisms of poor host defense are driven by similar mechanisms between T1D and T2D. If there are differences between T1D and T2D, this may indicate that treatment recommendations may need to be tailored depending on underlying conditions.

Balance of eicosanoids

Eicosanoids encompass a wide family of lipid mediators but all arise from arachidonic acid. From arachidonic acid, leukotrienes are produced from lipoxygenase activity and prostaglandins are produced from cyclooxygenase activity.

Diabetic mice have lower levels of PGE_2 in the skin during MRSA skin infection compared to nondiabetic control mice [176]. Host defense was restored when diabetic mice were treated with a topical ointment containing misoprostol, a PGE analog. Complementary to this, diabetic mice have high LTB_4 levels in the skin which drives poor host defense. In both instances, targeting the impairment restores host defense in diabetic mice. Whether host defense mechanisms are restored in similar mechanisms will be addressed. Low PGE_2 levels in diabetic impaired dendritic cell maturation and migration to the lymph nodes, which impaired the recruitment of beneficial Th17 cells to the site of infection. Whether BLT1 antagonist treatment restores Th17 activation and IL-17 production will be determined. Additionally, BLT1 antagonist treatment in diabetic mice reduced

neutrophil recruitment and allowed for better abscess formation and bacterial clearance. It will be determined whether topical misoprostol treatment improves these events. Additionally, diabetic mice will be treated with topical ointments containing BLT1 antagonist and the PGE analog misoprostol to evaluate combination therapy. These therapies will further be evaluated in combination with antibiotic therapy.

Biopsy samples will be collected at various time points during infection and mass spectrometry analysis will be used to measure the levels of eicosanoids and whether BLT1 antagonist of PGE analog treatments restore the eicosanoid balance in the skin. In order to determine whether PGE_2 or LTB_4 is more dominant, diabetic mice treated with misoprostol will also be treated with topical LTB_4 ointment, and diabetic mice treated with BLT1 antagonist will be treated with indomethacin or EP receptor antagonists. This will determine whether treating mice with the opposing treatment would inhibit the beneficial treatment.

Along with the balance of eicosanoids, the role of LTB_4 on BLT1 and BLT2 can be investigated in more detail. Whether BLT2 is involved during MRSA skin infections is not well understood. Although no significant effects were observed when diabetic mice were treated with BLT2 antagonist, the treatment dose and regime could be altered. Also, other cyclooxygenase products such as 12-HHT can signal through BLT2 and has been shown to improve wound healing in diabetic mice. Mice deficient in BLT1, BLT2, or both BLT1/2 will be studied. Also the use of U-75302 and LY255283 and LTB_4 and BLT2 agonists will be used to

treat mice and in vitro cell cultures. It would be expected that if 12-HHT is necessary for wound healing, that BLT2 antagonist treatment may exacerbate the infection.

Cell death pathways and mechanisms of clearance

Higher abundance of dead cells was observed in the skin of diabetic mice. The contribution of dead cell burden could result from one or a combination of the following: more neutrophil recruitment, signals in the skin triggering cell death, or inefficient efferocytosis to remove dead cells. TUNEL staining and flow cytometry analysis for 7AAD and AnnexinV show higher numbers of dead cells in skin of diabetic mice during infection. However, the majority of dead cells were not dying by caspase-3 activation for apoptosis (data not shown). The use of inhibitors or mice with genetic knockout for various proteins involved in the cell death pathways may reveal how the cells are dying in the skin.

How the cells die may alter the potential of the phagocytic cell to promote inflammation [221, 222]. Cells infected with *S. aureus* have been reported to die by various mechanisms [156, 209, 210]. Future experiments will help determine whether the cell death pathway is different in cells in the skin of diabetic mice, and whether BLT1 antagonist treatment alters this process. If there are differences in cell death mechanisms between diabetic and nondiabetic mice, future experiments will be performed to assess the activation and inflammatory profile of macrophages that engulf dead cells.

REFERENCES

[1] S.E. Turvey, D.H. Broide, Innate immunity, J Allergy Clin Immunol 125(2 Suppl 2) (2010) S24-32.

[2] M.G. Netea, E. Latz, K.H. Mills, L.A. O'Neill, Innate immune memory: a paradigm shift in understanding host defense, Nat Immunol 16(7) (2015) 675-9.

[3] S. Saeed, J. Quintin, H.H. Kerstens, N.A. Rao, A. Aghajanirefah, F. Matarese, S.C. Cheng, J. Ratter, K. Berentsen, M.A. van der Ent, N. Sharifi, E.M. Janssen-Megens, M. Ter Huurne, A. Mandoli, T. van Schaik, A. Ng, F. Burden, K. Downes, M. Frontini, V. Kumar, E.J. Giamarellos-Bourboulis, W.H. Ouwehand, J.W. van der Meer, L.A. Joosten, C. Wijmenga, J.H. Martens, R.J. Xavier, C. Logie, M.G. Netea, H.G. Stunnenberg, Epigenetic programming of monocyte-to-macrophage differentiation and trained innate immunity, Science 345(6204) (2014) 1251086.

[4] S.C. Cheng, J. Quintin, R.A. Cramer, K.M. Shepardson, S. Saeed, V. Kumar, E.J. Giamarellos-Bourboulis, J.H. Martens, N.A. Rao, A. Aghajanirefah, G.R. Manjeri, Y. Li, D.C. Ifrim, R.J. Arts, B.M. van der Veer, P.M. Deen, C. Logie, L.A. O'Neill, P. Willems, F.L. van de Veerdonk, J.W. van der Meer, A. Ng, L.A. Joosten, C. Wijmenga, H.G. Stunnenberg, R.J. Xavier, M.G. Netea, mTOR- and HIF-1alpha-mediated aerobic glycolysis as metabolic basis for trained immunity, Science 345(6204) (2014) 1250684.

[5] F.A. Bonilla, H.C. Oettgen, Adaptive immunity, J Allergy Clin Immunol 125(2 Suppl 2) (2010) S33-40.

[6] D.A. Vignali, L.W. Collison, C.J. Workman, How regulatory T cells work, Nat Rev Immunol 8(7) (2008) 523-32.

[7] J. Zhu, H. Yamane, W.E. Paul, Differentiation of effector CD4 T cell populations (*), Annu Rev Immunol 28 (2010) 445-89.

[8] A.C. Shaw, D.R. Goldstein, R.R. Montgomery, Age-dependent dysregulation of innate immunity, Nat Rev Immunol 13(12) (2013) 875-87.

[9] Y.J. Juhn, Risks for infection in patients with asthma (or other atopic conditions): is asthma more than a chronic airway disease?, J Allergy Clin Immunol 134(2) (2014) 247-57; quiz 258-9.

[10] M.F. Gregor, G.S. Hotamisligil, Inflammatory mechanisms in obesity, Annu Rev Immunol 29 (2011) 415-45.

[11] A.H. Sprague, R.A. Khalil, Inflammatory cytokines in vascular dysfunction and vascular disease, Biochem Pharmacol 78(6) (2009) 539-52.

[12] G. Feuerstein, J.M. Hallenbeck, Prostaglandins, leukotrienes, and platelet-activating factor in shock, Annu Rev Pharmacol Toxicol 27 (1987) 301-13.

[13] M.D. Turner, B. Nedjai, T. Hurst, D.J. Pennington, Cytokines and chemokines: At the crossroads of cell signalling and inflammatory disease, Biochim Biophys Acta 1843(11) (2014) 2563-2582.

[14] M.C. Basil, B.D. Levy, Specialized pro-resolving mediators: endogenous regulators of infection and inflammation, Nat Rev Immunol 16(1) (2016) 51-67.

[15] M.E. Kotas, R. Medzhitov, Homeostasis, inflammation, and disease susceptibility, Cell 160(5) (2015) 816-27.

[16] R. Medzhitov, Origin and physiological roles of inflammation, Nature 454(7203) (2008) 428-35.

[17] C.D. Bourke, J.A. Berkley, A.J. Prendergast, Immune Dysfunction as a Cause and Consequence of Malnutrition, Trends Immunol 37(6) (2016) 386-398.

[18] C. Shi, E.G. Pamer, Monocyte recruitment during infection and inflammation, Nat Rev Immunol 11(11) (2011) 762-74.

[19] L.C. Davies, S.J. Jenkins, J.E. Allen, P.R. Taylor, Tissue-resident macrophages, Nat Immunol 14(10) (2013) 986-95.

[20] S. Epelman, K.J. Lavine, G.J. Randolph, Origin and functions of tissue macrophages, Immunity 41(1) (2014) 21-35.

[21] S. Gordon, Alternative activation of macrophages, Nat Rev Immunol 3(1) (2003) 23-35.

[22] D.M. Mosser, J.P. Edwards, Exploring the full spectrum of macrophage activation, Nat Rev Immunol 8(12) (2008) 958-69.

[23] A. Mathur, A.S. Tripathi, M. Kuse, Scalable system for classification of white blood cells from Leishman stained blood stain images, J Pathol Inform 4(Suppl) (2013) S15.

[24] D.C. Doeing, J.L. Borowicz, E.T. Crockett, Gender dimorphism in differential peripheral blood leukocyte counts in mice using cardiac, tail, foot, and saphenous vein puncture methods, BMC Clin Pathol 3(1) (2003) 3.

[25] M. Faurschou, N. Borregaard, Neutrophil granules and secretory vesicles in inflammation, Microbes Infect 5(14) (2003) 1317-27.

[26] N. Borregaard, J.B. Cowland, Granules of the human neutrophilic polymorphonuclear leukocyte, Blood 89(10) (1997) 3503-21.

[27] V. Brinkmann, U. Reichard, C. Goosmann, B. Fauler, Y. Uhlemann, D.S. Weiss, Y. Weinrauch, A. Zychlinsky, Neutrophil extracellular traps kill bacteria, Science 303(5663) (2004) 1532-5.

[28] O.A. Chow, M. von Kockritz-Blickwede, A.T. Bright, M.E. Hensler, A.S. Zinkernagel, A.L. Cogen, R.L. Gallo, M. Monestier, Y. Wang, C.K. Glass, V. Nizet, Statins enhance formation of phagocyte extracellular traps, Cell Host Microbe 8(5) (2010) 445-54.

[29] M. Peters-Golden, M.M. Gleason, A. Togias, Cysteinyl leukotrienes: multi-functional mediators in allergic rhinitis, Clin Exp Allergy 36(6) (2006) 689-703.

[30] O. Werz, 5-lipoxygenase: cellular biology and molecular pharmacology, Curr Drug Targets Inflamm Allergy 1(1) (2002) 23-44.

[31] R. Nolfo, J.A. Rankin, U937 and THP-1 cells do not release LTB4, LTC4, or LTD4 in response to A23187, Prostaglandins 39(2) (1990) 157-65.

[32] A. Sala, G. Folco, R.C. Murphy, Transcellular biosynthesis of eicosanoids, Pharmacol Rep 62(3) (2010) 503-10.

[33] J.E. McGee, F.A. Fitzpatrick, Erythrocyte-neutrophil interactions: formation of leukotriene B4 by transcellular biosynthesis, Proc Natl Acad Sci U S A 83(5) (1986) 1349-53.

[34] L. Iversen, K. Fogh, V.A. Ziboh, P. Kristensen, A. Schmedes, K. Kragballe, Leukotriene B4 formation during human neutrophil keratinocyte interactions: evidence for transformation of leukotriene A4 by putative keratinocyte leukotriene A4 hydrolase, J Invest Dermatol 100(3) (1993) 293-8.

[35] J. Breton, D. Woolf, P. Young, M. Chabot-Fletcher, Human keratinocytes lack the components to produce leukotriene B4, J Invest Dermatol 106(1) (1996) 162-7.

[36] U. Janssen-Timmen, P.J. Vickers, U. Wittig, W.D. Lehmann, H.J. Stark, N.E. Fusenig, T. Rosenbach, O. Radmark, B. Samuelsson, A.J. Habenicht, Expression of 5-lipoxygenase in differentiating human skin keratinocytes, Proc Natl Acad Sci U S A 92(15) (1995) 6966-70.

[37] S.J. Feinmark, The role of the endothelial cell in leukotriene biosynthesis, Am Rev Respir Dis 146(5 Pt 2) (1992) S51-5.

[38] M. Peters-Golden, T.G. Brock, 5-Lipoxygenase and the Nucleus: Where, When, How, and Why?, in: B. Samuelsson, R. Paoletti, G.C. Folco, E. Granström, S. Nicosia (Eds.), Advances in Prostaglandin and Leukotriene Research: Basic Science and New Clinical Applications, Springer Netherlands, Dordrecht, 2001, pp. 9-15.

[39] S. Glover, M.S. de Carvalho, T. Bayburt, M. Jonas, E. Chi, C.C. Leslie, M.H. Gelb, Translocation of the 85-kDa phospholipase A2 from cytosol to the nuclear envelope in rat basophilic leukemia cells stimulated with calcium ionophore or IgE/antigen, J Biol Chem 270(25) (1995) 15359-67.

[40] M. Peters-Golden, R.W. McNish, Redistribution of 5-lipoxygenase and cytosolic phospholipase A2 to the nuclear fraction upon macrophage activation, Biochem Biophys Res Commun 196(1) (1993) 147-53.

[41] J.W. Woods, M.J. Coffey, T.G. Brock, Singer, II, M. Peters-Golden, 5-Lipoxygenase is located in the euchromatin of the nucleus in resting human alveolar macrophages and translocates to the nuclear envelope upon cell activation, J Clin Invest 95(5) (1995) 2035-46.

[42] M. Peters-Golden, Cell biology of the 5-lipoxygenase pathway, Am J Respir Crit Care Med 157(6 Pt 2) (1998) S227-31; discussion S231-2, S247-8.

[43] C. Canetti, B. Hu, J.L. Curtis, M. Peters-Golden, Syk activation is a leukotriene B4-regulated event involved in macrophage phagocytosis of IgG-coated targets but not apoptotic cells, Blood 102(5) (2003) 1877-83.

[44] J. Gosselin, P. Borgeat, Epstein-Barr virus modulates 5-lipoxygenase product synthesis in human peripheral blood mononuclear cells, Blood 89(6) (1997) 2122-30.

[45] M. Grone, J. Scheffer, W. Konig, Modulation of leukotriene generation by invasive bacteria, Immunology 77(3) (1992) 400-7.

[46] T.G. Brock, M. Peters-Golden, Activation and regulation of cellular eicosanoid biosynthesis, ScientificWorldJournal 7 (2007) 1273-84.

[47] O. Radmark, B. Samuelsson, 5-Lipoxygenase: mechanisms of regulation, J Lipid Res 50 Suppl (2009) S40-5.

[48] T. Yokomizo, Two distinct leukotriene B4 receptors, BLT1 and BLT2, J Biochem 157(2) (2015) 65-71.

[49] A.M. Tager, A.D. Luster, BLT1 and BLT2: the leukotriene B(4) receptors, Prostaglandins Leukot Essent Fatty Acids 69(2-3) (2003) 123-34.

[50] C.M. Peres, D.M. Aronoff, C.H. Serezani, N. Flamand, L.H. Faccioli, M. Peters-Golden, Specific leukotriene receptors couple to distinct G proteins to effect stimulation of alveolar macrophage host defense functions, J Immunol 179(8) (2007) 5454-61.

[51] A.J. Lee, K.J. Cho, J.H. Kim, MyD88-BLT2-dependent cascade contributes to LPS-induced interleukin-6 production in mouse macrophage, Exp Mol Med 47 (2015) e156.

[52] Y. Zhang, R.M. Olson, C.R. Brown, Macrophage LTB4 drives efficient phagocytosis of Borrelia burgdorferi via BLT1 or BLT2, J Lipid Res 58(3) (2017) 494-503.

[53] E.M. Soares, K.L. Mason, L.M. Rogers, C.H. Serezani, L.H. Faccioli, D.M. Aronoff, Leukotriene B4 enhances innate immune defense against the puerperal sepsis agent Streptococcus pyogenes, J Immunol 190(4) (2013) 1614-22.

[54] M. Liu, K. Saeki, T. Matsunobu, T. Okuno, T. Koga, Y. Sugimoto, C. Yokoyama, S. Nakamizo, K. Kabashima, S. Narumiya, T. Shimizu, T. Yokomizo, 12-Hydroxyheptadecatrienoic acid promotes epidermal wound healing by accelerating keratinocyte migration via the BLT2 receptor, J Exp Med 211(6) (2014) 1063-78.

[55] G.Y. Kim, J.W. Lee, S.H. Cho, J.M. Seo, J.H. Kim, Role of the low-affinity leukotriene B4 receptor BLT2 in VEGF-induced angiogenesis, Arterioscler Thromb Vasc Biol 29(6) (2009) 915-20.

[56] O. Takeuchi, S. Akira, Pattern recognition receptors and inflammation, Cell 140(6) (2010) 805-20.

[57] J.K. Dowling, A. Mansell, Toll-like receptors: the swiss army knife of immunity and vaccine development, Clin Transl Immunology 5(5) (2016) e85.

[58] K. Takeda, T. Kaisho, S. Akira, Toll-like receptors, Annu Rev Immunol 21 (2003) 335-76.

[59] P.P. Tak, G.S. Firestein, NF-kappaB: a key role in inflammatory diseases, J Clin Invest 107(1) (2001) 7-11.

[60] C.H. Serezani, C. Lewis, S. Jancar, M. Peters-Golden, Leukotriene B4 amplifies NF-kappaB activation in mouse macrophages by reducing SOCS1 inhibition of MyD88 expression, J Clin Invest 121(2) (2011) 671-82.

[61] L.R. Filgueiras, S.L. Brandt, S. Wang, Z. Wang, D.L. Morris, C. Evans-Molina, R.G. Mirmira, S. Jancar, C.H. Serezani, Leukotriene B4-mediated sterile inflammation promotes susceptibility to sepsis in a mouse model of type 1 diabetes, Sci Signal 8(361) (2015) ra10.

[62] E. Gaudreault, C. Paquet-Bouchard, S. Fiola, M. Le Bel, P. Lacerte, M.T. Shio, M. Olivier, J. Gosselin, TAK1 contributes to the enhanced responsiveness of LTB(4)-treated neutrophils to Toll-like receptor ligands, Int Immunol 24(11) (2012) 693-704.

[63] C.A. Leifer, A.E. Medvedev, Molecular mechanisms of regulation of Toll-like receptor signaling, J Leukoc Biol 100(5) (2016) 927-941.

[64] E. Gaudreault, J. Gosselin, Leukotriene B4 potentiates CpG signaling for enhanced cytokine secretion by human leukocytes, J Immunol 183(4) (2009) 2650-8.

[65] B.A. Croker, H. Kiu, S.E. Nicholson, SOCS regulation of the JAK/STAT signalling pathway, Semin Cell Dev Biol 19(4) (2008) 414-22.

[66] L. Huang, A. Zhao, F. Wong, J.M. Ayala, M. Struthers, F. Ujjainwalla, S.D. Wright, M.S. Springer, J. Evans, J. Cui, Leukotriene B4 strongly increases monocyte chemoattractant protein-1 in human monocytes, Arterioscler Thromb Vasc Biol 24(10) (2004) 1783-8.

[67] H. Saiwai, Y. Ohkawa, H. Yamada, H. Kumamaru, A. Harada, H. Okano, T. Yokomizo, Y. Iwamoto, S. Okada, The LTB4-BLT1 axis mediates neutrophil infiltration and secondary injury in experimental spinal cord injury, Am J Pathol 176(5) (2010) 2352-66.

[68] E.Y. Choi, S. Santoso, T. Chavakis, Mechanisms of neutrophil transendothelial migration, Front Biosci (Landmark Ed) 14 (2009) 1596-605.

[69] R.P. McEver, R.D. Cummings, Perspectives series: cell adhesion in vascular biology. Role of PSGL-1 binding to selectins in leukocyte recruitment, J Clin Invest 100(3) (1997) 485-91.

[70] K. Futosi, S. Fodor, A. Mocsai, Neutrophil cell surface receptors and their intracellular signal transduction pathways, Int Immunopharmacol 17(3) (2013) 638-50.

[71] B. Heit, S. Tavener, E. Raharjo, P. Kubes, An intracellular signaling hierarchy determines direction of migration in opposing chemotactic gradients, J Cell Biol 159(1) (2002) 91-102.

[72] B. Samuelsson, S.E. Dahlen, J.A. Lindgren, C.A. Rouzer, C.N. Serhan, Leukotrienes and lipoxins: structures, biosynthesis, and biological effects, Science 237(4819) (1987) 1171-6.

[73] T. Yokomizo, T. Izumi, K. Chang, Y. Takuwa, T. Shimizu, A G-protein-coupled receptor for leukotriene B4 that mediates chemotaxis, Nature 387(6633) (1997) 620-4.

[74] C.H. Woo, M.H. Yoo, H.J. You, S.H. Cho, Y.C. Mun, C.M. Seong, J.H. Kim, Transepithelial migration of neutrophils in response to leukotriene B4 is mediated by a reactive oxygen species-extracellular signal-regulated kinase-linked cascade, J Immunol 170(12) (2003) 6273-9.

[75] K. Goodarzi, M. Goodarzi, A.M. Tager, A.D. Luster, U.H. von Andrian, Leukotriene B4 and BLT1 control cytotoxic effector T cell recruitment to inflamed tissues, Nat Immunol 4(10) (2003) 965-73.

[76] A. Del Prete, W.H. Shao, S. Mitola, G. Santoro, S. Sozzani, B. Haribabu, Regulation of dendritic cell migration and adaptive immune response by leukotriene B4 receptors: a role for LTB4 in up-regulation of CCR7 expression and function, Blood 109(2) (2007) 626-31.

[77] B. Czarnetzki, Increased monocyte chemotaxis towards leukotriene B4 and platelet activating factor in patients with inflammatory dermatoses, Clin Exp Immunol 54(2) (1983) 486-92.

[78] P.V. Afonso, M. Janka-Junttila, Y.J. Lee, C.P. McCann, C.M. Oliver, K.A. Aamer, W. Losert, M.T. Cicerone, C.A. Parent, LTB4 is a signal-relay molecule during neutrophil chemotaxis, Dev Cell 22(5) (2012) 1079-91.

[79] A.P. Monteiro, C.S. Pinheiro, T. Luna-Gomes, L.R. Alves, C.M. Maya-Monteiro, B.N. Porto, C. Barja-Fidalgo, C.F. Benjamim, M. Peters-Golden, C. Bandeira-Melo, M.T. Bozza, C. Canetti, Leukotriene B4 mediates neutrophil migration induced by heme, J Immunol 186(11) (2011) 6562-7.

[80] D.J. Allendorf, J. Yan, G.D. Ross, R.D. Hansen, J.T. Baran, K. Subbarao, L. Wang, B. Haribabu, C5a-mediated leukotriene B4-amplified neutrophil chemotaxis is essential in tumor immunotherapy facilitated by anti-tumor monoclonal antibody and beta-glucan, J Immunol 174(11) (2005) 7050-6.

[81] T. Lammermann, P.V. Afonso, B.R. Angermann, J.M. Wang, W. Kastenmuller, C.A. Parent, R.N. Germain, Neutrophil swarms require LTB4 and integrins at sites of cell death in vivo, Nature 498(7454) (2013) 371-5.

[82] Y. Hirano, M. Aziz, P. Wang, Role of reverse transendothelial migration of neutrophils in inflammation, Biol Chem 397(6) (2016) 497-506.

[83] B. Colom, J.V. Bodkin, M. Beyrau, A. Woodfin, C. Ody, C. Rourke, T. Chavakis, K. Brohi, B.A. Imhof, S. Nourshargh, Leukotriene B4-Neutrophil Elastase Axis Drives Neutrophil Reverse Transendothelial Cell Migration In Vivo, Immunity 42(6) (2015) 1075-86.

[84] S. Gordon, Phagocytosis: An Immunobiologic Process, Immunity 44(3) (2016) 463-75.

[85] A.M. Kerrigan, G.D. Brown, C-type lectins and phagocytosis, Immunobiology 214(7) (2009) 562-75.

[86] T. Areschoug, S. Gordon, Scavenger receptors: role in innate immunity and microbial pathogenesis, Cell Microbiol 11(8) (2009) 1160-9.

[87] R.L. Silverstein, M. Febbraio, CD36, a scavenger receptor involved in immunity, metabolism, angiogenesis, and behavior, Sci Signal 2(72) (2009) re3.

[88] A. Aderem, D.M. Underhill, Mechanisms of phagocytosis in macrophages, Annu Rev Immunol 17 (1999) 593-623.

[89] P. Rougerie, V. Miskolci, D. Cox, Generation of membrane structures during phagocytosis and chemotaxis of macrophages: role and regulation of the actin cytoskeleton, Immunol Rev 256(1) (2013) 222-39.

[90] J.M. Kinchen, K.S. Ravichandran, Phagosome maturation: going through the acid test, Nat Rev Mol Cell Biol 9(10) (2008) 781-95.

[91] A.R. Mantegazza, J.G. Magalhaes, S. Amigorena, M.S. Marks, Presentation of phagocytosed antigens by MHC class I and II, Traffic 14(2) (2013) 135-52.

[92] V. Braun, F. Niedergang, Linking exocytosis and endocytosis during phagocytosis, Biol Cell 98(3) (2006) 195-201.

[93] J.J. Wirth, F. Kierszenbaum, Stimulatory effects of leukotriene B4 on macrophage association with and intracellular destruction of Trypanosoma cruzi, J Immunol 134(3) (1985) 1989-93.

[94] M.B. Bailie, T.J. Standiford, L.L. Laichalk, M.J. Coffey, R. Strieter, M. Peters-Golden, Leukotriene-deficient mice manifest enhanced lethality from Klebsiella pneumonia in association with decreased alveolar macrophage phagocytic and bactericidal activities, J Immunol 157(12) (1996) 5221-4.

[95] P. Mancuso, T.J. Standiford, T. Marshall, M. Peters-Golden, 5-Lipoxygenase reaction products modulate alveolar macrophage phagocytosis of Klebsiella pneumoniae, Infect Immun 66(11) (1998) 5140-6.

[96] P. Mancuso, P. Nana-Sinkam, M. Peters-Golden, Leukotriene B4 augments neutrophil phagocytosis of Klebsiella pneumoniae, Infect Immun 69(4) (2001) 2011-6.

[97] A. Secatto, L.C. Rodrigues, C.H. Serezani, S.G. Ramos, M. Dias-Baruffi, L.H. Faccioli, A.I. Medeiros, 5-Lipoxygenase deficiency impairs innate and adaptive immune responses during fungal infection, PLoS One 7(3) (2012) e31701.

[98] A. Secatto, E.M. Soares, G.A. Locachevic, P.A. Assis, F.W. Paula-Silva, C.H. Serezani, A.I. de Medeiros, L.H. Faccioli, The leukotriene B(4)/BLT(1) axis is a key determinant in susceptibility and resistance to histoplasmosis, PLoS One 9(1) (2014) e85083.

[99] C.H. Serezani, S. Kane, L. Collins, M. Morato-Marques, J.J. Osterholzer, M. Peters-Golden, Macrophage dectin-1 expression is controlled by leukotriene B4 via a GM-CSF/PU.1 axis, J Immunol 189(2) (2012) 906-15.

[100] P.C. Santos, D.A. Santos, L.S. Ribeiro, C.T. Fagundes, T.P. de Paula, T.V. Avila, M. Baltazar Lde, M.M. Madeira, C. Cruz Rde, A.C. Dias, F.S. Machado, M.M. Teixeira, P.S. Cisalpino, D.G. Souza, The pivotal role of 5-lipoxygenase-derived LTB4 in controlling pulmonary paracoccidioidomycosis, PLoS Negl Trop Dis 7(8) (2013) e2390.

[101] C.I. Morato, I.A. da Silva, Jr., A.F. Borges, M.L. Dorta, M.A. Oliveira, S. Jancar, C.H. Serezani, F. Ribeiro-Dias, Essential role of leukotriene B4 on Leishmania (Viannia) braziliensis killing by human macrophages, Microbes Infect 16(11) (2014) 945-53.

[102] N.M. Tavares, T. Araujo-Santos, L. Afonso, P.M. Nogueira, U.G. Lopes, R.P. Soares, P.T. Bozza, C. Bandeira-Melo, V.M. Borges, C. Brodskyn, Understanding the mechanisms controlling Leishmania amazonensis infection in vitro: the role of LTB4 derived from human neutrophils, J Infect Dis 210(4) (2014) 656-66.

[103] A. Talvani, F.S. Machado, G.C. Santana, A. Klein, L. Barcelos, J.S. Silva, M.M. Teixeira, Leukotriene B(4) induces nitric oxide synthesis in Trypanosoma cruzi-infected murine macrophages and mediates resistance to infection, Infect Immun 70(8) (2002) 4247-53.

[104] C.H. Serezani, D.M. Aronoff, R.G. Sitrin, M. Peters-Golden, FcgammaRI ligation leads to a complex with BLT1 in lipid rafts that enhances rat lung macrophage antimicrobial functions, Blood 114(15) (2009) 3316-24.

[105] M.R. Campos, C.H. Serezani, M. Peters-Golden, S. Jancar, Differential kinase requirement for enhancement of Fc gammaR-mediated phagocytosis in alveolar macrophages by leukotriene B4 vs. D4, Mol Immunol 46(6) (2009) 1204-11.

[106] C.H. Serezani, D.M. Aronoff, S. Jancar, P. Mancuso, M. Peters-Golden, Leukotrienes enhance the bactericidal activity of alveolar macrophages against Klebsiella pneumoniae through the activation of NADPH oxidase, Blood 106(3) (2005) 1067-75.

[107] M. Morato-Marques, M.R. Campos, S. Kane, A.P. Rangel, C. Lewis, M.N. Ballinger, S.H. Kim, M. Peters-Golden, S. Jancar, C.H. Serezani, Leukotrienes target F-actin/cofilin-1 to enhance alveolar macrophage anti-fungal activity, J Biol Chem 286(33) (2011) 28902-13.

[108] Y. Kobayashi, Neutrophil biology: an update, EXCLI J 14 (2015) 220-7.

[109] H. Widegren, M. Andersson, P. Borgeat, L. Flamand, S. Johnston, L. Greiff, LTB4 increases nasal neutrophil activity and conditions neutrophils to exert antiviral effects, Respir Med 105(7) (2011) 997-1006.

[110] K. Yoshimura, S. Nakagawa, S. Koyama, T. Kobayashi, T. Homma, Roles of neutrophil elastase and superoxide anion in leukotriene B4-induced lung injury in rabbit, J Appl Physiol (1985) 76(1) (1994) 91-6.

[111] E. Gaudreault, J. Gosselin, Leukotriene B4 induces release of antimicrobial peptides in lungs of virally infected mice, J Immunol 180(9) (2008) 6211-21.

[112] M. Wan, A. Sabirsh, A. Wetterholm, B. Agerberth, J.Z. Haeggstrom, Leukotriene B4 triggers release of the cathelicidin LL-37 from human neutrophils: novel lipid-peptide interactions in innate immune responses, FASEB J 21(11) (2007) 2897-905.

[113] M.P. Wymann, V. von Tscharner, D.A. Deranleau, M. Baggiolini, The onset of the respiratory burst in human neutrophils. Real-time studies of H2O2 formation reveal a rapid agonist-induced transduction process, J Biol Chem 262(25) (1987) 12048-53.

[114] C.H. Serezani, D.M. Aronoff, S. Jancar, M. Peters-Golden, Leukotriene B4 mediates p47phox phosphorylation and membrane translocation in polyunsaturated fatty acid-stimulated neutrophils, J Leukoc Biol 78(4) (2005) 976-84.

[115] C.H. Woo, H.J. You, S.H. Cho, Y.W. Eom, J.S. Chun, Y.J. Yoo, J.H. Kim, Leukotriene B(4) stimulates Rac-ERK cascade to generate reactive oxygen species that mediates chemotaxis, J Biol Chem 277(10) (2002) 8572-8.

[116] P. Mancuso, C. Lewis, C.H. Serezani, D. Goel, M. Peters-Golden, Intrapulmonary administration of leukotriene B4 enhances pulmonary host defense against pneumococcal pneumonia, Infect Immun 78(5) (2010) 2264-71.

[117] C. Bogdan, Nitric oxide and the immune response, Nat Immunol 2(10) (2001) 907-16.

[118] C.H. Serezani, J.H. Perrela, M. Russo, M. Peters-Golden, S. Jancar, Leukotrienes Are Essential for the Control of Leishmania amazonensis Infection and Contribute to Strain Variation in Susceptibility, The Journal of Immunology 177(5) (2006) 3201-3208.

[119] V.A. Rathinam, K.A. Fitzgerald, Inflammasome Complexes: Emerging Mechanisms and Effector Functions, Cell 165(4) (2016) 792-800.

[120] F.A. Amaral, V.V. Costa, L.D. Tavares, D. Sachs, F.M. Coelho, C.T. Fagundes, F.M. Soriani, T.N. Silveira, L.D. Cunha, D.S. Zamboni, V. Quesniaux, R.S. Peres, T.M. Cunha, F.Q. Cunha, B. Ryffel, D.G. Souza, M.M. Teixeira, NLRP3 inflammasome-mediated neutrophil recruitment and hypernociception depend on leukotriene B(4) in a murine model of gout, Arthritis Rheum 64(2) (2012) 474-84.

[121] M.G. Netea, F.L. van de Veerdonk, J.W. van der Meer, C.A. Dinarello, L.A. Joosten, Inflammasome-independent regulation of IL-1-family cytokines, Annu Rev Immunol 33 (2015) 49-77.

[122] L.S. Miller, E.M. Pietras, L.H. Uricchio, K. Hirano, S. Rao, H. Lin, R.M. O'Connell, Y. Iwakura, A.L. Cheung, G. Cheng, R.L. Modlin, Inflammasome-mediated production of IL-1beta is required for neutrophil recruitment against Staphylococcus aureus in vivo, J Immunol 179(10) (2007) 6933-42.

[123] H. Huang, N.M. Flynn, J.H. King, C. Monchaud, M. Morita, S.H. Cohen, Comparisons of community-associated methicillin-resistant Staphylococcus aureus (MRSA) and hospital-associated MSRA infections in Sacramento, California, J Clin Microbiol 44(7) (2006) 2423-7.

[124] L.R. Thurlow, G.S. Joshi, A.R. Richardson, Virulence strategies of the dominant USA300 lineage of community-associated methicillin-resistant Staphylococcus aureus (CA-MRSA), FEMS Immunol Med Microbiol 65(1) (2012) 5-22.

[125] M. Li, B.A. Diep, A.E. Villaruz, K.R. Braughton, X. Jiang, F.R. DeLeo, H.F. Chambers, Y. Lu, M. Otto, Evolution of virulence in epidemic community-associated methicillin-resistant Staphylococcus aureus, Proc Natl Acad Sci U S A 106(14) (2009) 5883-8.

[126] C.P. Montgomery, S. Boyle-Vavra, P.V. Adem, J.C. Lee, A.N. Husain, J. Clasen, R.S. Daum, Comparison of virulence in community-associated methicillin-resistant Staphylococcus aureus pulsotypes USA300 and USA400 in a rat model of pneumonia, J Infect Dis 198(4) (2008) 561-70.

[127] R.E. Hancock, A. Nijnik, D.J. Philpott, Modulating immunity as a therapy for bacterial infections, Nat Rev Microbiol 10(4) (2012) 243-54.

[128] S.D. Kobayashi, N. Malachowa, F.R. DeLeo, Pathogenesis of Staphylococcus aureus abscesses, Am J Pathol 185(6) (2015) 1518-27.

[129] R.N. Barker, L.P. Erwig, K.S. Hill, A. Devine, W.P. Pearce, A.J. Rees, Antigen presentation by macrophages is enhanced by the uptake of necrotic, but not apoptotic, cells, Clin Exp Immunol 127(2) (2002) 220-5.

[130] M. Martinez-Clemente, J. Claria, E. Titos, The 5-lipoxygenase/leukotriene pathway in obesity, insulin resistance, and fatty liver disease, Curr Opin Clin Nutr Metab Care 14(4) (2011) 347-53.

[131] K. Soumaya, Molecular mechanisms of insulin resistance in diabetes, Adv Exp Med Biol 771 (2012) 240-51.

[132] M. Spite, J. Hellmann, Y. Tang, S.P. Mathis, M. Kosuri, A. Bhatnagar, V.R. Jala, B. Haribabu, Deficiency of the leukotriene B4 receptor, BLT-1, protects

against systemic insulin resistance in diet-induced obesity, J Immunol 187(4) (2011) 1942-9.

[133] N. Ahmadzadeh, M. Shingu, M. Nobunaga, T. Tawara, Relationship between leukotriene B4 and immunological parameters in rheumatoid synovial fluids, Inflammation 15(6) (1991) 497-503.

[134] M. Chen, B.K. Lam, Y. Kanaoka, P.A. Nigrovic, L.P. Audoly, K.F. Austen, D.M. Lee, Neutrophil-derived leukotriene B4 is required for inflammatory arthritis, J Exp Med 203(4) (2006) 837-42.

[135] S. Mathis, V.R. Jala, B. Haribabu, Role of leukotriene B4 receptors in rheumatoid arthritis, Autoimmun Rev 7(1) (2007) 12-7.

[136] E. Sanchez-Galan, A. Gomez-Hernandez, C. Vidal, J.L. Martin-Ventura, L.M. Blanco-Colio, B. Munoz-Garcia, L. Ortega, J. Egido, J. Tunon, Leukotriene B4 enhances the activity of nuclear factor-kappaB pathway through BLT1 and BLT2 receptors in atherosclerosis, Cardiovasc Res 81(1) (2009) 216-25.

[137] D.M. Tobin, J.C. Vary, Jr., J.P. Ray, G.S. Walsh, S.J. Dunstan, N.D. Bang, D.A. Hagge, S. Khadge, M.C. King, T.R. Hawn, C.B. Moens, L. Ramakrishnan, The lta4h locus modulates susceptibility to mycobacterial infection in zebrafish and humans, Cell 140(5) (2010) 717-30.

[138] D.M. Tobin, F.J. Roca, S.F. Oh, R. McFarland, T.W. Vickery, J.P. Ray, D.C. Ko, Y. Zou, N.D. Bang, T.T. Chau, J.C. Vary, T.R. Hawn, S.J. Dunstan, J.J. Farrar, G.E. Thwaites, M.C. King, C.N. Serhan, L. Ramakrishnan, Host genotype-specific therapies can optimize the inflammatory response to mycobacterial infections, Cell 148(3) (2012) 434-46.

[139] D.M. Tobin, F.J. Roca, J.P. Ray, D.C. Ko, L. Ramakrishnan, An enzyme that inactivates the inflammatory mediator leukotriene b4 restricts mycobacterial infection, PLoS One 8(7) (2013) e67828.

[140] A.P. Monteiro, E. Soledade, C.S. Pinheiro, L. Dellatorre-Teixeira, G.P. Oliveira, M.G. Oliveira, M. Peters-Golden, P.R. Rocco, C.F. Benjamim, C. Canetti, Pivotal role of the 5-lipoxygenase pathway in lung injury after experimental sepsis, Am J Respir Cell Mol Biol 50(1) (2014) 87-95.

[141] X.J. Li, H.Y. Fu, W.J. Yi, Y.J. Zhao, J. Wang, J.B. Li, J.F. Wang, X.M. Deng, Dual role of leukotriene B4 receptor type 1 in experimental sepsis, J Surg Res 193(2) (2015) 902-8.

[142] M.A. Atkinson, The pathogenesis and natural history of type 1 diabetes, Cold Spring Harb Perspect Med 2(11) (2012) a007641.

[143] J. Casqueiro, J. Casqueiro, C. Alves, Infections in patients with diabetes mellitus: A review of pathogenesis, Indian J Endocrinol Metab 16 Suppl 1 (2012) S27-36.

[144] L.M. Muller, K.J. Gorter, E. Hak, W.L. Goudzwaard, F.G. Schellevis, A.I. Hoepelman, G.E. Rutten, Increased risk of common infections in patients with type 1 and type 2 diabetes mellitus, Clin Infect Dis 41(3) (2005) 281-8.

[145] B.A. Lipsky, Y.P. Tabak, R.S. Johannes, L. Vo, L. Hyde, J.A. Weigelt, Skin and soft tissue infections in hospitalised patients with diabetes: culture isolates and risk factors associated with mortality, length of stay and cost, Diabetologia 53(5) (2010) 914-23.

[146] N.T. Foss, M.C. Foss-Freitas, M.A. Ferreira, R.N. Cardili, C.M. Barbosa, M.C. Foss, Impaired cytokine production by peripheral blood mononuclear cells in type 1 diabetic patients, Diabetes Metab 33(6) (2007) 439-43.

[147] S.E. Geerlings, A.I. Hoepelman, Immune dysfunction in patients with diabetes mellitus (DM), FEMS Immunol Med Microbiol 26(3-4) (1999) 259-65.

[148] A. Lecube, G. Pachon, J. Petriz, C. Hernandez, R. Simo, Phagocytic activity is impaired in type 2 diabetes mellitus and increases after metabolic improvement, PLoS One 6(8) (2011) e23366.

[149] T.C. Alba-Loureiro, C.D. Munhoz, J.O. Martins, G.A. Cerchiaro, C. Scavone, R. Curi, P. Sannomiya, Neutrophil function and metabolism in individuals with diabetes mellitus, Braz J Med Biol Res 40(8) (2007) 1037-44.

[150] C. Parlapiano, C. Danese, M. Marangi, E. Campana, P. Pantone, T. Giovanniello, E. Zavattaro, S. Sanguigni, The relationship between glycated hemoglobin and polymorphonuclear leukocyte leukotriene B4 release in people with diabetes mellitus, Diabetes Res Clin Pract 46(1) (1999) 43-5.

[151] H. Matsushima, Y. Ogawa, T. Miyazaki, H. Tanaka, A. Nishibu, A. Takashima, Intravital imaging of IL-1beta production in skin, J Invest Dermatol 130(6) (2010) 1571-80.

[152] H.A. Schreiber, J. Loschko, R.A. Karssemeijer, A. Escolano, M.M. Meredith, D. Mucida, P. Guermonprez, M.C. Nussenzweig, Intestinal monocytes and macrophages are required for T cell polarization in response to Citrobacter rodentium, J Exp Med 210(10) (2013) 2025-39.

[153] N. Faust, F. Varas, L.M. Kelly, S. Heck, T. Graf, Insertion of enhanced green fluorescent protein into the lysozyme gene creates mice with green fluorescent granulocytes and macrophages, Blood 96(2) (2000) 719-26.

[154] R. Domingo-Gonzalez, S. Katz, C.H. Serezani, T.A. Moore, A.M. Levine, B.B. Moore, Prostaglandin E2-induced changes in alveolar macrophage

scavenger receptor profiles differentially alter phagocytosis of Pseudomonas aeruginosa and Staphylococcus aureus post-bone marrow transplant, J Immunol 190(11) (2013) 5809-17.

[155] R.D. Plaut, C.P. Mocca, R. Prabhakara, T.J. Merkel, S. Stibitz, Stably luminescent Staphylococcus aureus clinical strains for use in bioluminescent imaging, PLoS One 8(3) (2013) e59232.

[156] M.C. Greenlee-Wacker, K.M. Rigby, S.D. Kobayashi, A.R. Porter, F.R. DeLeo, W.M. Nauseef, Phagocytosis of Staphylococcus aureus by human neutrophils prevents macrophage efferocytosis and induces programmed necrosis, J Immunol 192(10) (2014) 4709-17.

[157] N. Malachowa, S.D. Kobayashi, K.R. Braughton, F.R. DeLeo, Mouse model of Staphylococcus aureus skin infection, Methods Mol Biol 1031 (2013) 109-16.

[158] B.C. Timmons, J. Reese, S. Socrate, N. Ehinger, B.C. Paria, G.L. Milne, M.L. Akins, R.J. Auchus, D. McIntire, M. House, M. Mahendroo, Prostaglandins are essential for cervical ripening in LPS-mediated preterm birth but not term or antiprogestin-driven preterm ripening, Endocrinology 155(1) (2014) 287-98.

[159] J. Liese, S.H. Rooijakkers, J.A. van Strijp, R.P. Novick, M.L. Dustin, Intravital two-photon microscopy of host-pathogen interactions in a mouse model of Staphylococcus aureus skin abscess formation, Cell Microbiol 15(6) (2013) 891-909.

[160] DiaComp, Low-Dose Streptozotocin Induction Protocol (Mouse), Diabetic Complications Consortium (2015).

[161] M.C. Deeds, J.M. Anderson, A.S. Armstrong, D.A. Gastineau, H.J. Hiddinga, A. Jahangir, N.L. Eberhardt, Y.C. Kudva, Single dose streptozotocin-induced diabetes: considerations for study design in islet transplantation models, Lab Anim 45(3) (2011) 131-40.

[162] S. Lenzen, The mechanisms of alloxan- and streptozotocin-induced diabetes, Diabetologia 51(2) (2008) 216-26.

[163] P.A. Pino-Tamayo, J.D. Puerta-Arias, D. Lopera, M.E. Uran-Jimenez, A. Gonzalez, Depletion of Neutrophils Exacerbates the Early Inflammatory Immune Response in Lungs of Mice Infected with Paracoccidioides brasiliensis, Mediators Inflamm 2016 (2016) 3183285.

[164] S. Krishna, L.S. Miller, Innate and adaptive immune responses against Staphylococcus aureus skin infections, Semin Immunopathol 34(2) (2012) 261-80.

[165] A. Abtin, R. Jain, A.J. Mitchell, B. Roediger, A.J. Brzoska, S. Tikoo, Q. Cheng, L.G. Ng, L.L. Cavanagh, U.H. von Andrian, M.J. Hickey, N. Firth, W.

Weninger, Perivascular macrophages mediate neutrophil recruitment during bacterial skin infection, Nat Immunol 15(1) (2014) 45-53.

[166] L.S. Miller, J.S. Cho, Immunity against Staphylococcus aureus cutaneous infections, Nat Rev Immunol 11(8) (2011) 505-18.

[167] V. Thammavongsa, D.M. Missiakas, O. Schneewind, Staphylococcus aureus degrades neutrophil extracellular traps to promote immune cell death, Science 342(6160) (2013) 863-6.

[168] A. Kubo, M. Kajimura, M. Suematsu, Matrix-Assisted Laser Desorption/Ionization (MALDI) Imaging Mass Spectrometry (IMS): A Challenge for Reliable Quantitative Analyses, Mass Spectrom (Tokyo) 1(1) (2012) A0004.

[169] A. Panday, M.K. Sahoo, D. Osorio, S. Batra, NADPH oxidases: an overview from structure to innate immunity-associated pathologies, Cell Mol Immunol 12(1) (2015) 5-23.

[170] J.S. Cho, Y. Guo, R.I. Ramos, F. Hebroni, S.B. Plaisier, C. Xuan, J.L. Granick, H. Matsushima, A. Takashima, Y. Iwakura, A.L. Cheung, G. Cheng, D.J. Lee, S.I. Simon, L.S. Miller, Neutrophil-derived IL-1beta is sufficient for abscess formation in immunity against Staphylococcus aureus in mice, PLoS Pathog 8(11) (2012) e1003047.

[171] R.C. Chou, N.D. Kim, C.D. Sadik, E. Seung, Y. Lan, M.H. Byrne, B. Haribabu, Y. Iwakura, A.D. Luster, Lipid-cytokine-chemokine cascade drives neutrophil recruitment in a murine model of inflammatory arthritis, Immunity 33(2) (2010) 266-78.

[172] C. Liu, A. Bayer, S.E. Cosgrove, R.S. Daum, S.K. Fridkin, R.J. Gorwitz, S.L. Kaplan, A.W. Karchmer, D.P. Levine, B.E. Murray, J.R. M, D.A. Talan, H.F. Chambers, Clinical practice guidelines by the infectious diseases society of america for the treatment of methicillin-resistant Staphylococcus aureus infections in adults and children: executive summary, Clin Infect Dis 52(3) (2011) 285-92.

[173] D.V. Serreze, J.W. Gaedeke, E.H. Leiter, Hematopoietic stem-cell defects underlying abnormal macrophage development and maturation in NOD/Lt mice: defective regulation of cytokine receptors and protein kinase C, Proc Natl Acad Sci U S A 90(20) (1993) 9625-9.

[174] D.V. Serreze, H.R. Gaskins, E.H. Leiter, Defects in the differentiation and function of antigen presenting cells in NOD/Lt mice, J Immunol 150(6) (1993) 2534-43.

[175] T. Pearson, T.G. Markees, D.V. Serreze, M.A. Pierce, L.S. Wicker, L.B. Peterson, L.D. Shultz, J.P. Mordes, A.A. Rossini, D.L. Greiner, Genetic

separation of the transplantation tolerance and autoimmune phenotypes in NOD mice, Rev Endocr Metab Disord 4(3) (2003) 255-61.

[176] N.N. Dejani, S.L. Brandt, A. Pineros, N.L. Glosson-Byers, S. Wang, Y.M. Son, A.I. Medeiros, C.H. Serezani, Topical Prostaglandin E Analog Restores Defective Dendritic Cell-Mediated Th17 Host Defense Against Methicillin-Resistant Staphylococcus Aureus in the Skin of Diabetic Mice, Diabetes 65(12) (2016) 3718-3729.

[177] N. Malachowa, S.D. Kobayashi, A.R. Porter, K.R. Braughton, D.P. Scott, D.J. Gardner, D.M. Missiakas, O. Schneewind, F.R. DeLeo, Contribution of Staphylococcus aureus Coagulases and Clumping Factor A to Abscess Formation in a Rabbit Model of Skin and Soft Tissue Infection, PLoS One 11(6) (2016) e0158293.

[178] M. Ferracini, F.J. Rios, M. Pecenin, S. Jancar, Clearance of apoptotic cells by macrophages induces regulatory phenotype and involves stimulation of CD36 and platelet-activating factor receptor, Mediators Inflamm 2013 (2013) 950273.

[179] B. Ha, Z. Lv, Z. Bian, X. Zhang, A. Mishra, Y. Liu, 'Clustering' SIRPalpha into the plasma membrane lipid microdomains is required for activated monocytes and macrophages to mediate effective cell surface interactions with CD47, PLoS One 8(10) (2013) e77615.

[180] E. Sezgin, I. Levental, S. Mayor, C. Eggeling, The mystery of membrane organization: composition, regulation and roles of lipid rafts, Nat Rev Mol Cell Biol 18(6) (2017) 361-374.

[181] Y. Ueda, M. Kondo, G. Kelsoe, Inflammation and the reciprocal production of granulocytes and lymphocytes in bone marrow, J Exp Med 201(11) (2005) 1771-80.

[182] L.S. Bisgaard, C.K. Mogensen, A. Rosendahl, H. Cucak, L.B. Nielsen, S.E. Rasmussen, T.X. Pedersen, Bone marrow-derived and peritoneal macrophages have different inflammatory response to oxLDL and M1/M2 marker expression - implications for atherosclerosis research, Sci Rep 6 (2016) 35234.

[183] R.K. Sivamani, Eicosanoids and Keratinocytes in Wound Healing, Adv Wound Care (New Rochelle) 3(7) (2014) 476-481.

[184] C.N. Serhan, Pro-resolving lipid mediators are leads for resolution physiology, Nature 510(7503) (2014) 92-101.

[185] H. Harizi, N. Gualde, Dendritic cells produce eicosanoids, which modulate generation and functions of antigen-presenting cells, Prostaglandins Leukot Essent Fatty Acids 66(5-6) (2002) 459-66.

[186] A.G. Cheng, A.C. DeDent, O. Schneewind, D. Missiakas, A play in four acts: Staphylococcus aureus abscess formation, Trends Microbiol 19(5) (2011) 225-32.

[187] B.L. Hahn, P.G. Sohnle, Direct translocation of staphylococci from the skin surface to deep organs, Microb Pathog 63 (2013) 24-9.

[188] N. Nippe, G. Varga, D. Holzinger, B. Loffler, E. Medina, K. Becker, J. Roth, J.M. Ehrchen, C. Sunderkotter, Subcutaneous infection with S. aureus in mice reveals association of resistance with influx of neutrophils and Th2 response, J Invest Dermatol 131(1) (2011) 125-32.

[189] E.B. Friedrich, A.M. Tager, E. Liu, A. Pettersson, C. Owman, L. Munn, A.D. Luster, R.E. Gerszten, Mechanisms of leukotriene B4--triggered monocyte adhesion, Arterioscler Thromb Vasc Biol 23(10) (2003) 1761-7.

[190] B. Lkhagvaa, K. Tani, K. Sato, Y. Toyoda, C. Suzuka, S. Sone, Bestatin, an inhibitor for aminopeptidases, modulates the production of cytokines and chemokines by activated monocytes and macrophages, Cytokine 44(3) (2008) 386-91.

[191] R.R. Craven, X. Gao, I.C. Allen, D. Gris, J. Bubeck Wardenburg, E. McElvania-Tekippe, J.P. Ting, J.A. Duncan, Staphylococcus aureus alpha-hemolysin activates the NLRP3-inflammasome in human and mouse monocytic cells, PLoS One 4(10) (2009) e7446.

[192] J. Munguia, V. Nizet, Pharmacological Targeting of the Host-Pathogen Interaction: Alternatives to Classical Antibiotics to Combat Drug-Resistant Superbugs, Trends Pharmacol Sci 38(5) (2017) 473-488.

[193] T.R. Martin, B.P. Pistorese, E.Y. Chi, R.B. Goodman, M.A. Matthay, Effects of leukotriene B4 in the human lung. Recruitment of neutrophils into the alveolar spaces without a change in protein permeability, J Clin Invest 84(5) (1989) 1609-19.

[194] S.E. Sampson, J.F. Costello, A.P. Sampson, The effect of inhaled leukotriene B4 in normal and in asthmatic subjects, Am J Respir Crit Care Med 155(5) (1997) 1789-92.

[195] L. Lin, P. Nonejuie, J. Munguia, A. Hollands, J. Olson, Q. Dam, M. Kumaraswamy, H. Rivera, Jr., R. Corriden, M. Rohde, M.E. Hensler, M.D. Burkart, J. Pogliano, G. Sakoulas, V. Nizet, Azithromycin Synergizes with Cationic Antimicrobial Peptides to Exert Bactericidal and Therapeutic Activity Against Highly Multidrug-Resistant Gram-Negative Bacterial Pathogens, EBioMedicine 2(7) (2015) 690-8.

[196] K. Leszczynska, A. Namiot, P.A. Janmey, R. Bucki, Modulation of exogenous antibiotic activity by host cathelicidin LL-37, APMIS 118(11) (2010) 830-6.

[197] S.J. Skerrett, W.R. Henderson, T.R. Martin, Alveolar macrophage function in rats with severe protein calorie malnutrition. Arachidonic acid metabolism, cytokine release, and antimicrobial activity, J Immunol 144(3) (1990) 1052-61.

[198] M.S. Balter, G.B. Toews, M. Peters-Golden, Multiple defects in arachidonate metabolism in alveolar macrophages from young asymptomatic smokers, J Lab Clin Med 114(6) (1989) 662-73.

[199] M.J. Coffey, S.E. Wilcoxen, S.M. Phare, R.U. Simpson, M.R. Gyetko, M. Peters-Golden, Reduced 5-lipoxygenase metabolism of arachidonic acid in macrophages rrom 1,25-dihydroxyvitamin D3-deficient rats, Prostaglandins 48(5) (1994) 313-29.

[200] M.J. Coffey, S.M. Phare, S. George, M. Peters-Golden, P.H. Kazanjian, Granulocyte colony-stimulating factor administration to HIV-infected subjects augments reduced leukotriene synthesis and anticryptococcal activity in neutrophils, J Clin Invest 102(4) (1998) 663-70.

[201] M.N. Ballinger, T.R. McMillan, B.B. Moore, Eicosanoid regulation of pulmonary innate immunity post-hematopoietic stem cell transplantation, Arch Immunol Ther Exp (Warsz) 55(1) (2007) 1-12.

[202] L. Flamand, M.J. Tremblay, P. Borgeat, Leukotriene B4 Triggers the In Vitro and In Vivo Release of Potent Antimicrobial Agents, The Journal of Immunology 178(12) (2007) 8036-8045.

[203] S. Khanna, S. Biswas, Y. Shang, E. Collard, A. Azad, C. Kauh, V. Bhasker, G.M. Gordillo, C.K. Sen, S. Roy, Macrophage dysfunction impairs resolution of inflammation in the wounds of diabetic mice, PLoS One 5(3) (2010) e9539.

[204] S. Li, Y. Sun, C.P. Liang, E.B. Thorp, S. Han, A.W. Jehle, V. Saraswathi, B. Pridgen, J.E. Kanter, R. Li, C.L. Welch, A.H. Hasty, K.E. Bornfeldt, J.L. Breslow, I. Tabas, A.R. Tall, Defective phagocytosis of apoptotic cells by macrophages in atherosclerotic lesions of ob/ob mice and reversal by a fish oil diet, Circ Res 105(11) (2009) 1072-82.

[205] M.R. Elliott, K.S. Ravichandran, Clearance of apoptotic cells: implications in health and disease, J Cell Biol 189(7) (2010) 1059-70.

[206] K.S. Ravichandran, Find-me and eat-me signals in apoptotic cell clearance: progress and conundrums, J Exp Med 207(9) (2010) 1807-17.

[207] S.W. Tait, G. Ichim, D.R. Green, Die another way--non-apoptotic mechanisms of cell death, J Cell Sci 127(Pt 10) (2014) 2135-44.

[208] T. Vanden Berghe, S. Grootjans, V. Goossens, Y. Dondelinger, D.V. Krysko, N. Takahashi, P. Vandenabeele, Determination of apoptotic and necrotic cell death in vitro and in vivo, Methods 61(2) (2013) 117-29.

[209] K. Kitur, S. Wachtel, A. Brown, M. Wickersham, F. Paulino, H.F. Penaloza, G. Soong, S. Bueno, D. Parker, A. Prince, Necroptosis Promotes Staphylococcus aureus Clearance by Inhibiting Excessive Inflammatory Signaling, Cell Rep 16(8) (2016) 2219-30.

[210] S. Accarias, G. Lugo-Villarino, G. Foucras, O. Neyrolles, S. Boullier, G. Tabouret, Pyroptosis of resident macrophages differentially orchestrates inflammatory responses to Staphylococcus aureus in resistant and susceptible mice, Eur J Immunol 45(3) (2015) 794-806.

[211] A. Puchta, A. Naidoo, C.P. Verschoor, D. Loukov, N. Thevaranjan, T.S. Mandur, P.S. Nguyen, M. Jordana, M. Loeb, Z. Xing, L. Kobzik, M.J. Larche, D.M. Bowdish, TNF Drives Monocyte Dysfunction with Age and Results in Impaired Anti-pneumococcal Immunity, PLoS Pathog 12(1) (2016) e1005368.

[212] F. Yin, R. Banerjee, B. Thomas, P. Zhou, L. Qian, T. Jia, X. Ma, Y. Ma, C. Iadecola, M.F. Beal, C. Nathan, A. Ding, Exaggerated inflammation, impaired host defense, and neuropathology in progranulin-deficient mice, J Exp Med 207(1) (2010) 117-28.

[213] A.S. Headley, E. Tolley, G.U. Meduri, Infections and the inflammatory response in acute respiratory distress syndrome, Chest 111(5) (1997) 1306-21.

[214] H.P. Ng, Y. Zhou, K. Song, C.A. Hodges, M.L. Drumm, G. Wang, Neutrophil-mediated phagocytic host defense defect in myeloid Cftr-inactivated mice, PLoS One 9(9) (2014) e106813.

[215] S.M. Aswani, U. Chandrashekar, K. Shivashankara, B. Pruthvi, Clinical profile of urinary tract infections in diabetics and non-diabetics, Australas Med J 7(1) (2014) 29-34.

[216] P. Li, D.Y. Oh, G. Bandyopadhyay, W.S. Lagakos, S. Talukdar, O. Osborn, A. Johnson, H. Chung, R. Mayoral, M. Maris, J.M. Ofrecio, S. Taguchi, M. Lu, J.M. Olefsky, LTB4 promotes insulin resistance in obese mice by acting on macrophages, hepatocytes and myocytes, Nat Med 21(3) (2015) 239-47.

[217] M.H. Braff, A. Di Nardo, R.L. Gallo, Keratinocytes store the antimicrobial peptide cathelicidin in lamellar bodies, J Invest Dermatol 124(2) (2005) 394-400.

[218] C.C. Lan, I.H. Liu, A.H. Fang, C.H. Wen, C.S. Wu, Hyperglycaemic conditions decrease cultured keratinocyte mobility: implications for impaired wound healing in patients with diabetes, Br J Dermatol 159(5) (2008) 1103-15.

[219] F.J. Eduardo Reategui, Aimal H. Khankhel, Elisabeth Wong, Hansang Cho, Jarone Lee, Charles N. Serhan, Jesmond Dalli, Hunter Elliott & Daniel Irimia, Microscale arrays for the profiling of start and stop signals coordinating human-neutrophil swarming, Nature Biomedical Engineering 1 (2017) 0094.

[220] M.E. Katt, A.L. Placone, A.D. Wong, Z.S. Xu, P.C. Searson, In Vitro Tumor Models: Advantages, Disadvantages, Variables, and Selecting the Right Platform, Front Bioeng Biotechnol 4 (2016) 12.

[221] X. Zhang, D.M. Mosser, Macrophage activation by endogenous danger signals, J Pathol 214(2) (2008) 161-78.

[222] O. Krysko, G. Holtappels, N. Zhang, M. Kubica, K. Deswarte, L. Derycke, S. Claeys, H. Hammad, G.G. Brusselle, P. Vandenabeele, D.V. Krysko, C. Bachert, Alternatively activated macrophages and impaired phagocytosis of S. aureus in chronic rhinosinusitis, Allergy 66(3) (2011) 396-403.

CURRICULUM VITAE

Stephanie Lillian Brandt

Education

2017	Ph.D. Microbiology and Immunology Indiana University	Indianapolis, IN
2011	B.Sc., Microbiology University of Washington	Seattle, WA

Research and Training Experience

08.2015	One week training at Dr. Victor Nizet's lab at University of California San Diego, La Jolla, CA
06.2011-07.2012	Summer intern in the Preclinical Research group at Seattle Genetics, Bothell, WA
01.2009-06.2011	Laboratory assistant in Dr. Sheila Lukehart's lab at University of Washington, Seattle, WA.

Teaching and mentoring opportunities

2017	Rotation student at VUMC
2016	High school student at Eastern HS
2016	Summer research 2nd year IU MD student
2015	Rotation student IUSM
2015	Summer research, 2nd year IU MD student
2015	Rotation student IUSM
2014	Teaching assistant for J210, Introduction to Microbiology and Immunology at IUPUI
2014	Summer research 2nd year IU MD student

Posters and presentations

2017	**Stephanie Brandt**, Soujuan Wang, Naiara Dejani, Seth Winfree, Brian McCarthy, Paul Territo, and C. Henrique Serezani. Skin Resident Macrophages Drive Detrimental Host Defense During Methicillin-Resistant Staphylococcus aureus Skin Infection in Diabetic Mice. Poster and oral presentation given at 2017 Gordon Research Seminar, Phagocytes in Waterville Valley, NH. Presented poster at the Phagocytes Gordon Research Conference.

2016 **Stephanie Brandt**, Soujuan Wang, Sebastian Carrasco, Naiara Dejani, Nicole Glosson-Byers, C. Henrique Serezani. Aberrant localized LTB4 production exacerbates methicillin-resistant Staphylococcus aureus skin infection in diabetic mice. Poster presented at the 2016 American Association of Immunologists Meeting in Seattle, WA.

2015 Presented at the Research in Pediatric Development Pharmacology meeting. October 2015. Washington DC.

2015 **Stephanie Brandt**, Soujuan Wang, Sebastian Carrasco, Stacy Blank, Nathan Delafield, C. Henrique Serezani. Leukotriene B4 is a homeostatic component of methicillin-resistant Staphylococcus aureus skin infection. Poster presented at the 2015 Midwest Microbial Pathogenesis Conference.

2015 **Stephanie Brandt**, Soujuan Wang, Sebastian Carrasco, Stacy Blank, Nathan Delafield, C. Henrique Serezani. Leukotriene B4 is a homeostatic component of methicillin-resistant Staphylococcus aureus skin infection. Poster presented at the 2015 World Congress on Inflammation meeting in Boston, MA

2014 **Stephanie Brandt**, Soujuan Wang, Stacy Blank, Nathan Delafield, Sebastian Carrasco, C. Henrique Serezani. Leukotriene B4 controls methicillin-resistant Staphylococcus aureus skin infection. Poster and oral presentation presented at the 2014 Autumn Immunology Conference in Chicago, IL.

2014 **Stephanie Brandt**, Sue Wang, Nathan Delafield, Sebastian Carrasco, and Henrique Serezani. Leukotriene B4 controls methicillin-resistant Staphylococcus aureus skin infection. Poster presented at the 2014 American Association of Immunologists Meeting in Pittsburgh, PA.

2011 **Stephanie L. Brandt**. Arturo Centurion-Lara. Treponemal Outer Membrane Protein Candidate: TP0126. Poster presented at the 2011 University of Washington Mary Gates Research Symposium in Seattle, WA.

Awards

2014-2017	Immunology and Infectious Diseases training grant T32 AI 60519-12
2016	Harold Raidt Graduate Student Teaching Award
2016	American Association of Immunologists Trainee Poster Award
2016	IUPUI Graduate Office Travel Fellowship Award
2015	IUPUI Graduate Office Travel Fellowship Award
2015	Midwest Microbial Pathogenesis Conference Poster Award

Publications

2017	**Stephanie L. Brandt**, Soujuan Wang, Naiara Dejani, Seth Winfree, Brian McCarthy, Paul Territo, and C. Henrique Serezani. Diabetes promotes excessive leukotriene B4 levels driven by macrophages impairing host defense to skin infection. In preparation.
2017	**Stephanie L. Brandt**, Soujuan Wang, Seth Winfree, Brian McCarthy, Paul Territo, Lloyd Miller, and C. Henrique Serezani. Leukotriene B4 orchestrates abscess architecture during methicillin-resistant Staphylococcus aureus skin infections. Submitted.
2017	**Stephanie L. Brandt** and C. Henrique Serezani. Too much of a good thing: how leukotriene B4 influences host defense mechanisms. In press at Seminars in Immunology.
2017	Annie Piñeros, Nicole Glosson-Byers, **Stephanie Brandt**, Soujuan Wang, Hector Wong, Sarah Sturgeon, Brian McCarthy, Paul Territo, Jose C. Alves-Filho, C. Henrique Serezani. SOCS1 is a negative regulator of metabolic reprogramming during sepsis. JCI Insight. 2017; 2(13):e92530. doi:10.1172/jci.insight.92530.
2017	Nuclear PTEN drives microRNA maturation regulon to mediate MyD88-dependent susceptibility to sepsis. Flavia Sisti[#], Soujuan Wang[#], **Stephanie L. Brandt[#]**, Nicole Glosson-Byers, Lindsey Mayo, Young min Son, Luciano Filgueiras, Sonia Jancar, Hector Wong, Charles S. Dela Cruz, Nathaniel Andrews, Jose Carlos Alves-Filho, Fernando Q. Cunha, C. Henrique Serezani. [#]Co-first authors. Under review at Science Signaling.

2017 Luciano Filgueiras, **Stephanie L. Brandt**, Theresa Raquel de Oliveira Ramalho, Sonia Jancar, Carlos Henrique Serezani. Imbalance between HDAC and HAT activities drives aberrant Stat1/Myd88 expression in macrophages from type 1 diabetic mice. Journal of Diabetes and its Complications. 2017 Feb;31 (2):334-339. doi: 10.1016/j.jdiacomp.2016.08.001.

2016 Naiara N. Dejani, **Stephanie L. Brandt**, Annie Piñeros, Nicole L. Glosson-Byers, Sue Wang, Alexandra I. Medeiros, C. Henrique Serezani. PGE2 imbalance in diabetic skin impairs dendritic cell-mediated Th17 host defense against methicillin-resistant Staphylococcus aureus. Diabetes. 2016 Dec;65 (12):3718-3729.

2016 Barbara J. Molini, Lauren C. Tantalo, Sharon K. Sahi, Veronica I. Rodriguez, **Stephanie L. Brandt**, Mark C. Fernandez, Charmie B. Godornes, Christina M. Marra, Sheila A. Lukehart. Macrolide Resistance in Treponema pallidum Correlates With 23S rDNA Mutations in Recently Isolated Clinical Strains. Sexually Transmitted Diseases: September 2016 - Volume 43 - Issue 9 - p 579–583 doi:10.1097

2016 Xing Jun Li, Lisa Deng, **Stephanie Brandt**, Charles Goodwin, Peilin Ma, Zhenyun Yang, Raghuveer Mali, Ziyue Liu, Reuben Kapur, C. Henrique Serezani, and Rebecca Chan. Role of p85α in Neutrophil Extra- and Intra-Phagosomal ROS Generation. Oncotarget 10.18632/oncotarget.8500

2015 Sebastian Carrasco, Bryan Troxell, Youyun Yang, **Stephanie Brandt**, Hongxia Li, George Sandusky, Keith Condon, C. Henrique Serezani*, and X. Frank Yang*. Outer Surface Protein OspC is an anti-phagocytic factor that protects Borrelia burgdorferi from phagocytosis by macrophages. Infection and Immunity, 2015 Dec;83(12):4848-60. doi: 10.1128/IAI.01215-15. *co-last author

2015 Lorenzo Giacani, **Stephanie L. Brandt**, Wujian Ke, Tara B. Reid, Barbara J. Molini, Stefanie Iverson-Cabral, Giulia Ciccarese, Francesco Drago, Sheila A. Lukehart, and Arturo Centurion-Lara. Transcription of TP0126, Treponema pallidum Putative OmpW Homolog, Is Regulated by the Length of a Homopolymeric Guanosine Repeat. Infection and Immunity, 2015 Jun;83(6):2275-89. doi: 10.1128/IAI.00360-15.

2015 Zhuo Wang, **Stephanie Brandt**, Alexandra Medeiros, Soujuan Wang, Hao Wu, Alexander Dent, C. Henrique Serezani. MicroRNA 21 is a homeostatic regulator of macrophage polarization and prevents prostaglandin E2-mediated M2 generation. PLoS ONE 2015 Feb 23;10(2):e0115855. doi: 10.1371/journal.pone.0115855.

2015 Luciano Filguerias, **Stephanie Brandt**, Soujuan Wang, Zhuo Wang, David Morris, Carmella Evans-Molina, Raghavendra G. Mirmira, Sonia Jancar, C. Henrique Serezani. Leukotriene B4-mediated sterile inflammation favors susceptibility to sepsis in murine type 1 diabetes. Science Signaling. 2015 Jan 27;8(361):ra10. doi: 10.1126/scisignal.2005568.

2014 Ana Elisa Ferreira, Flavia Sisti, Fabiane Sonego, Soujuan Wang, Luciano Filgueiras, **Stephanie Brandt**, Ana Paula Moreira Serezani, Hong Du, Fernando Q. Cunha, Jose Carlos Alves-Filho, and Carlos Henrique Serezani. PPAR-gamma /IL-10 Axis Inhibits MyD88 Expression and Ameliorates Murine Polymicrobial Sepsis. Journal of Immunology. 2014 Mar 1;192(5):2357-65. doi: 10.4049/jimmunol.1302375.

2012 Lorenzo Giacani, **Stephanie L. Brandt**, Maritza Puray-Chaveza, Tara Brinck Reid, Charmie Godornes, Barbara J. Molini, Martin Benzler, Jörg S. Hartig, Sheila A. Lukehart, Arturo Centurion-Lara. Comparative investigation of the genomic regions involved in antigenic variation of the TprK antigen among treponemal species, subspecies, and strains. Journal of Bacteriology. 2012 Aug;194(16):4208-25. doi: 10.1128/JB.00863-12.